UNIVERSITY OF TECHNOLOGY SYDNEY

Data-driven structural condition assessment for highway bridges under operational environments

by Ye Yuan

Thesis submitted in fulfilment of the requirements for the degree of

Master of Engineering (Research)

under the supervision of

A/Professor **Xinqun Zhu** and Dr **Jun Li**

University of Technology Sydney
Faculty of Engineering and Information Technology (FEIT)

August 2022

CERTIFICATE OF ORIGINAL AUTHORSHIP

I, **Ye Yuan** declare that this thesis, is submitted in fulfilment of the requirements for the award of Master of Engineering (Research), in the School of Civil and Environmental Engineering at the University of Technology Sydney.

This thesis is wholly my own work unless otherwise referenced or acknowledged. In addition, I certify that all information sources and literature used are indicated in the thesis.

This document has not been submitted for qualifications at any other academic institution.

This research is supported by the Australian Government Research Training Program.

Signature: Production Note:
Signature removed prior to publication.

Date: 31.08.2022

ACKNOWLEDGEMENT

Foremost, I would like to express my sincere gratitude to my supervisors, Prof. Xinqun Zhu and Dr. Jun Li for the continuous support of my Master study and research. Their patience, motivation, enthusiasm and immense knowledge are like the brightness shinning and penetrating dense fog and darkness, illuminating and guiding my academic path in all the time of research and writing of this thesis. I could not have imagined having a better supervisor and mentor for my Master study.

Besides my supervisor, I would like to thank the assessors who have attended my Candidature Assessment: Drs. Mina Mortazavi, Jianguang Fang, Yancheng Li and Prof. Chengqing Wu for their encouragement, insightful comments, and hard questions.

Many thanks to other group members of the lab team: Dr. Jiantao Li, Bing Zhang, Jiajia Hao, Chenguang Li, Nico Xu and Mingzhe Gao, for the stimulating discussions about research, coursework assignments, review of progress and other interesting topics.

My sincere thank also goes to Prof. Zhongrong Lv and Dr. Zhiyi Yin in Sun Yat-sen University for enlightening me the first glance of research. Prof. Lv's face to face supervision and weekly held group meetings that I have attended were very helpful in the initial stage of my research.

In particular, I am grateful to Prof. Xiangrong Yuan in Guangzhou University.

Last but not the least, I would like to thank my parents Jingbo Yuan and Weirong Bu, for giving birth to me at the first place and supporting me materially and spiritually throughout my life.

TABLE OF CONTENTS

ABSTRACT

Bridges are key transportation infrastructure. In Australia, over 60% of bridges on local roads are over 50 years old. With the deterioration of the bridge performance and ever-increasing amount of traffic, the bridge safety is becoming a concern for engineering community. A method that can assess the bridge's condition in real-time is urgently needed. Structural health monitoring (SHM) provides a practical tool to assess and predict the condition of bridges. From the perspective of the real-time monitoring, the main factor that hinders an ideal bridge condition assessment is the uncertain operational environment. Existing SHM methods either try to assess the structural performance under the controlled environmental conditions or eliminate the influence of the operational environment using long-term monitoring data to train or calibrate the condition assessment model. These two ideas cannot fit the target of the real-time monitoring.

To achieve the real-time monitoring, this study proposes a new damage sensitive feature (DSF) based on moving principal component analysis (MPCA). The two main operational environmental factors: environmental temperature and traffic loads, are studied in the assessment process to verify the robustness and practicality of the proposed DSF. The numerical and experimental study has been carried out to show the reliability and accuracy of the proposed method. The mechanism of the DSF variation induced by changes in environmental parameters are discussed to show the interpretability of the proposed DSF. The value of the DSF can precisely reflect bridge's overall vibration 'rhythm' which is reliable to reflect the bridge's instantaneous vibration state. This DSF is not restricted to several few pre-considered parameters but reflects the bridge's damage condition from a dynamic perspective.

Chapter 1 Introduction

1.1 Research Background

Bridges are key component of transportation infrastructure that is crucial for a society to function well. They are under increasing pressure from continuing deterioration, in particular, due to ageing and the overloading as results of population growth and heavy vehicle deregulation. In Australia, over 60% of bridges on local roads are over 50 years old and approximately 55% of all highway bridges are over 20 years old (Austroads 2012). The catastrophic Genova Bridge collapsed in Italy in 2018 with 43 people killed and the Nanfang'ao Bridge in Taiwan suddenly gave way, injuring more than 20 people. These failures highlighted the importance of accurately assessing, maintaining and prolonging the design life of our ageing highway infrastructure. The visual inspection is a traditional method that has been widely used and is still evolving (Khan et al. 2020). However, the reliability and effectiveness of the structural condition assessment are largely based on the inspector's performance and experience. Since civil structures are usually on a large scale with many areas that cannot be accessed directly, the process of the inspection is always time-consuming and laborious (Avci et al. 2021). Along with the development of the computation technology and data science, plenty of new concepts and methods known as structural health monitoring (SHM) began to emerge since the 1970s (Cawley 2018). SHM provides a practical tool to assess and predict the structural performance of bridges.

SHM is a multi-discipline field involving the data collection by sensor networks and the diagnosis of structural health based on the collected data. The collected

data are processed to extract the valuable features that can be analysed through model-based or data-driven techniques to enhance the decision making for the structural condition assessment (An et al. 2019; Bao et al. 2019). The model-based method intends to construct an accurate bridge finite-element model to simulate real structures by correcting model parameters and will readily be affected by structural modelling errors, high measurement noise and uncertain operational environments (Law and Zhu 2009). Based on the machine learning (ML) technique, the data-driven method shows a promising future and has already performed better in practical cases (Avci et al. 2021; Yuan et al. 2020). In practice, two main factors that hinder algorithms from obtaining the ideal result:

1) For the traditional SHM system, it is time-consuming and expensive to install a lot of sensors on bridges and there are some other practical difficulties for the system maintenance.
2) The operational environmental effect cannot be neglected.

This project aims to develop a data-driven method that is competent for the structural condition assessment under the two main factors mentioned above for highway bridges.

1.2 Research objectives

This project aims to develop a data-driven structural damage detection approach using the moving principal component analysis (MPCA) method for bridge long-terming monitoring under operational environments. The detailed objectives are as follows,

1) To develop a data-driven structural damage detection approach for highway bridges under moving vehicles.
2) To develop a data-driven structural damage detection approach which

can extract damage features considering environmental temperature effect.

3) Numerical and experimental verification of the proposed approach.

1.3 Significance

The time series vibration signals have drawn great attention since they are easy to obtain and can provide sufficient information. Currently a large branch of bridge damage indicators is constructed based on modal analysis theory. Modal analysis concentrates more on the global behaviour of the system. It assumes that the parameters of the bridge system are time-invariant. However, the two most common factors: the moving load and temperature, will directly affect the parameters of the bridge system (Yuen 2010; Law and Zhu 2009; Law and Zhu 2011; Han et al. 2021). The bridge system is a time-varying system when the environmental factors are considered. Thus, they still face challenges in the real time monitoring of bridges. Another type is the time series regression method based statistical models such as Kalman filtering or Autoregressive Moving Average (ARMA). In the training stage, they require the training data to cover the bridge's all potential states as much as possible to generate the statistical distribution of target parameters more comprehensively. Therefore, they put a high requirement of the data in the training phase with certain difficulties in the actual operation. If numerous influencing factors of bridges are considered together, the bridge is a complex high-dimensional information source. Bridges are always simplified as specific physical and mathematical models for further research. The damage is defined on specific bridge parameters, but these parameters are far from the completely representative of the actual bridge. Damage can affect the actual bridge on the arbitrary number of parameters or dimensions, and the theoretical simplification will cause part of these impacts to be ignored. Therefore, we need more perspectives to observe and obtain the actual state of the bridge.

This study will describe the state of bridges from a dynamic perspective. As a machine learning method, this study will more concentrate on mining out the state of bridges from data itself. A new damage sensitive feature (DSF) is extracted from vehicle induced bridge acceleration responses through MPCA. This DSF can reflect the bridge status in real time with enough accuracy and robustness. Its computational cost is low. The results obtained from it have a good interpretability since the changes of features can be corresponded to the variations of operational environments. For the real time monitoring of the bridge health considering the temperature impact and moving loads, this method has a better prospect for practical applications.

1.4 Layout of the thesis

This thesis is organised as follows:

Chapter 1 presents an overview of thesis including background, research objectives, significance, and the layout.

Chapter 2 reviews recent developments of vibration-based bridge SHM methods. Bridge SHM under operational environment including moving loads and temperature are listed in Section 2.2. Bridge SHM methods of each operational environment are introduced separately in corresponding Subsection according to two categories: model-based and data-driven based. Section 2.3 introduces model-based bridge SHM methods. Section 2.4 introduces data-driven based bridge SHM methods including online learning methods and offline monitoring methods. Sections 2.2 to 2.4 show the modal analysis-based methods are grouped together and introduced into one category in each Subsection according to the classification. Section 2.5 introduces bridge SHM methods using PCA. Section 2.6 introduces bridge SHM methods using MPCA.

Chapter 3 presents the development and numerical verification of the proposed approach including introduction of PCA and MPCA, establishment of numerical model, results of numerical simulation, results obtained by PCA and MPCA with comparison, parametric study of MPCA, and the construction of damage sensitive feature with discussions.

Chapter 4 presents the laboratory experimental study including introduction of experimental setup, and experimental results and discussions with an improved MPCA.

Chapter 5 presents the field experimental study including introduction of long-term monitoring system, and the results and discussions using monitored data from different operational conditions.

Chapter 6 lists conclusions and recommendations from this thesis.

Chapter 2 Literature review

2.1 Overview

For structural condition assessment, it aims to obtain the information that represents the structure's inner situation from outside. Since the vibration signal is convenient to obtain with the sufficient information, a large number of methods based on vibration measurements have been developed (Cawley 2018). In this study, I will focus on vibration-based methods. SHM is an emerging field that covers different types of structures, and the review will be specialized in the bridge SHM here. This section covers exist and representative studies among bridge SHM. From the perspective of the practical use, two characteristics become interested points to judge the quality of a method: robustness and practicality. These two goals result in two research objectives in this study. The next two sections review recent developments in these two aspects.

2.2 Bridge structural condition assessment under operational environments

2.2.1 Bridge structural health monitoring under moving loads

As an essential factor throughout the whole SHM, the operational environmental impact has drawn much attention and two main research trends to deal with it have been studied: utilization and elimination. The elimination is a traditional thinking that enhances the robustness of the method to confront uncertainty from environmental impact. On the contrary, the utilization, known as ambient vibration survey (AVS), aims at obtaining dynamic responses under natural excitation such as traffic loads, wind and micro-tremors. Since it does not require a special excitation on structures, the AVS is usually economical, convenient and time-saving (Yuen 2010). For bridge engineering, vehicle-bridge interaction is a common problem that will affect the analytic accuracy for

dynamic analysis. Scholars have done a great effort to fully understand its mechanism for further practical applications (Law and Zhu 2011). Based on these studies, we can extract useful bridge information from the response of the bridge subjected to the moving load excitation. Therefore, as the most common live loads in bridges, the moving-load is more preferred to be used as the excitation for bridge SHM considering operational environments.

2.2.1.1 Model based methods

For moving loads driven methods, most of them are based on vehicle-bridge interaction model. Martinez et al. (2020a) used an instrumented moving vehicle with installed sensors as both the moving exciter and the moving sensor, by solving an inverse problem to obtain bridge's deflection based on the vehicle-bridge interaction model for structural condition assessment. The characteristics of the vehicle are known and the measurement noise should be low for the method. This method is not suitable for the practical application. Another moving loads-driven method has been developed using three displacement transducers on the bridge (Martinez et al. 2020b). The absolute deflection of the bridge is predicted using the displacement measurements, and then the vehicle axle loads and bridge structural element stiffness are identified. This method is very sensitive to the measurement noise and it is relatively expensive to measure the absolute deflection using displacement transducers on the bridge. Shahbaznia et al. (2020) proposes a model updating approach which is based on the response sensitivity in time-domain to identify damage in railway bridges under unknown moving loads. The damage is introduced as a reduction in the stiffness of structural elements, and it may not be suitable for other damage scenarios such as changing in boundary conditions. Mao et al. (2020) put forward a state-space based statistical method using the response sensitivity. It is tested on a simply supported beam model under moving loads. The acceleration

measurements are used to predict the damage using the finite element model and the results are compared with that by Monte Carlo method. Since the environmental uncertainties are not considered, the application in real structures is limited. Based on the above, the traditional moving loads driven methods can perform precisely with good interpretability as they have a relatively strong theoretical basis. However, these methods are only suitable to the controlled environmental condition, and it is laborious and time-consuming to ensure their performance due to their limited anti-noise ability.

2.2.1.2 Data driven methods

For moving loads-based data-driven methods, Yeung and Smith (2005) proposed a pattern recognition method for structural damage detection using two unsupervised artificial neural networks (ANNs): DIGNET and probabilistic resource allocating network (PRAN). The finite element model (FEM) of a suspension bridge subjected to traffic excitation is established to obtain the frequency spectra included the first five vibration modes under the undamaged condition as the feature vectors for the training stage of ANNs, and the test feature vectors under damaged condition are generated for verifying. The responses generated from the FEM are polluted by the thermal stressing and the Gaussian noise of 0.5 mm to 3.0 mm standard deviation, and the overall identification accuracy is about 70% since the sensitivity thresholds of ANNs can be tuned according to the noise level. Ma et al. (2020) provide a variation auto-encoder based unsupervised deep-learning method using measured accelerations for structural damage detection under moving loads. It is a baseline-free approach and received good performances from both the numerical study and a scaled-model test of a simply supported beam under a single moving load. It needs to further verify under complex environmental conditions like real traffic condition to test its robustness. Since most of moving

loads-based data-driven damage detection methods base on principal component analysis (PCA), it will be further discussed in Section 2.5.1.

2.2.2 Bridge structural health monitoring under environmental temperature

Although traffic-load is most common operational loads on bridges, the temperature effect is far more complicated than the traffic effect. For the abnormal detection, the temperature impacts had drawn enormous research since it could lead to periodically or anomaly variations in measurements (Zhu et al. 2018; Han et al. 2021).

2.2.2.1 Model based methods

Since model-based methods use responses from real structures to update the FEM model by iteration. The temperature effect takes a leading position for some large bridges. Some methods utilize the temperature-induced response to identify the stiffness changes and those methods are known as structural identification (st-id). Murphy and Yarnold (2018) proposed a temperature-driven st-id method based on the thermal response of a highway bridge. They deploy different kinds of sensors to monitor the temperature gradient, thermal strain, environmental temperature and displacement of the bridge. 70 days' data have been collected for a FEM model’s validation and updating. Kulprapha and Warnitchai (2012) proposed a model-based approach using ambient thermal responses to adjust the analytical model and forecast the bridge's behaviour. It uses discrepancy between prediction and measured data to judge structure's state. The method has been verified using a scaled bridge model in laboratory. Jesus et al. (2019) proposed a model-based hybrid modular Bayesian approach (MBA) using Markov chain Monte Carlo (MCMC). The MBA is used to forecast the discrepancy between the model and MCMC for multi-parameter identification.

This method has been verified on a suspension bridge to predict natural frequencies and mid-span displacements under thermal and traffic loads.

Rather than st-id approach which is based on static responses (e.g., deflection or strain), another group of model-based methods concentrate on dynamic features like modal parameters and they aim to eliminate the temperature effect. Meruane and Heylen (2012) proposed a model-based damage detection method using parallel genetic algorithm to solve inverse problem under various environmental temperatures using I40 bridge monitored data. The objective function includes the changes of the natural frequency and mode-shape. Structural damage detection becomes a nonlinear optimization problem which is solved by genetic algorithm. Although the accuracy of numerical results can be ensured by the input and the iteration of temperature and damage parameters, a large number of temperature measured points are required to collect the enough information for precisely simulating the temperature field. Huang et al. (2018) proposed a similar model-based method using genetic algorithm. The objective function is based on the weighted frequency and mode shape changes and this method shows good robustness. Wang et al. (2020) proposed a model-based damage detection method based on particle swarm optimization (PSO) using autoregressive with exogenous input model (ARX) or linear regression (LR) to correlate the temperature and frequency. It is tested using one year monitored data of a reinforced concrete slab with the temperature range from 0 to 5 Celsius. It proves the temperature change will induce large changes of the natural frequency. Therefore, for model-based method, the key issue is laborious, time-consuming for the process of collecting enough data to reduce the effect of measurement noise and a high requirement of the operator's knowledge and experience for ensuring the accuracy of the established model.

2.2.2.2 Data-driven methods

For data-driven methods based on static responses, the temperature-driven approach has drawn some attention recently. Kromanis and Kripakaran (2016) proposed a two-stage data-driven temperature-based measurement interpretation (TB-MI) method for online monitoring. This method has been verified using a scaled truss bridge model. The regression based thermal response prediction (RBTRP) is used firstly to generate a statistical model by the statistical or machine learning algorithms and then the signal subtraction method (SSM) is used for anomaly detection from prediction errors obtained from RBTRP. Since it does not rely on the physical model, the regression model can be easily transferred to other type of structures. Wang and Ni (2020) proposed a Bayesian dynamic linear model (BDLM) to forecast structure's strain responses using Gibbs sampling to calculate hidden parameters. The approach is aimed at eliminating temperature's effect, and it can forecast strain responses of a bridge under seasonal temperature fluctuation that provides a foundation for a real-time structural damage detection.

For data-driven methods using dynamic responses, a large category of studies uses modal parameters as damage features. Kim et al. (2007) proposed a frequency-based damage detection method using a control chart for early warning of damage occurrence under temperature's impact of modal parameters. As the damage sensitive feature, nature frequencies extracted from measured accelerations are used for damage localization and extent evaluation based on analysis of modal strain energy (a model-based method), and the temperature's effect is eliminated by the empirical equation obtained at 20 degrees Celsius based on linear regression. Since the accuracy of the empirical equation will reduce when the gap of the temperature between reference and actual value raises, this method is inconvenient for practical application. Gu et al. (2017) proposed an unsupervised damage detection method using multiple ANNs to eliminate the temperature's effect. Natural frequencies are processed by multiple

ANNs, and the state of the structure is identified by using Euclidean distance as a novelty index. This method has been verified on the FEM and laboratory experiment with good performances. Sarmadi and Karamodin (2020) proposed an adaptive Mahalanobis-squared distance (AMSD) based unsupervised damage detection method using natural frequencies as input. K-nearest neighbor (kNN) method is used for clustering similar state's vectors into the same group based on AMSD, and the generalized extreme value distribution (GEV) constructed by the block maxima (BM) method is used to decide the threshold. It performs well on two real bridge datasets with a high requirement of training samples due to its strong theoretical hypotheses.

For other data-driven methods, Erazo et al. (2019) proposed a residual-based damage detection method using spectrum analysis to extract damage features which are peak indicators of the spectral density measured from velocity responses. It has been verified using a continuous beam bridge model with the uniform and non-uniform temperature fields and Kalman filter is used to filter temperature effect. Kostić and Gül (2017) proposed a residual-based damage detection method using ARX to extract damage features which are the fit ratio of ARX measured from acceleration measurements. It has been verified using a footbridge model under different temperature conditions and a back-propagation artificial neural networks is used to eliminate temperature's effect. Zhang et al. (2019) proposed an adapted method based on auto-associative neural networks (AANNs). Both of these two methods are verified with 5% noise measurements. As above, the data-driven method under varying temperature conditions shows great potential for practical application with high robustness and low operation difficulty. These methods are mainly for anomaly detection, and they cannot provide the accurate estimation of damage severity as the model-based method does. So the further study on actual structure under complex conditions is needed. However, since these methods concentrate more on the features of

uncertain operational environments, they need to take all of possible operational environments in which the bridge is in normal operation into account. The biggest obstacle to the effect of these methods comes from the unpredictability of the future since it is impossible to traverse all possible interference factors in bridge health monitoring. The performance of the regression models or neural networks on a bridge that has been affected by unconsidered factors cannot be ensured.

2.3 Model based bridge structural condition assessment methods

The model-based method extracts the information from structure's responses to rebuild the physical-model which is simplified by some theoretic hypothesis and focuses on interested parameters or features. This model is updated by continuous monitored data input aimed at matching actual situation and finally we can obtain target information from the updated model. By contrast, the data-driven method processes structure's response directly based on statistical learning methods. A noteworthy point is that the statistical learning model should be distinguished from the physical model. The difference between them is that the physical model is used to simulate real conditions, while the other is constructed in the data space (mathematical space), mainly a series of mathematical algorithms designed to extract interested features from the complex and assorted information (Li 2019). As discussed above, these models propose a high demand of operator's experience and knowledge, and it is time-consuming and laborious to adjust these models to fit the real structure.

Although many statistical methods are introduced, the uncertainty in real case is far beyond than we can take into consideration in advance based on a theoretic hypothesis. The performance of model-based methods in real scenarios under the complex environment situation need to be further tested.

A large category of model-based methods uses modal parameters as damage features. Miguel et al. (2012) proposed a model-based damage detection method using time domain stochastic subspace identification (SSI) technique with evolutionary harmony search algorithm (HS) to identify, locate and quantity severity of damage. The natural frequencies obtained by SSI from measured acceleration are used as damage sensitive feature for model updating using HS algorithm. This method has been verified using the experimental and numerical study under 5% noise. Since the damage severity is set more than 20%, it may not be suitable for early warning which usually aims at detecting slight damage. Cao et al. (2021) proposed a model-based damage detection and quantification method specialized for the bridge structure with a parked vehicle on it. Frequency change rate (FCR) obtained from the measured acceleration is used to construct structure's baseline as a damage sensitive feature. This method has been verified on numerical and experimental study in which 5% stiffness deviation is detected under 7% measurement noise with the standard normal distribution of elastic modulus' modeling error. It needs further verification on real parked vehicle-bridge system. Meixedo et al. (2021) proposed a traditional model-based monitoring system using environment vibration. Static responses induced by the temperature variation and dynamic responses by traffic loading are used to calibrate a nonlinear FEM of a real railway bridge under operational environments. Aided with visual inspection, the hourly measured data from different types of sensors in five years are used to update the FEM. This FEM shows a good performance of estimating modal parameters and static responses but requires further study of different damage scenarios in bridge's different components. The modal parameters are sensitive to moisture, temperature, and measurement noise and they are not robust enough and often make false alarm (Moughty and Casas 2016;Avci et al. 2021). Therefore, current model-based

method using modal parameters is always combined with other methods or under controlled situation to eliminate the disturbance from these factors.

For other model-based methods, since the accuracy of the model will be affected by uncertainty of the material, boundary conditions and simplification theoretical hypotheses (Law and Zhu 2009), many mathematical methods are introduced. Pai et al. (2019) introduced error-domain model falsification (EDMF) and the modified Bayesian model updating (mBMU) to obtain structure's parameters under numerous uncertainties. This method has been verified on a real bridge with a good performance. The EDMF does not require a complete restart between iterations of identification and could define target reliability levels at the beginning. Thus, it is more compatible for practical application with low computational cost and robust to deal with biased and correlated error sources since it sacrifices precision. Zhang et al. (2021) proposed a model-based stress monitoring system using partial least-squares regression (PLSR). It has been verified on numerical and experimental steel bridge. The boundary condition is estimated from the fusion of measured strains, rotations and displacements, and the stress distribution is calculated when the location of vehicle loads is known. This method is suitable for small and medium bridges since nonlinear effects are not considered. Guidio and Jeong (2021) proposed a real-time identifying method using finite element method to back-calculate elastic modulus's variation. Genetic Algorithm (GA) is used as the inversion solver and its anti-noise ability will reduce when the number of controlled parameters increases. For practical application, this method needs to be extended to three dimensions since it is based on one dimension beam model currently. As mentioned above, the model-based methods are more concentrating on the accuracy than robustness since they can quantify the severity of damage. Due to the high cost of achieving both goals simultaneously,

these methods need to create a criterion to control the balance of accuracy and robustness in practical use.

2.4 Data driven based bridge condition assessment methods

2.4.1 Online learning methods

Among data-driven methods, a large category of studies that concentrate on the online learning. They are usually semi-supervised methods with two stages: the offline learning for training and the online learning for monitoring. The training stage uses representative data to form identification methods (most of them are classification or cluster approaches) and the monitoring stage is for the identification. The online learning methods aim at establishing a monitoring system which can self-update automatically while encountering a new and unknown condition. It is unrealistic to obtain the data covering all structures' conditions and not easy to acquire the enough data from real structures for training. Thus, a big challenge for the online learning methods is that they should be robust and accurate enough for unknown conditions. This difficulty puts a higher request for monitoring algorithms. Entezami et al. (2019) proposed a new autoregressive modeling (AR)-based classification approach using partition-based Kullback-Leibler (KL) divergence for measuring statistical distance. The residuals of AR coefficients are obtained as damage sensitive features by AR model's time-series auto-regress and classified into damaged or undamaged clusters for condition assessment based on KL divergence. The bridge experiment is on a scaled model with indoor environment condition and the online stage is absolutely executed by the program itself after limited data training. Therefore, the performance of this method under unscheduled conditions on real bridges needs to be further studied since some non-ignorable false alarms still appear in this study. Rogers et al. (2019) proposed a modified Dirichlet process (DP)-finite Gaussian mixture models (GMM) based Bayesian

non-parametric clustering method. It is an ease of use online method with the simple feedback since a single user-tunable hyperparameter is set after little information input. It has been verified on the Z24 bridge dataset. An essential issue is that at the beginning stage, this method needs more interventions that require experts to match algorithm with structure's behaviour under different environment situations. Santos et al. (2016) proposed an online unsupervised early warning method for cable-stayed bridge. The feed-forward multi-layer perception (MLP) neural networks are used to model the structure's response and calculate the residual errors for one step ahead estimation, and the advanced k-means clustering-based statistical method is for creating damage index. Two methods are used to achieve automatic monitoring without operator's intervention. The Gowda-Diday dissimilarity is used to measure distance for clustering, and the global silhouette index (SIL) is used to automatically select the cluster's number to construct the average dissimilarity value, which is defined as t-student distribution to form damage index. Since this method is specialized for damage in stay cables and they cannot detect the damage occurred far away from the sensors, it may not be suitable for other types' bridge. Silva et al. (2017) proposed an unsupervised and non-parametric online monitoring clustering method using agglomerative concentric hypersphere (ACH) algorithm. This method is compared with Mahalanobis Squared Distance (MSD) and GMM method. It has been verified on the Z24 bridge dataset and shows a promising future for practical application since it does not require any input after the training data matrix has been constructed as baseline. Since the initialization of each iteration will affect clustering's results, it needs further verification under more complex scenarios.

Another type of online learning methods uses modal analysis. Since traditional modal analysis requires modal testing that cannot be performed when the bridge is in operation, a technique called the operational modal analysis (OMA) is

developed. The modal parameters, which are sensitive to the occurrence of damage, can be extracted by OMA continuously and in real time when the bridge is in running. Cheema et al. (2021) proposed an automatic operational modal analysis (OMA) method to identify the natural physical modes out of the mathematically spurious modes. It has been verified on an actual cable-stayed bridge with higher accuracy than other DP-GMM based OMA method. The stabilization diagram contained with many artificial modes are obtained by covariance driven stochastic subspace identification (SSI-Cov) method, and then real physical modes with uncertainty bounds are calculated by a two consecutive DP-GMM approach (cluster and identify). Since the traffic load excitation and damage are not considered in this study, this method needs further tests under complex situations. Favarelli and Giorgetti (2021) proposed a similar OMA based online damage detection method. The stabilization diagram calculated by SSI from acceleration signals is used to obtain natural frequencies of real modes based on four-mode selection criteria. The natural frequencies are selected as damage features by k-means clustering algorithm and frequencies density-based time-domain tracking method. One-class classifier neural network (OCCNN) is used for anomaly detection on damage features. This method has been verified on the Z24 bridge dataset with a satisfactory performance compared to other traditional methods like ANN, GMM, KPCA and ANN. It needs a further test on other real bridges under complex situations to confirm its practicality. Santos et al. (2020) proposed an advanced data-driven OMA method using SSI-Cov method and k-medoids algorithm. It has been verified on an actual suspension bridge under complex environmental conditions. The natural frequencies are obtained by modified SSI-Cov method using Moore-Penrose pseudo-inverse with moving frequency windows. Modal assurance criterion (MAC) based dissimilarity measurement of natural frequencies are used in k-medoids clustering for modal parameters' identification. The SIL

index is used to judge the clustering's performance and bilinear regression method is used to decide initial cluster's number. Except OMA, de Almeida Cardoso et al. (2019) proposed an unsupervised symbolic data objects (SDOs) based real-time damage detection method called time-frequency interquartile range median object (TF-IQRM). Two triple vectors contained with quartiles in frequency domain are extracted as SDOs by fast Fourier transform (FFT) from acceleration signals. The quartiles in time domain calculated from statistical distribution of acceleration's amplitude values, are used to create dissimilarity matrix. The damage index is constructed by the dissimilarity matrix based on k-medoids algorithm and a statistical threshold called confidence boundaries. Since the structural reinforcement is detected simultaneously when the signal is truncated in this study, the operational and environmental factors' impact of this method needs further verification. The modal parameters can be easily affected by the uncertain operational environments (e.g., traffic, temperature or wind). Currently OMA is more deployed on the large and complex bridges to study the impact of these uncertain factors. The statistical analysis-based technique is widely used to make the decision for the damage detection after the modal parameters are identified.

These online learning methods usually state that they have considered the operational environmental impact. However, their primary target is to establish an automatic long-term SHM system which can hardly be achieved by the traditional way. The influence of operational environmental impact is a considerable obstacle for these emerging methods to achieve automatic process without human's interference. Thus, although these methods show their robustness by highlighting these factors, their topic is concentrating more on automation since most of their experiments do not consider the conditions that environmental factors take the principal place. These methods are essentially black box models. Instead of the robustness, the accuracy of these methods

should be further verified on more examples that have been deeply studied for evaluating the performance of these online methods to avoid false alarm. Currently, the Z24 bridge dataset is famous and has been extensively used among online monitoring methods. These methods should be verified on other actual bridges' dataset with different bridge types and damage scenarios to avoid overfitting.

2.4.2 Offline monitoring methods

The online monitoring methods which can incorporate the unknown operational environmental impact into the corresponding structure's state (i.e., damaged or undamaged) by the method itself at the monitoring stage without the requirement of the labeled (damaged) data input. Other data-driven methods use some algorithms to eliminate the operational environmental factors' effect by learning the labeled input data. These data are usually generated from the FEM simulation since the damaged data of an actual bridge are not easy to obtain.

Some offline data-driven methods use modal analysis called the parametric approach. Zhou et al. (2014) proposed a modal frequency-based damage localization method specialized for long-span bridges using a probabilistic neural network (PNN). The modal frequency change ratios generated from two bridges' FEM with measurement noise, are used for training and testing in PNN. This frequency-only method shows 90% accuracy rate of damage identification and localization in two numerical studies when the noise level is within 10%. Niu et al. (2021) proposed a practical method to identify modal parameters of a real bridge using Chebyshev filter-complementary ensemble empirical mode decomposition (CF-CEEMD) with data-driven SSI (DD-SSI) method and real-time kinematic of a global navigation satellite system (GNSS-RTK). Since measured dynamic displacements by GNSS-RTK will include background noise, the CF-CEEMD is used to reduce noise. The FFT with DD-SSI are used to

obtain the natural frequency and other modal parameters. The DD-SSI is a combination of several data-driven algorithms with SSI. This real-time method has been verified on a numerical study with a good performance and it is practical since the displacements of a real long-span bridge can be directly obtained. Zhou et al. (2018) proposed a modal parameter identification method using DD-SSI and exploratory data analysis (EDA) with morphological filter (MF). The EDA is used to inspect wrong data generated by sensor fault, and the MF with an automatic structural element size determination process is deployed to filter the white noise. The DD-SSI is used to extract modal parameters. This method has been verified on a numerical study and a real long-span cable-stayed bridge's study with good performances. Gul and Catbas (2008) proposed a modal analysis-based damage detection approach using complex mode indicator functions (CMIFs) with the random decrement method (RD). The measured deflection from ambient vibration is used to calculate unscaled FRFs by FFT. The RD is used to solve leakage problem, high computational cost and random loading's effect. The CMIFs are used to obtain modal parameters from the unscaled FRFs. This method has been verified on an actual suspension bridge and successfully obtains the first 20 modes. Currently the data-driven modal-based damage detection methods are more concentrating on how to precisely extract bridges' modal parameters under the influencing factors such as sensor fault and noise among data collection since they have a solid theoretical basis. Most of them are studied on the result of the finite-element model simulation. These methods need to be implemented on real bridges.

Other data-driven methods usually consist of the combined machine learning or optimization algorithm. Zhu and Hao (2007) proposed a data-driven damage detection approach using wavelet support vector machine (WSVM). The energy of wavelet packet components is calculated from measured accelerations as feature vectors. The feature vectors are used in tightening SVM for training and

identifying. This method has been verified on a FE beam under a low noise level and can precisely predict location and severity of damage. Entezami et al. (2020) proposed a statistical damage detection method using ARMA with partition-based Kullback-Leibler divergence-nearest neighbour method (PKLD-NN). The ARMA coefficients are calculated from measured accelerations as damage features for damage detection by PKLD-NN. This method is compared with the classical Euclidean-squared distance-NN (ESD-NN) and MSD method on a real cable-stayed bridge's study. The result shows PKLD-NN is more sensitive and accurate to damage than ESD-NN and MSD. The coefficient-based feature extraction in ARMA modelling requires much less computational cost than residual-based feature extraction in ARMA modelling. Pan et al. (2018) proposed a data-driven damage detection method using SVM with three fast feature extraction method for comparison: wavelet transform (WT), Hilbert-Huang transform (HHT) and Teager-Huang transform (THT). It has been verified on a cable-stayed bridge's FEM. The result shows the WT has a better anti-noise ability, and the THT with HHT run ten times faster than WT. Since this method has been verified on the FEM with ideal performance, it needs to be implemented on real bridges for practical application. Carden and Brownjohn (2008) proposed a time-series damage detection method using ARMA modelling technique. The ARMA parameters obtained from measured responses are used as damage features to classify the bridge's state based on the sum of residuals' square. This method has been verified on the Z24 bridge and a real bridge with good performances. They concentrate more on extracting the features of damage rather than the influence on the features induced by the operational environment. The performance of them under different uncertain operational environments is related to how many these different uncertain operational environments are included in the labeled input data. The results obtained from them are only meaningful (interpretable) if the environmental

conditions of actual bridges are close to the scenarios included in the training data. So in terms of the interpretability, these methods require a more in-depth study. Although these offline methods cannot run as robust as the online methods, they are suitable for bridges that are suspiciously under damage. These operational methods are specially designed for certain kinds of structures with an accurate damage localization and estimation ability.

2.5 Bridge structural damage assessment using principal component analysis

As one of the most widely used methods, principal component analysis (PCA) was first developed by Pearson and then extended by Hotelling (1933). Among SHM, the traditional PCA was mainly used in data dimension reduction and feature extraction. As an unsupervised machine learning algorithm, PCA is mostly used in the data-driven damage detection approach. Thus, this section will concentrate on PCA's role in the data-driven structural damage detection since the model-based approach normally uses PCA only for data dimension reduction.

2.5.1 Data driven bridge damage detection under operational environment

For moving loads driven methods, Mei et al. (2019) proposed an indirect damage detection approach using Mel-frequency cepstral coefficients (MFCCs) and PCA. PCA is used to construct the baseline and extend this method to a multi-vehicle version since the MFCCs is based on a single passing vehicle. Yu and Zhu (2011) proposed a PCA based moving force identification (MFI) approach. The results show that PCA is effective for MFI and the effect of two computation patterns with the PCs' number for PCA is discussed. Eshkevari et al. (2020) proposed an indirect approach using the vehicular sensor network for bridge modal identification with matrix completion (MIMC) method. PCA is

used to extract the modal properties from the completed response matrix by factorizing it into orthogonal mode shapes.

Among the temperature-driven approach, PCA was widely applied for temperature-induced response separation procedure (Han et al. 2021). Deraemaeker et al. (2008) proposed a spectrum analysis-based damage detection approach for a scaled cable-stayed bridge using SSI, Shewhart-T control charts and PCA. PCA is used to model and eliminate the temperature effect using a residual-based least-square approach. A statistical-based threshold for PCA is also proposed to enhance the performance (Deraemaeker and Worden 2018). Li et al. (2020) proposed a PCA-based estimation approach to reconstruct the missing temperature data using statistical analysis and the expectation-maximization (EM) algorithm on an actual cable-stayed bridge. PCA is used to calculate the correlation of the time-series SHM dataset for estimation. Sen et al. (2019) proposed a modal analysis-based damage detection method for the Z24 bridge. PCA is used to remove the temperature effect in modal frequencies for structural damage detection.

Some PCA based approaches consider temperature's effect with moving loads excitation. Kumar et al. (2019) use PCA for feature vector extraction to construct a model space method for damage localization and detection under different temperatures and moving loads. PCA is used to extract feature vectors for constructing damage index, and the temperature effect is treated as the fluctuation on the modulus of elasticity and coefficient of thermal expansion of the steel material. Guo et al. (2018) proposed a train recognition approach using symbolic data analysis (SDA) and clustering methods on an actual bridge in which two temperature sensors are installed to record temperature data. As the critical step, PCA is used to reduce noise's effect and extract essential characteristics of the signals with good performances. Sakiyama et al. (2021)

proposed a real-time abnormal detection approach for the actual large-scale bridges using a large number of the long-gauge fibre Bragg grating sensors (LGFBG). PCA is used to calculate the sensors' correlation and determine its contribution to specific structure's behaviour from hundreds of gigabytes of data with satisfactory results. Kromanis and Kripakaran (2017) proposed a detection approach using the RBTRP with traffic-induced responses to assess structural performance and it cointegrated with the signal subtraction method (SSM) for anomaly detection. The temperature distribution measured from a thermal imaging camera with thermocouples and the traffic loads with its location measured by contact sensors are used as input to predict the bridge's traffic and thermal response. PCA is used in RBTRP to reduce the temperature data's dimension and transform the temperature data into principal components as input of the regression model. Shokrani et al. (2018) proposed a mode shape curvature-based damage detection, localisation and quantification approach on a bridge model under varying temperature conditions. PCA is used to capture the feature from temperature fluctuation and noise on the bridge for creating the baseline of damage index.

2.5.2 Data driven bridge damage detection assessment

For data-driven damage detection methods, Roveri et al. (2019) use PCA to extract damage features from strain responses of a truss bridge for clustering and detecting damage. Dackermann et al. (2010) proposed a modal strain energy (MSE) based damage detection, localization and quantification approach using ANNs ensembles. PCA is used to eliminate the noise in MSE based damage index for training ANNs ensembles. Nguyen et al. (2015) proposed an FRFs based damage detection and quantification approach on a replica of an actual bridge using ANNs ensembles. PCA is used to reduce residual FRFs' size as the damage sensitive feature for training ANNs ensembles.

Jayasundara et al. (2020) proposed an FRFs based damage location and quantification approach on a simulated deck-type arch bridge using ANNs ensembles. PCA is used to reduce the size of residual FRFs and remove the noise for training ANNs ensembles. In general, PCA is an intermediate step that concentrates on improving the data quality in most PCA-based bridge SHM studies. The effectiveness of PCA among the removing environmental effects (e.g., temperature effect and noise), data size reduction and feature extraction have been sufficiently proved.

2.6 Bridge structural damage assessment using moving principal component analysis

As for traditional PCA, the computational cost of the covariance matrix will significantly increase according to the number of measurements and the length of the time series. Additionally, the weight of the new data in the covariance matrix will be reduced with the increasing number of measurements which will dilute everything (Lanata et al. 2007). Thus, Posenato et al. (2008) proposed moving principal component analysis (MPCA) for long-term structural monitoring. This algorithm calculates the covariance matrix in a fixed size window and the data outside of the window's range could not affect results. This improved algorithm is competent to reduce the computational cost in long-term monitoring. Lanata et al. (2007) deployed MPCA on a real highway bridge for damage detection. MPCA is used to capture the correlation in each small cluster obtained by the K-means method overlapping for the damage detection. Cavadas et al. (2013) compared the performance of damage detection and location between MPCA with robust regression analysis (RRA) on a quasi-bridge rigid frame's quasi-static only response. Compared to RRA, MPCA can locate the damage and detect the early damage. Zhu et al. (2019) proposed a temperature-driven damage detection approach using the independent

component analysis (ICA) on the numerical and experimental study under temperature fluctuations and traffic loads. MPCA successfully detected damage from the temperature-induced response separated by ICA from environmental factors in a two-year data record. Jin et al. (2015) compared results of the modal analysis-based damage detection performance under varying temperature conditions using PCA or MPCA. The numerical study of a Bernoulli-Euler beam shows that MPCA has lower false alarm rates with more vital anti-noise ability than PCA. Zhang et al. (2019) deployed MPCA on a rigid frame bridge under seasonal temperature fluctuations for damage detection with time and space windows. The one-year-length time window of MPCA is for the damage detection, and the grouped space window is to locate the damage by incorporating the damage sensitive sensors, which are defined by the residuals of the sensor's response between the damaged and healthy states. Jin and Jung (2018) compared modified MPCA with the static linear principal component analysis (SPCA) and incremental linear principal component analysis (IPCA) for Z24 bridge using the k-means clustering with Linde-Buzo-Gray algorithm (KMC-LBG) and Bayesian information criterion (BIC) to judge the window size of MPCA. The proposed three PCA-based approaches are for damage features extraction from natural frequencies, and only MPCA successfully achieves early detection of two nonlinear damage cases with more than 100 hour's window size. These MPCA methods have a relatively large window size. Since it is not suitable for the real-time monitoring, Nie et al. (2020) developed a narrow moving window for MPCA and successfully detected an abnormal behaviour of an actual suspension bridge. The window's size is calculated based on the cumulative contribution ratio with a convergent spectrum. Compared with PCA, MPCA is mainly used for damage detection with a better performance under complex environmental conditions since the suitable window size can enlarge the inconspicuous fluctuation in the measured data. It

has a promising future for early warning and slight damage detection since it can reveal the data's inherent correlation and structure in more detail. Currently, it performs well on early damage detection under temperature variations.

However, how to judge the most appropriate window size has been studied a little and requires a further discussion since the size of the moving window will greatly affect the effectiveness of the MPCA-based method with varying computational cost. From the perspective of frequency domain, the longer the length of the window, the lower the frequency of the signal is concerned. The window length of current studies is usually determined based on the fundamental frequency of bridges or the period of temperature fluctuations. This causes a longer window length (e.g., for months or years) is chosen for MPCA in current studies. The longer the window, the higher the computational cost. Additionally, a series of window selection criteria, such as the fundamental frequency of bridges and the temperature fluctuation period, will change with uncertain operational environments. Thus, the challenge of this idea is how to adjust the window length flexibly and accurately according to the changing environmental conditions and the influencing factors to be analysed. For the real-time monitoring, A narrow window size (e.g., within a day) seems better for the real-time detection, but the small amount of data may not provide the sufficient information for the highly accurate detection. Also, this will lead to a greatly increase of the impact from the uncertain operational environments on the measured data. Since MPCA is a linear method, it may not be enough to deal with the nonlinear behaviour of the bridge (Jin and Jung 2018). In different studies, the form of external loads and damage is usually inconsistent. This inconsistency prevents the comparison of the results obtained by MPCA in different studies.

2.7 Summary

- Moving loads driven methods

The moving load driven bridge damage detection has drawn much attention since the moving load excited part can take the dominant place in the bridge response compared with other environmental factors in normal condition. The moving load induced part can be easily extracted from the bridge response since it has an obvious and interpretable pattern.

Since the traditional moving loads driven methods are based on vehicle-bridge interaction theory, they can detect, locate and quantify the severity of damage accurately with good interpretability but work in a controlled environment which is time-consuming and laborious due to their limited anti-noise ability.

The data-driven methods concentrate on constructing damage sensitive features from data space rather than physical space. Aided by algorithms, they provide a convenient and economical way for moving loads driven damage detection compared with the traditional methods. As the novelty approach, they are underdeveloped with a promising future since they can achieve the real-time damage detection under complex environmental conditions.

- Temperature driven methods

The study of temperature's effect has attracted significant interest and can be categorised into several research branches since the temperature factor is not negligible among bridge SHM.

For model-based methods, they aim to construct a FEM that can represent the actual bridge as close as possible for damage detection and behaviour prediction. Currently these methods can precisely forecast real bridge's behaviour even under complex environmental conditions. However, the critical issue is that the model updating procedure is time-consuming and laborious, with a high demand

for operator's experience and has limited transferability. Some optimization algorithms or machine learning methods are combined into model-based methods to eliminate the effect of uncertainties.

For data-driven methods, a branch of study concentrates on static responses for bridge's behaviour prediction based on regression approaches. They can predict bridge's static responses in a relatively long period (e.g., several months) with enough accuracy. The others are dynamic responses-based anomaly detection approaches that show great practical application potentials like easy operation and robustness on the service stage. As recently developed methods, they require further verification on the actual structure under complex conditions. However, they cannot quantify the severity of damage compared with the model-based method. Since they focus more on the effects of uncertain operational environments, they try to consider every possible operational environment under the normal operation of the bridge. The main challenge to these methods is from the unpredictability of the future as it can hardly take every possible interference factor into account in bridge health monitoring. The performance of the neural networks or regression models on a bridge that has been influenced by not considered factors cannot be guaranteed.

- Model-based damage detection methods

The model-based methods can identify, locate and quantify damage. As previously mentioned, current model-based methods are always combined with other algorithms or under conditioned circumstances to eliminate the disturbance of uncertainties. They are more concentrated on accuracy than robustness since they can quantify damage's severity. Due to the high cost of achieving both goals simultaneously, these methods need to create a standard to control the balance of accuracy and robustness in practical use.

The model-based methods using modal analysis have many practical applications currently. Since the modal parameters are sensitive to moisture, temperature, and measurement noise instead of damage, they can be easily affected by environmental conditions and often make false alarm. Thus, they are always combined with several algorithms to enhance their performance. Also, this is why a large branch concentrating on modal analysis is derived from the model-based approach to the data-driven approach under the temperature-driven damage detection field.

As discussed above, the model-based method proposes a high requirement of operator's knowledge and experience. It is laborious and time-consuming to adjust these models to fit actual structure.

- Data-driven damage detection methods

As the ultimate aim, the online learning methods are dedicated to replacing human beings as the automatic long-term monitoring method. To achieve this goal, the effect of the environment and operation impacts is a considerable obstacle for these emerging methods. Currently they can correctly categorise the state of the bridge (i.e., damaged or undamaged) based on its behaviour in experimental conditions. Their accuracy requires further verification on more instances that have been deeply studied for improving their performance by reducing false alarm rather than enhancing robustness. Currently, the Z24 bridge dataset has been widely used among them. They should be tested on other actual bridges' dataset with different bridge types and damage scenarios to avoid overfitting.

The modal analysis has drawn great attention in the online learning. Since the modal testing which is used to extract bridge's modal parameters in traditional modal analysis cannot be deployed when bridge is in running, a method called

the operational modal analysis (OMA) is constructed. The modal parameters, which can sensitively reveal the existence of damage, can be continuously identified by OMA in real time when bridge is in operation. But the uncertain operational environments (e.g., traffic, temperature or wind) can also directly influence them. Currently OMA is mainly deployed on complex and large bridges to study the effect of these uncertain factors. After identifying modal parameters, the statistical analysis-based method is extensively adopted to make decision for damage detection. The modal-based methods focus more on practical use since they have a solid theoretical foundation. They need to be implemented on real bridges.

As for the offline methods, they may not act as robust as the online methods. They focus more on extracting damage's feature instead of the operational environment induced effects in obtained features. Their performance on the dataset under different uncertain operational environments is based on how many these uncertain operational environments are pre-considered in the labeled input data. The interpretability of the obtained results from them are ensured only if the environmental circumstances of real bridges are pre-considered in the training data. From the perspective of interpretability, they need more in-depth study. They are appropriate for bridge damage detection. They are specially designed for the particular type of bridges with a precise damage localization and quantification ability.

Some modal analysis based offline methods are called the parametric approach. They focus on how to accurately extract modal parameters of bridges under the interference factors like noise or sensor fault since they have a strong theoretical background. Most of these studies use the finite-element model simulation. They need to be more deployed on real bridges.

- PCA-based damage detection methods

PCA is an intermediate step used for data size decrease, feature extraction and eliminating environmental effects with noise reduction. As a convenient tool, it shows a fascinating performance in improving the data's quality.

MPCA is mainly deployed for damage detection and performs better compared to PCA under complex environmental conditions. Since it can extract the inherent structure and correlation of data in more detail, it shows great potential for slight damage detection and early warning. Currently, it shows good performances on early damage detection under temperature variations. However, the most appropriate window size is still under discussion, and it will directly influence the availability of the MPCA-based approach with different computational cost. A narrow window size may be more suitable to achieve the real-time detection, but the insufficient data cannot provide the enough information to ensure detection's accuracy. This also will result in a significant increase of the uncertain operational environments induced impact on the detection result. Since MPCA is based on linear theory, it may not be competent to cope with the bridge's nonlinear behaviour. The load forms and the causes of bridge anomalies (e.g., damage) are often inconsistent in different studies. This inconsistency causes the results of MPCA are not interpretable and without a specific pattern for the comparison between the studies.

- Solutions to address the research gaps

To address the research gaps, there are two promising perspectives worth investigating: the *real-time* and the *monitoring.* The real-time requires the bridge condition assessment model to evaluate the bridge state in a timely manner. The monitoring requires that the model can reflect the information of the bridge more comprehensively. Not only the overall health condition, the detailed information of the operational environment in which the bridge operates is needed for providing a more reliable evaluation of the bridge. The

existing monitoring methods require a lot of preparations, so it is difficult to accurately assess the bridge state in real-time when encountering unknown situations. For the temperature-driven cases, a longer time observation dimension (e.g., the MPCA window length in months or years) can more easily and clearly reflect the more stable change pattern of the bridge state under the temperature impact. But this cannot meet the requirement of the real-time. Most of the methods concentrate on the general distinction between the damaged and undamaged states of the bridge. The real-time assessments can be more reliable if the model can provide more relevant information about the bridge beyond its damage state. In general, breakthroughs in these two perspectives can significantly improve the practicability of the existing methods and make the existing methods have grater application value.

Chapter 3 Numerical study

This chapter presents the moving principal component analysis (MPCA) approach for structural condition assessment of bridges under moving vehicle considering the temperature environment using the numerical study. To understand the effect of operational environments such as moving vehicles and the temperature environment, the basic mathematical theory is briefly introduced and then the proposed method is verified using the numerical simulation. The arrangement of this chapter as the following: the theory PCA and MPCA is introduced firstly and the main target for current existed data processing algorithm is discussed. The second part is to construct the bridge finite element model. The details of the simulation of a bridge subjected to a moving vehicle, the temperature influence and the crack damage model are presented. The third part is the results. The simulation result of the numerical model is presented, and the results analysed by PCA and MPCA are compared. The parametric study is conducted including the effect of individual parameter variations from the bridge finite element model and interactions among these parameters' variations. The fourth part, the damage sensitive feature is constructed based on the analysis above in this chapter. The influence of the crack's location with the mechanism behind the variations on this constructed damage sensitive feature is interpreted in the discussion part.

3.1 Introduction of the detection method: PCA and MPCA

Principal component analysis (PCA) and moving principal component analysis (MPCA) are briefly introduced in this section. The detail information could be found the textbook (Li, 2019).

3.1.1 Principal component analysis (PCA)

As the foundation of MPCA, PCA is a statistical learning method that decomposes the original data into linearly uncorrelated vectors-principal components (PCs) according to the maximum variance's direction. At the same time, the new coordinate axis's direction should be orthogonal to all previous coordinate axis's directions. This transformation ensures that the selection of the coordinate axis's direction can make each PC contain as much information as possible. It is widely used in data compression and feature extraction.

In this study, the singular value decomposition (SVD) method is adopted for PCA. Considering a data (signal) matrix $\mathbf{X}_{m\times n}$ with the k-order PCs, suppose the matrix's rank is r that is greater than or equal to k. The $\mathbf{X}_{m\times n}$ can be factorized according to truncated SVD as

$$\mathbf{X}_{m\times n} \approx \mathbf{U}_k \mathbf{\Sigma}_k \mathbf{V}_k^T \tag{3-1}$$

where $\mathbf{U}_k$ is $m \times k$ matrix, $\mathbf{V}_k$ is $n \times k$ matrix and $\mathbf{\Sigma}_k$ is diagonal matrix of the order k. $\mathbf{U}_k$, $\mathbf{V}_k$ are respectively taken from the first k columns of matrices $\mathbf{U}$, $\mathbf{V}$ that are singular vectors of the matrix $\mathbf{X}_{m\times n}$. $\mathbf{\Sigma}_k$ is obtained from the first k diagonal elements of matrix $\mathbf{\Sigma}$ which is the singular value matrix of the matrix $\mathbf{X}_{m\times n}$.

Before using PCA, the data in the matrix $\mathbf{X}_{m\times n}$ needs to be standardized to obtain the matrix $\mathbf{X}'$ according to Eq. (3-2).

$$x_{ij}^* = \frac{x_{ij}-\overline{x_i}}{\sqrt{s_{ii}}} \tag{3-2}$$

where $\overline{x_i} = \frac{1}{n}\sum_{j=1}^{n} x_{ij}$, $i = 1,2,\ldots,m$ and $s_{ii} = \frac{1}{n-1}\sum_{j=1}^{n}(x_{ij} - \overline{x_i})^2$, $i = 1,2,\ldots,m$. x_{ij} is the $\mathbf{X}_{m\times n}$'s element at row i and column j. x_{ij}^* is the standardized matrix $\mathbf{X}'$'s element at row i and column j. $\overline{x_i}$ is the average value in row i of the matrix $\mathbf{X}'$.

After obtaining the standardized data matrix $\mathbf{X}'$, the traditional PCA uses the eigenvalue decomposition of the $\mathbf{X}'$'s correlation matrix or covariance matrix to calculate the principal component matrix. According to characteristic of SVD, the principal component matrix can be obtained

$$\mathbf{X}'' = \frac{1}{\sqrt{n-1}}\mathbf{X}'^{T} \tag{3-3}$$

$$\mathbf{X}'' = \mathbf{U}\mathbf{\Sigma}\mathbf{V}^{T} \tag{3-4}$$

$$\mathbf{Y}_{k\times n} = \mathbf{V}^{T}\mathbf{X}' \tag{3-5}$$

where $\mathbf{X}''$ is constructed for the truncated SVD. The row of $\mathbf{V}^{T}$ is the eigenvector of the $\mathbf{X}'$'s covariance matrix. $\mathbf{Y}_{k\times n}$ is the principal component matrix and it is also called the score matrix. $\mathbf{V}^{T}$ is called the weight or coefficient matrix.

3.1.2 Moving principal component analysis (MPCA)

PCA extracts the feature of data on entire signals. This ignores subtle trends implied by the observed data on the time axis. MPCA is a method that deploys PCA on the signal truncated into the window length instead of the full signal. With an additional moving window, MPCA can excavate the inner structure of time series signals in detail and reveal the variation trend of data itself. The window is like a filter that slides and decomposes the original signals along the time axis to different PCs. These PCs obtained from MPCA have more significant features than the PCs obtained from PCA. Also, the obtained eigenvalue is no longer a constant, but a changing curve. This curve can reflect the instantaneous trend of data variations at each moment and provides a new approach to calculate the energy of bridge vibration signals. In other words, the main difference between MPCA and PCA is that Eq. (3-1) in MPCA is

calculated using a window length's signal instead of the whole. MPCA will slide the moving window on the data matrix along the whole time axis. The time axis location of the window center column vector corresponds to the current time t. Within each movement, MPCA will calculate the principal component matrix and eigenvalue vector on the current window's location according to Eqs. (3-2) to (3-5). The obtained PC (a single column vector) at the window's location from each movement will be saved sequentially to form the final principal component matrix of MPCA. Similarly, the eigenvalue vector will be saved in the eigenvalue matrix sequentially to form the eigenvalue curves of each principal components. Figure 3-1 shows the schema of MPCA.

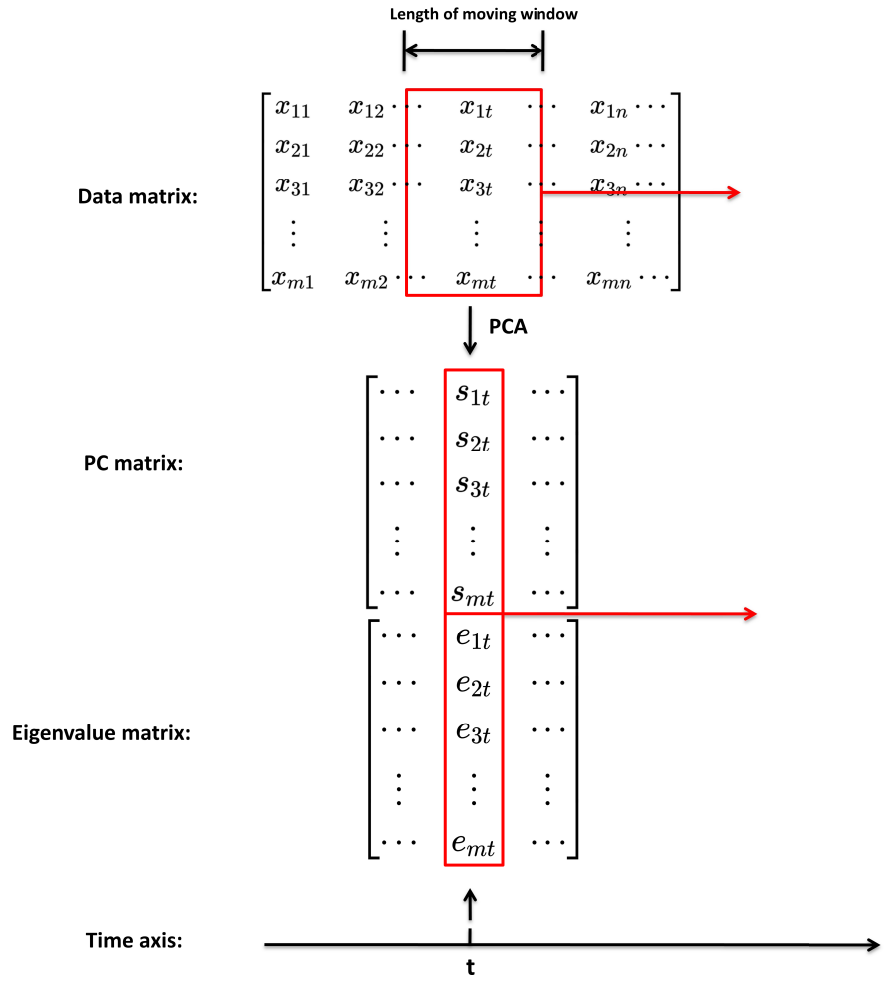

Figure 3-1. The schema of MPCA

3.1.3 Data preprocessing

For bridge SHM, time series signals are affected by some factors. These signals cannot be directly used as the algorithm's input. For every already existed data processing algorithm, currently the main target is to find out how to preprocess the source signals as the input data. Time series signal processing mainly concentrates on two aspects:

1) How to excavate and expose the intrinsic feature from the source signals. This step concentrates on improving the input data's quality and density (amount of information).
2) How to filter out the interference caused by other factors. This step is to ensure the robustness.

Among the data-driven approaches, a large branch of study is on the modal analysis. Modal analysis uses some mathematical methods to extract the modal parameters from the measured vibration responses. Mode shape decomposition factorizes the vibrations into different mode bases which are corresponding to natural frequencies. Modal analysis focuses more on the global behaviour of the bridge system and presumes the bridge's parameters are time-invariant. However, Eq. (3-13) shows that $\mathbf{M}$, $\mathbf{C}$ and $\mathbf{K}$ are time varying when a beam is under a moving mass. The temperature impact will also cause the time-varying of these matrices. Thus, the parameters of the bridge under the operational environmental conditions are time-varying. This is one reason why the current bridge damage detection approach under the moving vehicle excitation using the modal analysis needs a lot of preparation before the damage detection model training. Although the mathematical approach to deal with time-varying problems is segmentation and approximation, the time series signals processed by the modal analysis will lose a lot of information in time-domain. Numerous information of structure's state in time-domain excited by moving vehicles is

lost when the signals are converted into frequency-domain and the basis mode. A lot of work is needed to extract the enough information for the damage detection algorithm. Thus, the traditional modal analysis may not be suitable for this study.

3.2 Construction of the bridge finite element model

The research objectives of this study place a higher demand on the required numerical model. As a specific problem, this study requires a numerical model which can simulate the behaviour of the undamaged or damaged bridge subjected to a moving vehicle considering the environmental temperature effect. In the existing research, the damage, moving vehicles and temperature are often selected as the main influencing factors of the bridge individually. This study integrates these factors for the first time to establish a bridge numerical model that meets the research objectives. The first subsection in this section describes the establishment process of the bridge finite element model. The rest subsections introduce the simulation method of these influencing factors on the established bridge model. The damage on the bridge is simulated as the breathing crack. This allows the model to simulate the behaviour of a slightly damaged bridge more realistically.

3.2.1 Finite element model for a beam bridge

The bridge is simplified as an Euler-Bernoulli beam and it is evenly discretized in this study. The element mass matrix and stiffness matrix of a beam element can be obtained as

$$\mathbf{M}_e = \frac{\rho A l}{420}\begin{bmatrix} 156 & 22l & 54 & -13l \\ 22l & 4l^2 & 13l & -3l^2 \\ 54 & 13l & 156 & -22l \\ -13l & -3l^2 & -22l & 4l^2 \end{bmatrix}, \mathbf{K}_e = \frac{EI}{l^3}\begin{bmatrix} 12 & 6l & -12 & 6l \\ 6l & 4l^2 & -6l & 2l^2 \\ -12 & -6l & 12 & -6l \\ 6l & 2l^2 & -6l & 4l^2 \end{bmatrix} \quad (3\text{-}6)$$

where ρ, A, l are the density, section's area and length of the beam element respectively.

Figure 3-2 shows the i[th] beam element. The response at point x and time t can be obtained by the Hermite interpolation $H(x)$ from the node responses. Eq. (3-7) shows the Hermite interpolation $H(x)$:

$$\begin{aligned} H_1(x) &= 1 - 3\left(\frac{x}{L}\right)^2 + 2\left(\frac{x}{L}\right)^3 \\ H_2(x) &= x\left(1 - \frac{x}{L}\right)^2 \\ H_3(x) &= 3\left(\frac{x}{L}\right)^2 - 2\left(\frac{x}{L}\right)^3 \\ H_4(x) &= \frac{x^2}{L}\left(\frac{x}{L} - 1\right) \end{aligned} \tag{3-7}$$

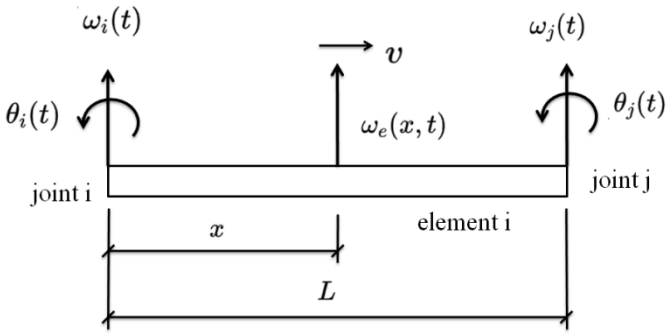

Figure 3-2. The Hermite interpolation on beam element

Eq. (3-8) shows the displacement at point x and time t:

$$\omega_e(x,t) = \mathbf{H}(x)^T\mathbf{R}(t) = \{H_1(x) \quad H_2(x) \quad H_3(x) \quad H_4(x)\}\begin{Bmatrix} \omega_i(t) \\ \theta_i(t) \\ \omega_j(t) \\ \theta_j(t) \end{Bmatrix} \tag{3-8}$$

where $\omega_e(x,t)$ is the displacement at point x and time t. $\omega_a(t)$, $\theta_a(t)$ are the displacement and rotation at corresponding joint a and time t of the beam element. x is the position in the beam element and L is the length of the beam element. $\mathbf{R}(t)$ is the node responses.

The strain at point x and time t can also be obtained (Law and Zhu 2009) as

$$\varepsilon(\mathrm{x},\mathrm{t}) = -\mathrm{z}\frac{\partial \mathbf{H}(x)\mathbf{R}(t)}{\partial x^2} \tag{3-9}$$

where z is the distance from the bottom to the neutral axis.

3.2.2 Equation of motion for the bridge subjected to a moving vehicle

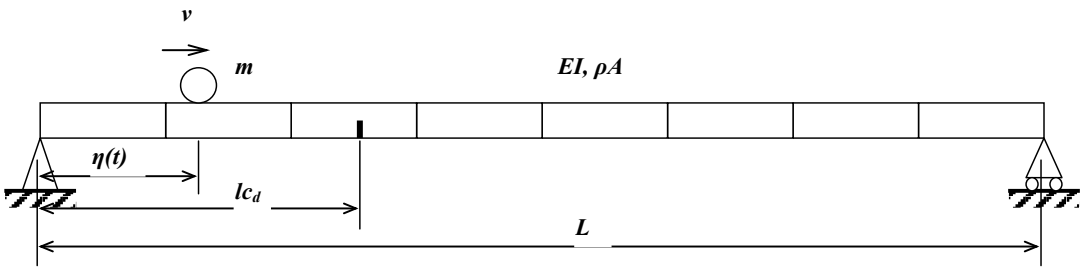

Figure 3-3. The damaged beam under a moving mass

The bridge is modelled as a simply supported beam and the vehicle is modelled as a mass m, as shown in Figure 3-3. The bridge length is L. The vehicle is moving along the bridge at a constant speed v. The crack damage is considered in this study. lc_d is the crack's location from the left support. The beam bridge is discretized into $N-1$ elements and N is the number of nodes. Considering Rayleigh damping for the bridge, the motion of equation for the bridge subjected to a moving vehicle can be obtained as

$$\mathbf{M}_b\ddot{\mathbf{R}}(t) + \mathbf{C}_b\dot{\mathbf{R}}(t) + \mathbf{K}_b\mathbf{R}(t) = \mathbf{H}_m\mathbf{P} \tag{3-10}$$

where $\mathbf{M}_b$, $\mathbf{C}_b$ and $\mathbf{K}_b$ are the mass, damping and stiffness matrices of the bridge respectively. The $\ddot{\mathbf{R}}(t)$, $\dot{\mathbf{R}}(t)$ and $\mathbf{R}(t)$ are the node's acceleration, velocity and displacement response vectors respectively. $\mathbf{H}_m\mathbf{P}$ is the node's equivalent force vector induced by the moving mass. $\mathbf{P}$ is the equivalent resultant force vector induced by the moving mass. The interaction force between the bridge and the mass is $P(x(t),t)$ that can be obtained as

$$P(x(t),t) = m\left\{g - \frac{\mathrm{d}^2(\omega(x(t),t))}{\mathrm{d}t^2}\right\} \tag{3-11}$$

where m is the mass of a moving vehicle. $\mathbf{H}_m = \{0 \quad \cdots \quad \mathbf{H}(\eta(t))_j^T \quad 0 \quad \cdots \quad 0\}^T$ when $(j-1)l \leqslant \eta(t) \leqslant jl$. $H(x)$ is the Hermite interpolation as the beam element's shape function. The beam's deflection at point x and time t can be written as

$$\omega(x,t) = \mathbf{H}(x)\mathbf{R}(t) \tag{3-12}$$

where $\mathbf{H}(x) = \{0 \quad \cdots \quad H(x)_j^T \quad 0 \quad \cdots \quad 0\}^T$ when $(j-1)l \leqslant \eta(t) \leqslant jl$. Combining Eqs. (3-10)-(3-12), the equation of motion can be written as

$$\mathbf{M}(t)\ddot{\mathbf{R}}(t) + \mathbf{C}(t)\dot{\mathbf{R}}(t) + \mathbf{K}(t)\mathbf{R}(t) = mg\mathbf{H}_m \tag{3-13}$$

where $\mathbf{M}(t) = \mathbf{M}_b + m\mathbf{H}_m\mathbf{H}(x)$, $\mathbf{C}(t) = \mathbf{C}_b + 2mv\mathbf{H}_m\mathbf{H}'(x)$, $\mathbf{K}(t) = \mathbf{K}_b + mv^2\mathbf{H}_m\mathbf{H}''(x)$. $\mathbf{H}'(x)$, $\mathbf{H}''(x)$ are the first and second derivatives of the Hermite interpolation vector $\mathbf{H}(x)$. Eq. (3-13) can be solved using the Newmark-β method. The parameters are: $\alpha = 0.5, \beta = 0.25$. The time step is 0.01 s. Then, the bridge response at point x can be obtained by Eqs. (3-7) to (3-9).

3.2.3 Temperature influence

The temperature's impact can be divided into two parts. The first one is the variation of the beam's parameters which will directly influence the beam's dynamic property. In the model, the thermal coefficients of the temperature impact on each parameter are listed in Table 3-1 (Yuen, 2010). A_0, E_0 and I_0 are the cross-section area, Young's modulus and second moment of inertia at the reference temperature T_0 respectively. The influence of the temperature on the section's Young's modulus is linearly weights according to the steel and concrete's bearing ratio of the section's ultimate bending moment at the

reference temperature. The section's expansion only considers the concrete's area growth.

Table 3-1. The temperature coefficients of beam's parameters (Yuen, 2010)

Parameters	Formula	Coefficient	Steel ($/^{\circ}C$)	Concrete ($/^{\circ}C$)
Expansion	$A = A_0(1 + \alpha_L \Delta T)^2$	α_L	1.2×10^{-5}	1.3×10^{-5}
Young's modulus	$E = E_0(1 + \alpha_E \Delta T)$	α_E	-3.2×10^{-4}	-7.2×10^{-3}
Second moment of inertia	$I = I_0(1 + \alpha_L \Delta T)^4$	α_L	1.2×10^{-5}	1.3×10^{-5}

The second impact is induced by vertical temperature gradient. This temperature gradient is to influence the bending curvature of the beam. For a simply supported beam, the influence of the vertical temperature gradient can be taken as (Zhou et al. 2021):

$$r_1 = -\frac{\alpha l_0 \cdot \Delta T}{2\sqrt{3} \cdot h} \cdot \frac{\lambda+1}{\lambda-1} \tag{3-14}$$

$$r_2 = -r_1 \tag{3-15}$$

$$M_1 = \left[1 - \frac{1}{\sqrt{3}} \cdot \frac{\lambda+1}{\lambda-1}\right] \cdot \frac{\alpha EI \cdot \Delta T}{h} \tag{3-16}$$

$$M_2 = M_1 \tag{3-17}$$

where r_1 and M_1 are the vertical temperature gradient induced rotation and moment at the beam's left support. r_2 and M_2 are the vertical temperature gradient induced rotation and moment at the beam's right support. ΔT is the temperature difference between the top surface and bottom, and the positive reflects the top surface is warmer. h is the cross-section's height. EI is the

beam's rigidity. α is the concrete's thermal expansion coefficient in Table 3-1. λ is a constant and it is equal to $\frac{\sqrt{3}+1}{\sqrt{3}-1}$. l_0 is the beam's length. According to Eqs. (3-14) to (3-17), the vertical temperature gradient induced effect is obtained and considered as the boundary condition of the simulated beam.

3.2.4 Crack damage model

The beam's damage starts from initial microcracks and develops by many factors such as degradation, loads, temperature impact, etc. While expanding, these microcracks keep opening and closing due to external dynamic excitation. This phenomenon is known as the breathing crack and dominates the beam's crack behavior in incipient crack stage (Voggu and Sasmal 2021). Besides, since the prestress is widely applied, the crack in the prestressed concrete bridges will perform as the breathing crack. Thus, it is necessary to simulate the breathing crack in the bridge model since it is close to the actual cracks' behaviour.

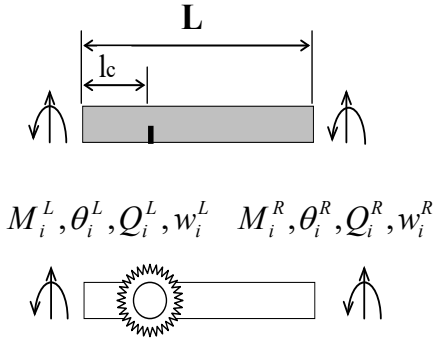

Figure 3-4. The cracked beam element

In this study, the breathing crack is studied. Law and Zhu's damage model is used to simulate the breathing crack (Law and Zhu 2006). The breathing crack is simulated as a rotational spring at the crack's location l_c. Figure 3-4 shows the beam element with a breathing crack. This element is considered as two undamaged beam sections connected by the proposed rotational spring. EI is the

undamaged beam's flexural rigidity and L is the length of this element. The stiffness matrix of this element can be written as

$$\begin{Bmatrix} Q_i \\ M_i \\ Q_d^L \\ M_d^L \end{Bmatrix} = \frac{EI}{l_c^3} \begin{bmatrix} 12 & 6l_c & -12 & 6l_c \\ 6l_c & 4l_c^2 & -6l_c & 2l_c^2 \\ -12 & -6l_c & 12 & -6_c \\ 6l_c & 2l_c^2 & -6l_c & 4l_c^2 \end{bmatrix} \begin{Bmatrix} w_i \\ \theta_i \\ w_d^L \\ \theta_d^L \end{Bmatrix} \tag{3-18}$$

$$\begin{Bmatrix} Q_d^R \\ M_d^R \\ Q_j \\ M_j \end{Bmatrix} = \frac{EI}{(l-l_c)^3} \begin{bmatrix} 12 & 6(l-l_c) & -12 & 6(l-l_c) \\ 6(l-l_c) & 4(l-l_c)^2 & -6(l-l_c) & 2(l-l_c)^2 \\ -12 & -6(l-l_c) & 12 & -6(l-l_c) \\ 6(l-l_c) & 2(l-l_c)^2 & -6(l-l_c) & 4(l-l_c)^2 \end{bmatrix} \begin{Bmatrix} w_d^R \\ \theta_d^R \\ w_j \\ \theta_j \end{Bmatrix}$$

(3-19)

Eqs. (3-18) and (3-19) link up the deformation and force at two beam sections' ends. The w_i, w_j, θ_i, θ_j are the displacement and rotation angle of two beam sections' joint. The Q_i, Q_j, M_i, M_j are the transverse shear force and moment. The w_d^L, θ_d^L, w_d^R, θ_d^R are the spring's displacement and rotation angle at the joint. The Q_d^L, M_d^L, Q_d^R, M_d^R are corresponding the shear force and moment.

According to equilibrium and compatibility condition at the crack's location, the cracked beam's element stiffness matrix can be obtained

$$\mathbf{K}_d = \mathbf{K}_1 + \mathbf{K}_2 \mathbf{K}_3^{-1} \mathbf{K}_4 \tag{3-20}$$

where

$$\mathbf{K}_1 = \frac{EI}{l^3} \begin{bmatrix} \frac{12}{\delta^3} & \frac{6l}{\delta^2} & 0 & 0 \\ \frac{6l}{\delta^2} & \frac{4l^2}{\delta} & 0 & 0 \\ 0 & 0 & \frac{12}{(1-\delta)^3} & -\frac{6l}{(1-\delta)^2} \\ 0 & 0 & -\frac{6l}{(1-\delta)^2} & \frac{4l^2}{(1-\delta)} \end{bmatrix}, \quad \mathbf{K}_2 = \frac{EI}{l^3} \begin{bmatrix} -\frac{12}{\delta^3} & \frac{6l}{\delta^2} & 0 & 0 \\ -\frac{6l}{\delta^2} & \frac{2l^2}{\delta} & 0 & 0 \\ 0 & 0 & -\frac{12}{(1-\delta)^3} & -\frac{6l}{(1-\delta)^2} \\ 0 & 0 & \frac{6l}{(1-\delta)^2} & \frac{2l^2}{(1-\delta)} \end{bmatrix}$$

$$\mathbf{K}_3 = \begin{bmatrix} -\frac{12}{\delta^3} & \frac{6l}{\delta^2} & 0 & 0 \\ \frac{6l}{\delta^2} & S-\frac{4l^2}{\delta} & 0 & 0 \\ 0 & 0 & \frac{12}{(1-\delta)^3} & \frac{6l}{(1-\delta)^2} \\ 0 & -S & -\frac{6l}{(1-\delta)^2} & S-\frac{4l^2}{(1-\delta)} \end{bmatrix}, \quad \mathbf{K}_4 = \begin{bmatrix} -\frac{12}{\delta^3} & -\frac{6l}{\delta^2} & 0 & 0 \\ \frac{6l}{\delta^2} & \frac{2l^2}{\delta} & 0 & 0 \\ 0 & 0 & -\frac{12}{(1-\delta)^3} & \frac{6l}{(1-\delta)^2} \\ 0 & 0 & -\frac{6l}{(1-\delta)^2} & \frac{2l^2}{(1-\delta)} \end{bmatrix}$$

$$\delta = \frac{l_c}{l}, S = \frac{K_{rd} l^3}{EI}$$

The K_{rd} is the tangent stiffness which reveals the spring's instant rigidity. As shown in Figure 3-5, there is a crack opening at the edge of a rectangular section. $2h$ is the cracked element's length and b is the element's height. The crack is started on the center of the element's long edge. The rotational displacement due to the crack opening at the edge can be obtained using linear-elastic fracture mechanics (Tada et al. 2000) as

$$\theta_{crack} = \frac{4\sigma}{E} S\left(\frac{a}{b}\right) \tag{3-21}$$

where σ is the applied stress of the whole cracked element induced by bending moment. The $\frac{\mathrm{a}}{\mathrm{b}}$ is the ratio of the crack's depth. For $\frac{h}{b} > 2$, the $S(\frac{a}{b})$ can be written (Tada et al. 2000) as

$$S\left(\frac{a}{b}\right) = \left(\frac{\frac{a}{b}}{1-\frac{a}{b}}\right)^2 \left\{5.93 - 19.69\left(\frac{a}{b}\right) + 37.14\left(\frac{a}{b}\right)^2 - 35.84\left(\frac{a}{b}\right)^3 + 13.12\left(\frac{a}{b}\right)^4\right\} \tag{3-22}$$

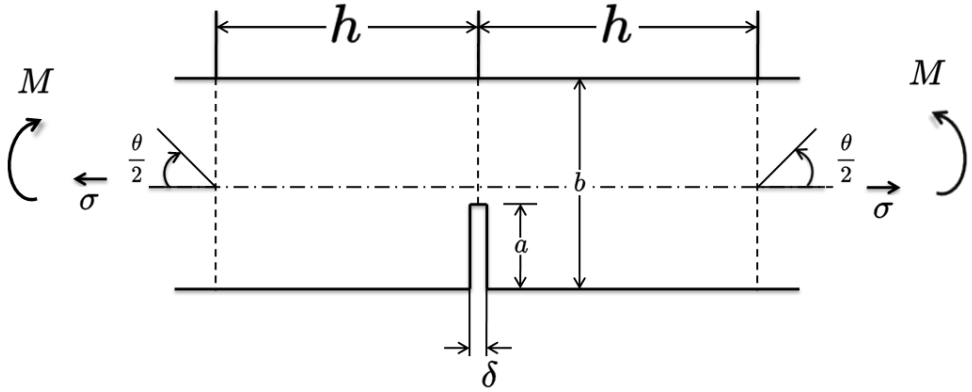

Figure 3-5. The crack opening at edge

The relationship of σ and M for the pure bending element can be written as

$$\sigma = \frac{6M}{\mathrm{b}^2} \tag{3-23}$$

where M is the cracked element's bending moment. b is the length of the section's short edge. Integrating Eqs. (3-21) to (3-23), the K_{rd} which is the instant tangent stiffness of the virtual rotational spring, is obtained.

$$K_{rd} = \frac{M}{\theta_{crack}} = \frac{Eb^2}{24S(\frac{a}{b})} \tag{3-24}$$

3.3 Results

3.3.1 Numerical simulation

The numerical model is verified by comparing with the results by Zhu and Law (2006). A simply supported beam with a 50 m length, a 0.5 m width and a 1 m high is used. The elastic modulus of the beam is 2.1×10^{11} Pa, and the density is $7860\ \mathrm{kg/m^3}$. The moving force is 10 kN. The first six natural frequencies are listed in Table 3-2.

Table 3-2. The numerical model's natural frequencies

Natural frequencies	
Zhu and Law	In this study
0.94	0.9375
3.75	3.7501
8.44	8.4377
15.00	15.0004
23.44	23.4390
33.75	33.7547

Figure 3-6 shows the normalized deflection curve at the mid-span. The sampling rate is 100 Hz. The deflection is normalized by $\frac{\mathrm{F_0 L^3}}{48\mathrm{EI}}$ which is the static

deflection when the force is at the mid-span. The scattered points are the analytical solution obtained by Zhu and Law (2006) and the line curves are the numerical solution obtained by the proposed model in this study. a/h is the crack depth ratio at the mid-span. For v=5 m/s, the number of elements is 13. For v=40 m/s, the number of elements is 7. The number of elements is consistent with the compatibility condition in Eq. (3-22). The results by the proposed model are close to those in the reference paper (Zhu and Law 2006). The results show that the higher frequency components to obtain when the larger number of elements are used. The proposed damage detection method will be deployed on this numerical model with enough accuracy. As shown in Fig. 3.6, the occurrence of the fluctuations in the responses reflects the high frequency components. The number of elements for the case v=5 m/s is 13 and it is 7 for the case with 40 m/s. To obtain the higher frequency components in the response, the larger number of elements should be used.

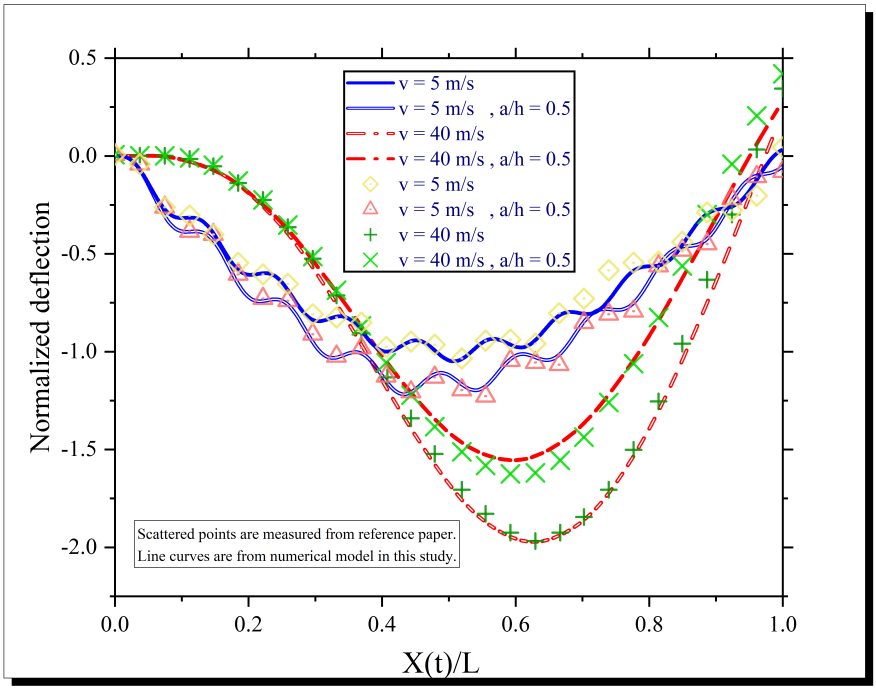

Figure 3-6. The normalized deflection at mid-span by (Zhu and Law 2006) and this study

3.3.2 Comparison between principal component analysis and moving principal component analysis

With a moving window, MPCA can reveal more intrinsic feature of the data than PCA. A comparison study will be shown here to illustrate this point. The simulated beam is taken from Section 3.3.1. The moving load is 10 kN. The velocity of the moving load is 5 m/s and the number of elements is 13. The beam is undamaged. A sudden and slight change of the load's mass is simulated to illustrate the sensitivity and reliability of MPCA. The acceleration signals are taken as the input data. Table 3-3 shows simulated three cases.

Table 3-3. The simulated three cases

Case	Mass change	Time duration	
		Start time	End time
1	0%		
2	1%	5 s	6 s
3	1%	5 s	10 s

Figure 3-7 shows the results of PCA for those three cases in Table 3-3. The first PC is shown for comparison. The unit of the results obtained by PCA-based methods (PCs and eigenvalues) depends on the unit and amount of the input data. The property of the covariance matrix determines that the total amount of eigenvalues obtained by PCA is equal to the sum of the norms' squares of all input vectors. Also, the metric of the obtained eigenvectors depends on the corresponding eigenvalues. Thus, the number and size of input vectors will directly determine the magnitude of the obtained result by PCA. The meaning of the obtained result depends on the unit of the input vectors. This also makes the obtained result comparable, as long as the vectors can be input according to a same rule. Additionally, the Gaussian window proposed in the next chapter will scale the magnitude of the obtained results.

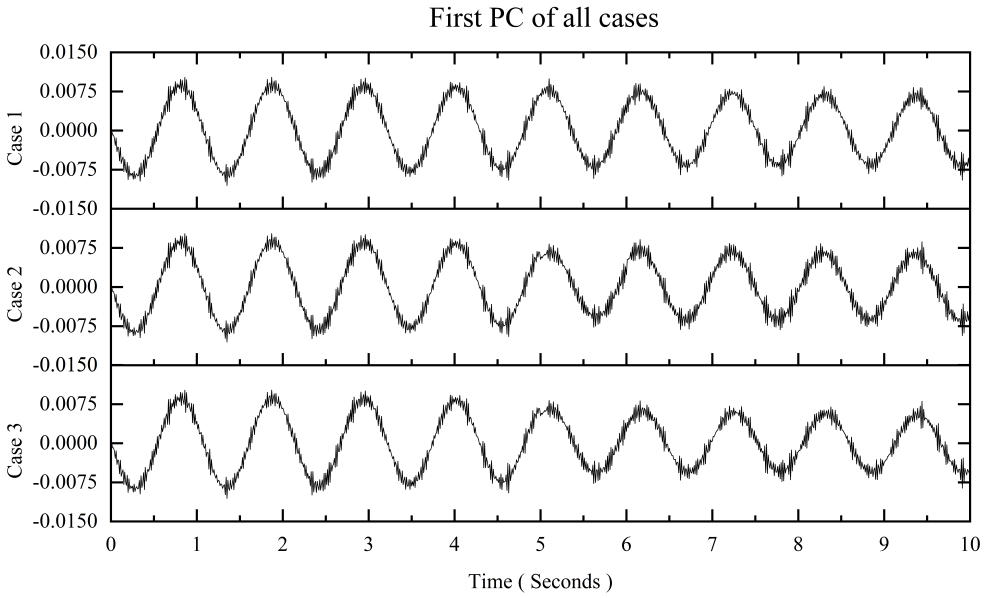

Figure 3-7. Results of PCA with three different masses

There are some slight but not obvious changes at the fifth second in Figure 3-7. It is difficult to distinguish the difference in the results of PCA. Without a moving window, the eigenvalue obtained by PCA is a constant and cannot be used as the feature for a time-varying process.

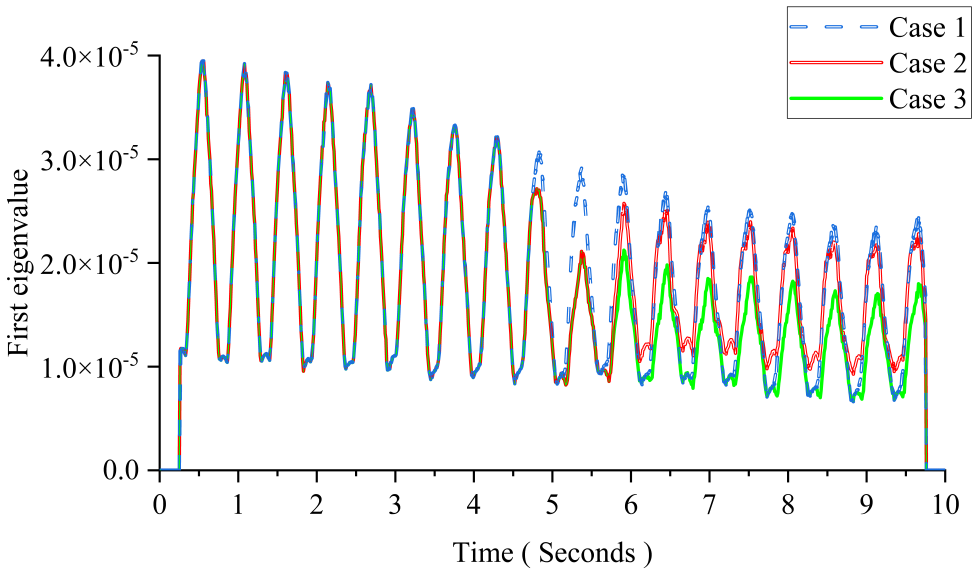

Figure 3-8. Result of MPCA with the mass change

The eigenvalues are more sensitive to abrupt changes than PCs (Nie et al. 2020). The first eigenvalue is taken for comparison in this study. The size of the window is 50 times the sampling interval. Figure 3-8 shows the result using MPCA. As shown in Figure 3-8, there are clear changes at 5 s in Cases 2 and 3. The results show that the 1% mass variation can be detected immediately in the first eigenvalue curve by using MPCA. For Case 2, the magnitude of the first eigenvalue is the same with Case 1 after 6 s as the mass returns back the original value. For Case 3, the first eigenvalue keeps the same magnitude after 5 s since the mass of the moving load does not change after that.

3.3.3 The effect of damage patterns

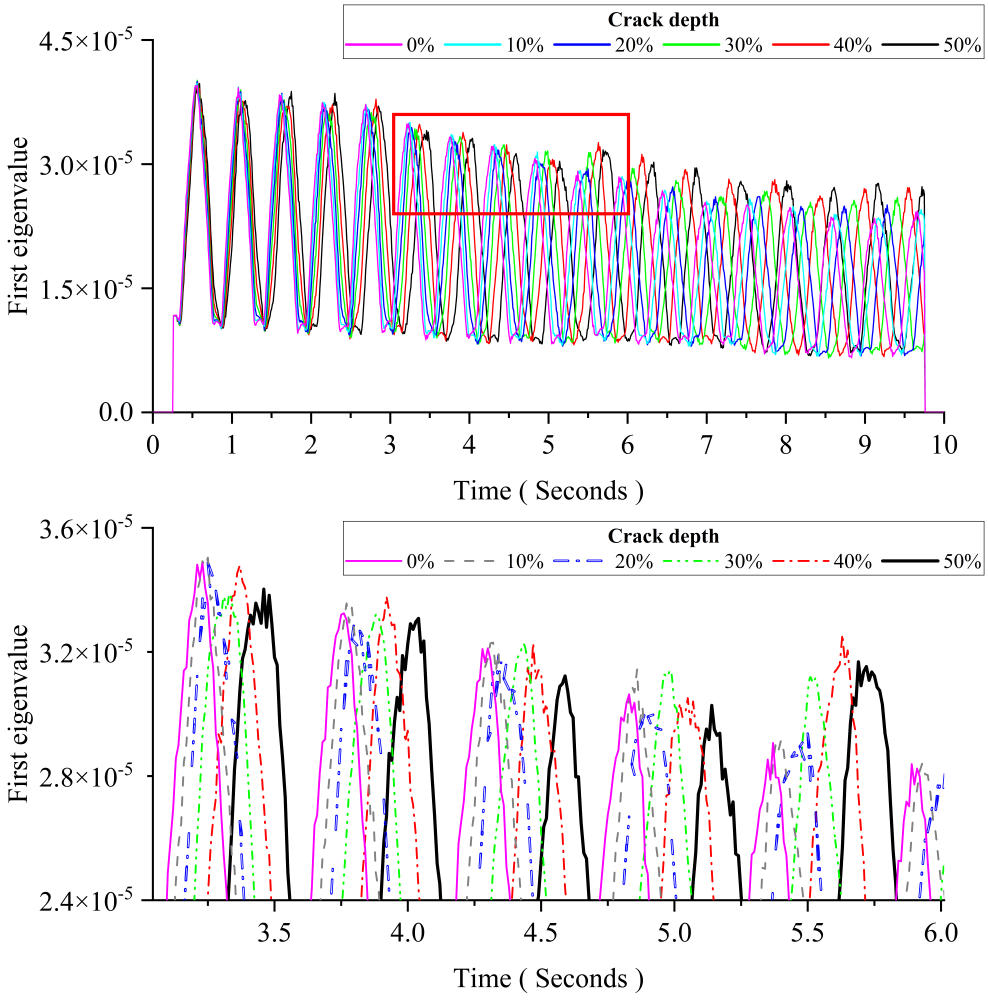

Figure 3-9. The influence of the crack depth for MPCA

Figure 3-9 shows the pattern change of the first eigenvalue induced by the growing crack depth. Other parameters are the same as Case 1 in Section 3.3.2. The crack occurred at the mid-span. The image below is an enlarged view of the area in the red box of the image above. Figure 3-9 reveals that changes of the crack depth mainly affect the distance between each pair of adjacent peaks in the first eigenvalue curve. If the damage occurs, the distance between each pair of adjacent peaks will increase and this increment will increase with the crack depth. This pattern was also observed in Hester and González (2015).

3.3.4 Orthogonality

The efficiency of the proposed method requires to be proved by the orthogonality. MPCA can decompose the data into different coordinate axes in which each axis is orthogonal with other axes. For bridge SHM, the changes occurred by damage need to be orthogonal with changes induced by other factors such as the vehicle's mass, the temperature, road surface roughness, etc. In this section the orthogonality between the vehicle's mass and damage is studied. Six cases have been studied. The parameters of the first three cases are the same with those in Section 3.3.2. The parameters of the remaining three cases are also the same as those in Section 3.3.2 except for the crack depth. Table 3-4 shows all six simulated scenarios.

Table 3-4. Six cases for the orthogonality

Case	Mass change	Time duration		Crack depth
		Start time	End time	
1	0%			0
2	1%	5 s	6 s	0
3	1%	5 s	10 s	0
4	0%			50%
5	1%	5 s	6 s	50%
6	1%	5 s	10 s	50%

Figure 3-10 shows the result of six simulated scenarios. The image below is an enlarged view of the area in the red box of the image above. Comparing Cases 1 to 3 with Cases 4 to 6, we can see the influence of the damage is orthogonal with the influence of the moving load's mass. The influence of the damage is embodied in the distance between each pair of adjacent peaks. Cases 4 to 6 show similar patterns which are different with the undamaged beam's patterns in Cases 1 to 3. The influence of the moving load's mass is embodied in the magnitude of each peak. The first eigenvalue represents the amount of information at the corresponding time in acceleration signals. For the undamaged beam, the increase of the moving load's mass will lead to the decrease of the first eigenvalue. For the damaged beam, the increase of the moving load's mass will lead to the increase of the first eigenvalue. For Cases 1, 2, 4 and 5, the peak magnitude after 6 s is the same and the result shows that the proposed method also has the potential for moving load identification.

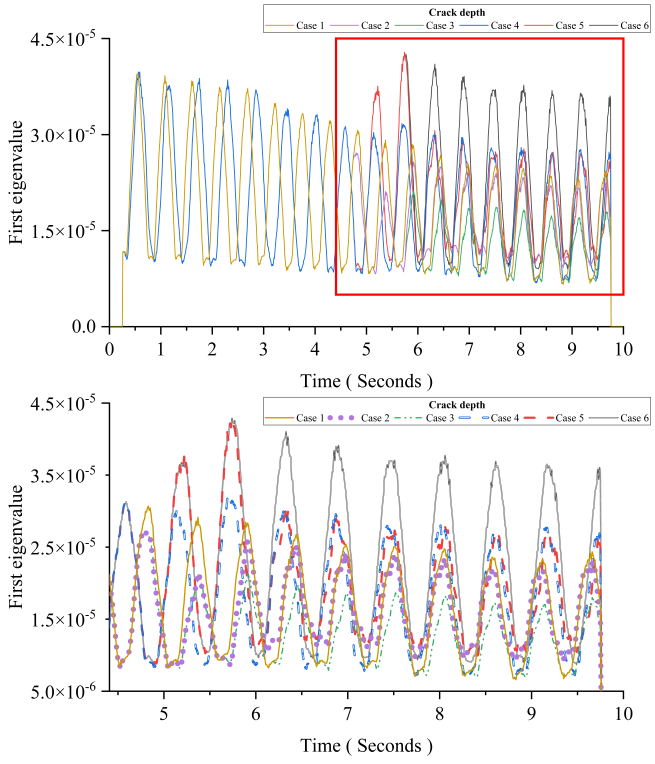

Figure 3-10. Result of six cases for the orthogonality

3.3.5 Temperature influence

To investigate temperature's impact on MPCA, the following cases are considered for comparison. Table 3-5 summaries all considered scenarios.

Table 3-5. Cases to investigate temperature's impact on MPCA

Case	Average temperature difference(℃)	Vertical temperature difference(℃)		Crack depth
		Start time	End time	
1	0	0	0	0
2	0	0	0	50%
3	+15	28	25	0
4	+15	28	25	50%
5	-15	20	15	0
6	-15	20	15	50%

The two kinds of temperature changes are based on the reference temperature. The average temperature difference means the average temperature of the whole beam in different cases. The +15 means that the average beam temperature is 15 degrees Celsius higher than the reference temperature. The -15 means that the average beam temperature is 15 degrees Celsius lower than the reference temperature. The vertical temperature difference will slightly change when the vehicle is passing the bridge. All the considered temperature changes are linear since the moving load will pass the beam in a short time. The average temperature difference between Cases 3, 4 and Cases 5, 6 reaches 30 degrees Celsius to simulate the temperature difference between day and night in mid-summer, and the corresponding vertical temperature difference is to simulate strong sunlight conditions. The other parameters are the same as Case 1 in Section 3.3.4.

Figure 3-11 shows the temperature's impact on the first eigenvalue of MPCA. The image below is an enlarged view of the area in the red box of the image

above. Since the temperature difference considered in this section is relatively extreme, a small amount of deviation is caused to the first eigenvalue curve's fluctuations. However, the deviation caused by the temperature difference is concentrated in a specific small range, which is an order of the magnitude different from the change in the curve pattern caused by the damage.

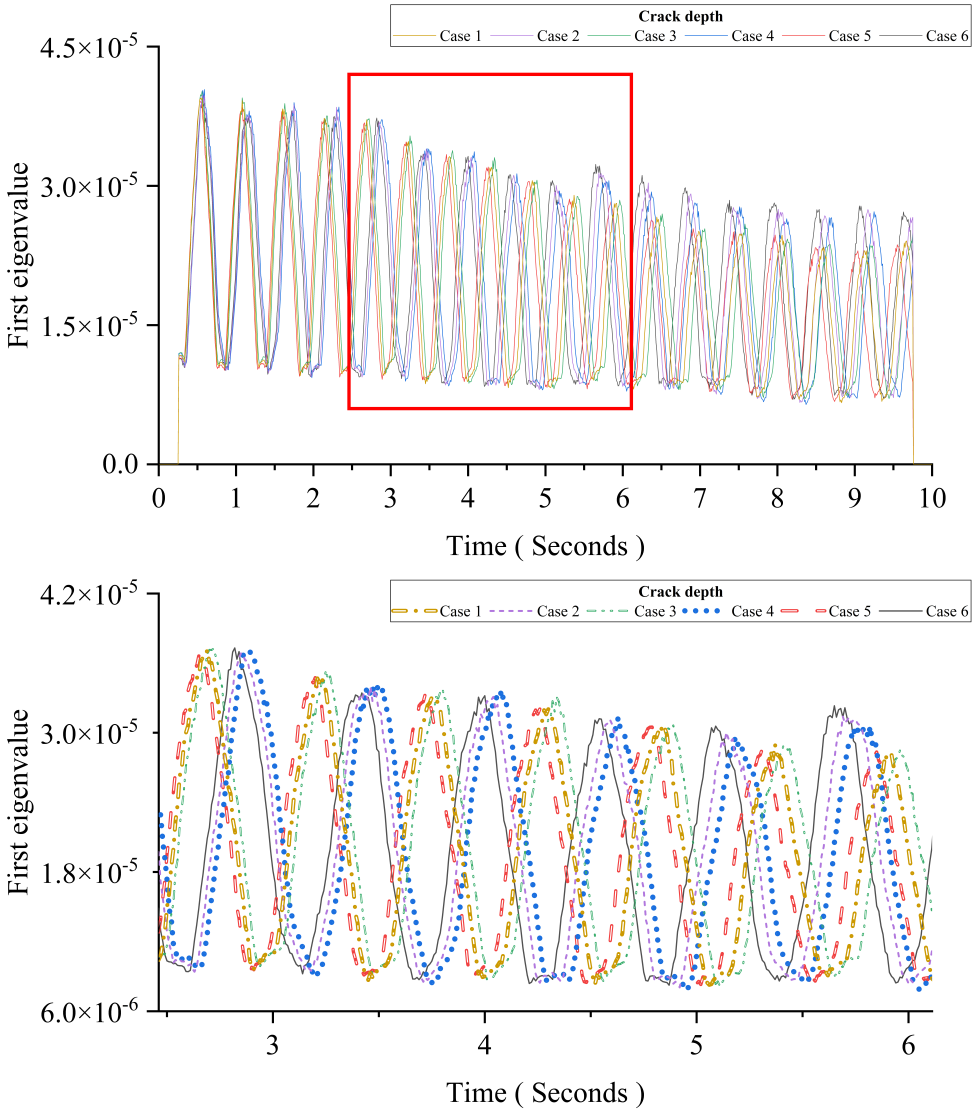

Figure 3-11. Temperature impact on MPCA

3.4 Damage sensitive feature

3.4.1 Observation

According to previous discussions, the crack depth mainly affects the distance between each pair of adjacent peaks in the first eigenvalue curve. If damage occurs, the distance between each pair of adjacent peaks will increase and this increment will grow along with the growth of the crack depth. Although the first eigenvalue curve has an obvious and identifiable pattern, some sawtooth-like interference information occurs near the peak and trough areas. This information will greatly affect the accuracy of the detection. To avoid the influence of these perturbation, a special treatment is adopted. Following the idea of PCA, the information we actually need is the principal component in the first eigenvalue curve. Figure 3-12 shows that the steadiest part which can reflect the main trend of the first eigenvalue is the two limbs of each peak. Thus, the mean line of the first eigenvalue curve is taken to cut the first eigenvalue curve. The midpoints of each pair of intersections in each peak are taken as the foundation of the DSF's construction.

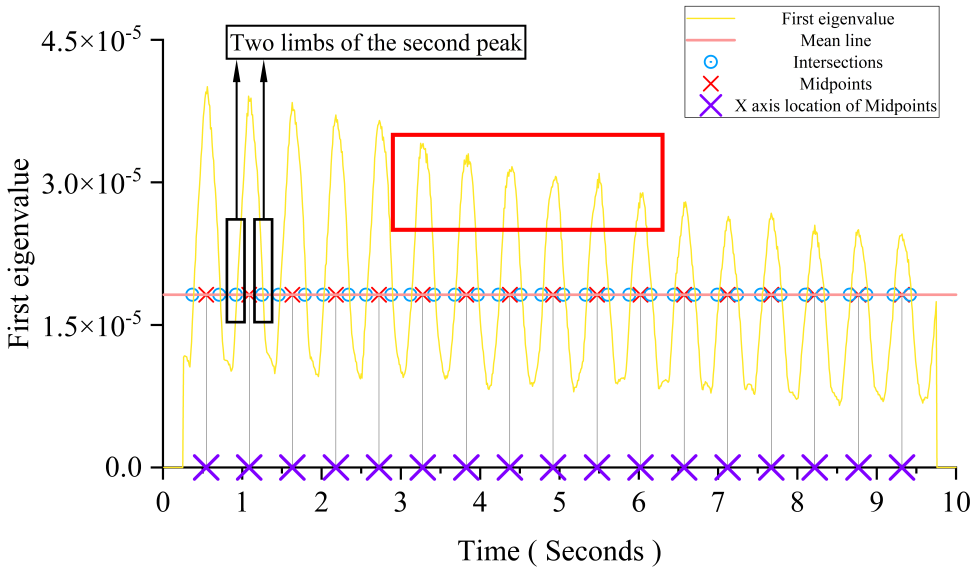

Figure 3-12. The detail of DSF's construction

3.4.2 Construction

Figure 3-13 shows that the growth trend of the x-axis location of each midpoint is linear. The thumbnail in this figure is an enlarged view of the red boxed area. The crack depth's change will influence the inclination of each midpoint's x-axis location's growth trend line. In this section all cracks are occurred at the mid-span.

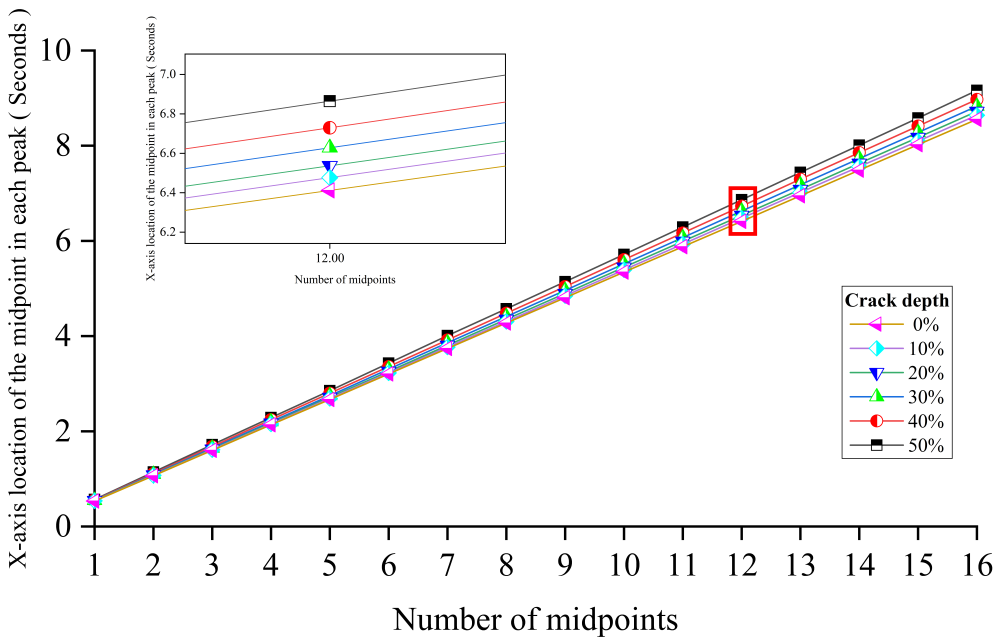

Figure 3-13. The growth trend of each peak's midpoints

Thus, the gradient of the line in Figure 3-13 can be used as the DSF. The numerical derivatives of each pair of discrete midpoints are obtained. The mean of all numerical derivatives in each line is calculated corresponding to its crack depth. The angle of each line is obtained by the mean's arctangent. Figure 3-14 shows the angle of each line corresponding to its crack depth.

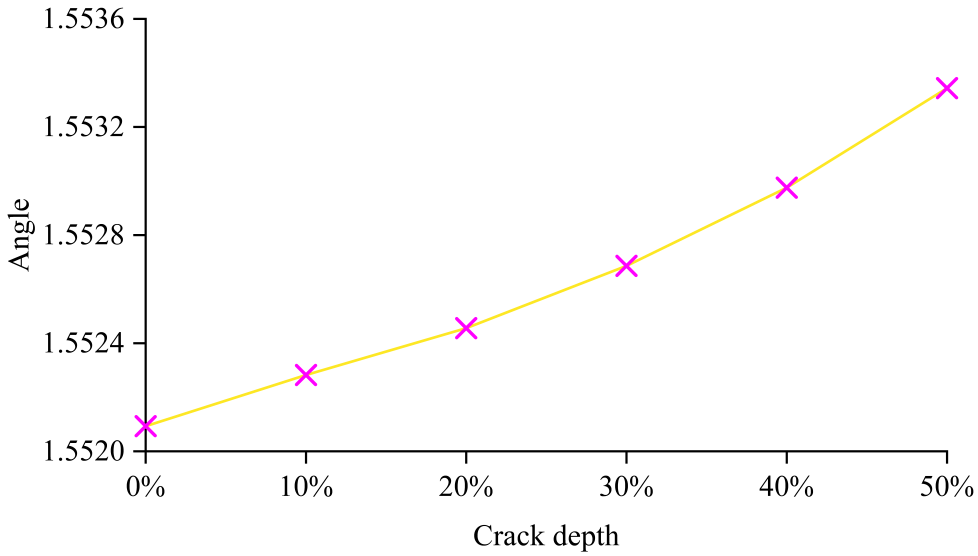

Figure 3-14. The angle of each line when crack is growing

3.4.3 Influence by crack's location

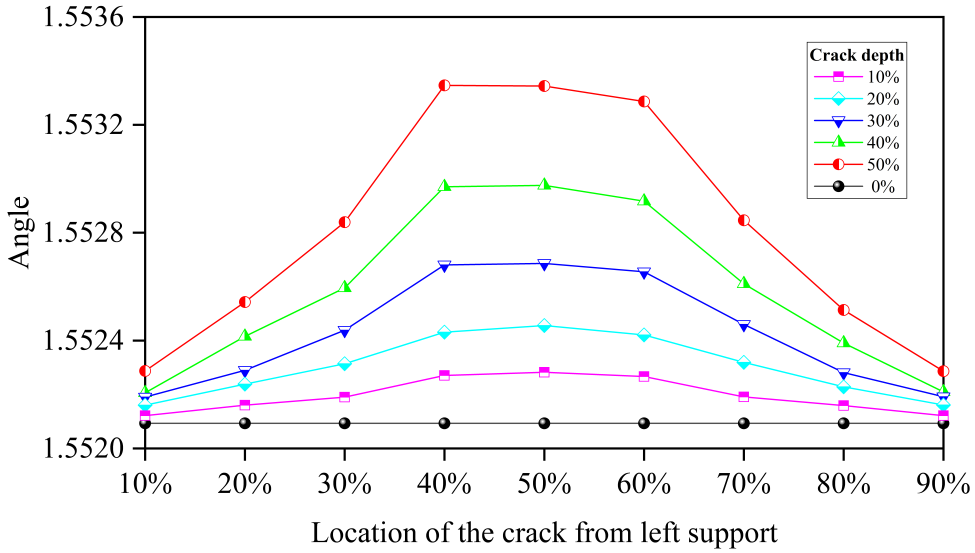

Figure 3-15. The angle of each line when crack locates at different position

Figure 3-15 shows the crack location's influence. The result reveals that for each crack depth the crack located around the midpoint of the beam has a larger influence than the crack located near the beam's end. This phenomenon will be more obvious when the crack grows deeper. This result complies with the

beam's dynamic analysis theory. In PCA, the first eigenvalue represents the variance of the first dimension. In this study, the first dimension is dominated by the acceleration changes caused by the moving loads. The vertical fluctuation and slow decline of the first eigenvalue reveal that the amount of the information (energy) brought by the moving load is gradually dissipated in the beam's response over time due to the beam's vibration. The existence of cracks will change the rate of this dissipation. Therefore, the increases in the distance between each midpoint represent these crack induced changes. Additionally, this DSF reflects the damage of the beam from the overall perspective, which is the so-called equivalent crack depth. Since cracks in actual structure are distributed near the damaged area of the beam, this DSF can provide a more realistic beam damage situation. When the crack depth is greater than 30%, the Maxwell-Betti reciprocal theorem is no longer valid due to the nonlinearity caused by the cracks. Thus, although the two damage locations with a distance of the 1/10 L on both sides of the beam’s midpoint are symmetrical in space, the damage extent reflected by these two DSFs is no longer consistent due to the directionality of the moving load on the time axis. In this case, the first eigenvalue is dominated by the moving load and the breathing crack. Within this range, the moving load passing through the crack earlier means that the beam has more time to dissipate, so the reflected degree of the damage will be slightly higher than the other places that the moving load passes the crack later. Therefore, the proposed DSF describes the damage extent of the beam from a dynamic perspective. In other words, it depicts beam's "rhythm". The traditional modal analysis describes the beam’s vibration from a static perspective. Since the analysis is based on the simply supported beam model, the magnitude of the first eigenvalue represents a measure of the maximum variance direction dimension. For a simply supported beam, the direction of the maximum variance of the measuring points' acceleration is in the direction of the gravity

axis when a uniaxial moving load is passing. Therefore, MPCA can capture a continuous peak fluctuation of the same magnitude in the first eigenvalue curve.

3.5 Summary

- Introduction of PCA and MPCA

As the used detection method in this study, PCA and MPCA are first introduced at the beginning of this chapter. For PCA, the obtained eigenvalue is a constant and the resolution of the corresponding principal component vector (eigenvector) depends on the length of the input data. In other words, the obtained eigenvalues and eigenvectors reflect the unweighted statistical characteristics over the entire length of the input data. This can cause some local subtle features to be overwhelmed by the overall features of the entire signal. For MPCA, the additional moving window expands the constant eigenvalues obtained by PCA into the eigenvalue curves along the time axis based on local fluctuations of the data. The corresponding eigenvectors also have higher resolution and become more sensitive to local subtle variations. This enables MPCA to excavate the inner structure of time series signals in detail and reveal the variation trend of the data itself. For current existed data processing algorithms, their main target is to extract the enough inherent features of the data and filter out the interference caused by the other factors as possible.

- Construction of bridge finite element model

The numerical model is used to develop the damage detection method for the bridges under the moving vehicles considering the environmental temperature effect. The bridge is simulated as a simply supported Euler Bernoulli beam with the breathing crack subjected to a moving vehicle. The Hermite interpolation and Newmark-β method are used to solve the equation of motion and obtain the bridge response. The temperature influence is simulated as the variation of the

beam's parameters and thermal stress induced by the vertical temperature difference. The cracked beam element is modelled with a virtual rotational spring and its stiffness matrix is obtained based on the equilibrium and compatibility condition and the linear-elastic fracture mechanics. The result in a reference paper is used to ensure the accuracy of the proposed numerical model.

- Results of numerical simulation

By the comparison with the result in the reference paper, this numerical model is accurate enough to develop the damage detection method.

- Results of comparison between PCA and MPCA

According to the results, it is difficult to observe and distinguish the slight changes detected by PCA in the input data. The first eigenvalues obtained by MPCA are more sensitive to the abrupt and slight changes in the input data. The sudden slight changes in the input data can be timely and clearly detected and observed on the first eigenvalue curves. This comparison study is used to illustrate the superior of MPCA. Based on this conclusion, the first eigenvalue curve is used as the foundation to create the damage sensitive feature.

- Parametric study

The parametric study is conducted to investigate the effect of the single parameter variations and the interactions between these parameters' variations on the changes of the first eigenvalue. This is to demonstrate the feasibility and robustness of using the first eigenvalue curve to construct the damage sensitive feature. The pattern change of the first eigenvalue induced by the growing crack depth is presented. The first eigenvalue curve can obviously reveal the occurrence of the damage induced by the breathing crack. In the first eigenvalue curve, the changes induced by a moving vehicle are orthogonal with the changes induced by the breathing crack, and the changes caused by the temperature

difference are an order of the magnitude different from the changes caused by the breathing crack. These conclusions ensure the feasibility and robustness of using the first eigenvalue curve to construct the damage sensitive feature.

- Construction of damage sensitive feature with discussion

Based on the results above in this chapter, the final form of the damage sensitive feature is determined. The mean line of the first eigenvalue curve is taken to cut the first eigenvalue curve and a series of intersections are obtained. The midpoints' x-axis location of each pair of intersections in each peak is obtained. Connect these x-axis coordinate values into a line, and the gradient of this line is used as the damage sensitive feature. The effects of the different damage depth and location on the damage sensitive feature are studied, and the discussions are conducted based on these results. From the perspective of mechanics and MPCA, the mechanism and meaning behind the feature changes are analysed. The result shows that the proposed damage sensitive feature can reflect the damage of the bridge more truly. In bridge, the cracks are actually formed by the accumulation of small cracks distributed in different positions. The equivalent crack depth reflected by the proposed damage sensitive feature can more accurately measure the damage extent caused by these distributed cracks on the bridge. This feature provides the bridge information from a dynamic perspective and is strongly interpretable.

Chapter 4 Laboratory Study

A laboratory study has been conducted in this study. The acceleration data of the experimental beam subjected to a moving model vehicle load under undamaged and damaged states from Zhu and Law (2006) have been used. The wavelet transform is used to extract the discontinuity of the displacement response for the potential damage detection in Zhu and Law (2006). In this study, the acceleration response is adopted. The first eigenvalue curve has been obtained using the proposed method in Chapter 3. The Gaussian window is adopted to reduce the measurement noise and the vehicle-bridge interaction. The selection of the window parameters is also discussed. The results of the obtained damage sensitive feature on this laboratory data using the proposed method in Chapter 3 are presented and discussed.

4.1 Experimental setup

Figure 4-1 shows the experimental setup. The cross-section of the concrete beam is shown in Figure 4-1 (a). As shown in Figure 4-1 (b), the whole experimental beam is composed of three T-section reinforcement concrete beams: the front beam, the main beam and the tail beam. The front and tail beams are 4.5 m long each. The main beam is 5.0 m long. The gaps between these three beams are 10 mm. An electric motor is used to pull the vehicle along the beam at a speed of approximately 0.5 m/s. The vehicle's axle spacing is 0.8 m, and its wheel spacing is 0.39 m. There are two vehicle models with different weights in this study. The whole weight of the first vehicle model (without elastic spring) is 10.60 kN with the front axle load 5.58 kN and the rear axle load 5.02 kN. The whole weight of the second vehicle model (with elastic spring) is 15.00 kN with the front axle load 6.20 kN and the rear axle load 9.00 kN. Since the mass of the whole concrete beam is 1050 kg, the weight ratios

between the vehicle and the beam bridge for these two vehicle models are 1.01 and 1.43 respectively. Figures 4-1 (c) and (d) are the photos taken during this experiment. Figure 4-1 (c) shows the vehicle model passing through the beam and Figure 4-1 (d) shows the large damage case being generated.

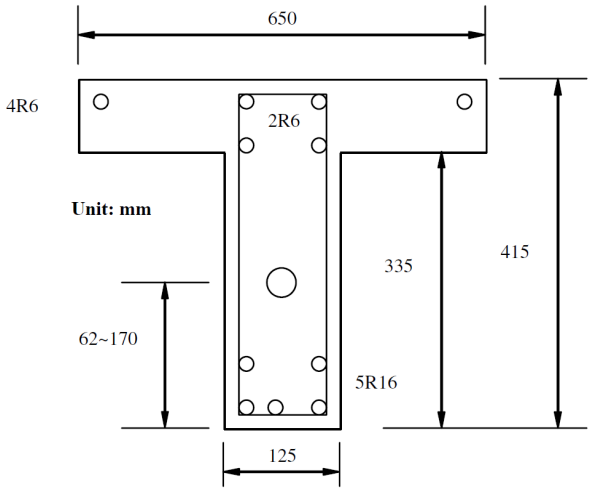

(a) Cross-section of the concrete beam

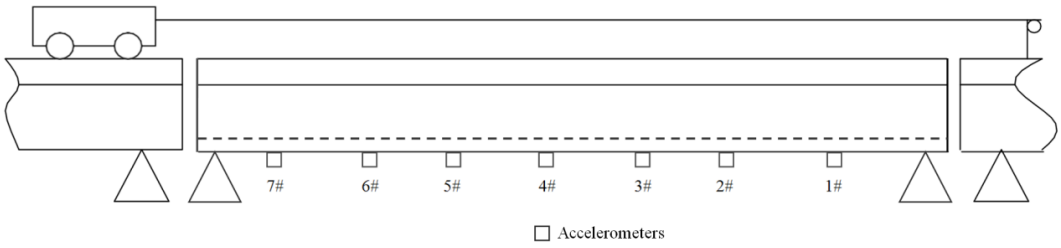

(b) Sensor location

(c) Moving vehicle model (d) Generating large damage case

Figure 4-1. Experimental setup

As shown in Figure 4-1 (b), seven accelerometers are evenly installed along the beam at the bottom surface. Thirteen photo-electric sensors are distributed on the lead and main beams with 0.56 m spacing to measure the vehicle's moving velocity. The third and thirteenth photo-electric sensors are installed at the entry and exit points of the main beam respectively. The INV300E data acquisition system is used to obtain the response data. The duration for each test is 30 seconds and the sampling frequency is 2024.292 Hz.

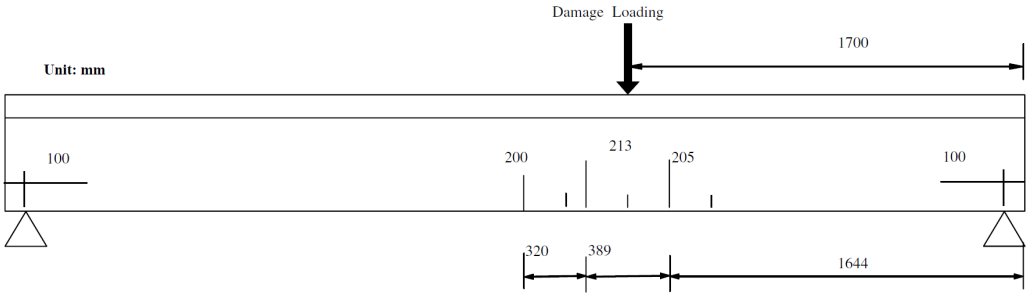

(a) Small damage

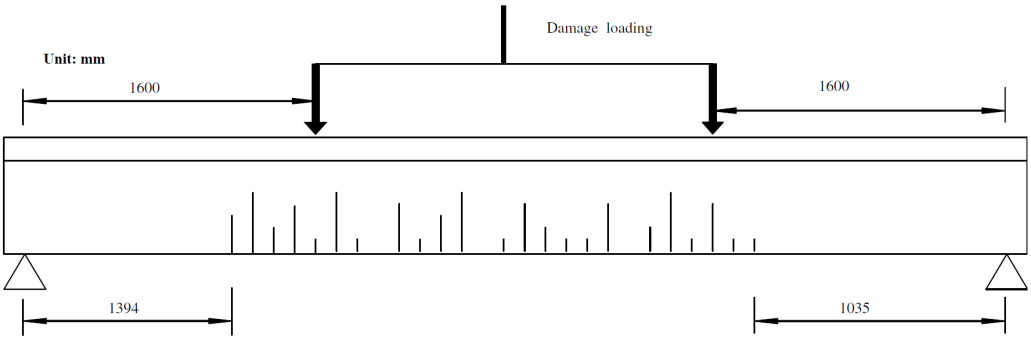

(b) Large damage

Figure 4-2. The damage loading and the crack zone

A three-point load system is used to create the damage. The small damage is created by deploying the load at the 1/3 L from the beam's right support as marked in Figure 4-2 (a). The load is gradually added with a 2 kN increment. Several tensile cracks are obviously appeared on the beam rib when the load reaches 36 kN. When the load is 50 kN, the largest crack at the beam's bottom is

measured as a 0.10 mm width. This crack is located close to the loading point but on the span inside with a 213 mm depth and a 760 mm wide crack zone visually. The beam is unloaded after the load is kept for 30 minutes. Then the crack at the beam's bottom decreases to a 0.025 mm width and closes partly. These descriptions are referred to as the small damage case.

For the large damage case, a 50 kN load is first loaded at the 2/3 L of the beam from the right support by the three-point load system. This produces a crack pattern similar in the extent and magnitude to the existing crack zone at the 1/3 L. After that, a four-point load system is used for a further loading as marked in Figure 4-2 (b). The final total load was 105 kN without the main reinforcement yielding and the largest crack is located near the beam's midpoint with a 281 mm depth. This crack is a 0.1 mm width at the beam's bottom when the load is 105 kN. When the beam is unloaded after keeping the 105 kN static load on the top surface for 30 minutes, this crack width reduces to 0.038 mm. The crack zone is 2371 mm long.

4.2 Results

4.2.1 The Gaussian window

Figure 4-3 shows the first eigenvalue curves under different moving vehicle models. Figure 4-3 (a) shows the results for the undamaged beam, and the beams with the small and large damage under a 10.6 kN moving vehicle. Figure 4-3 (b) shows the results under a 15 kN moving vehicle. The results show that the pattern of the first eigenvalue curve is severely affected due to the existence of measurement noise and the vehicle-bridge interaction. Measurement noise and the vehicle-bridge interaction are two main influencing factors for the first eigenvalue curve. Comparing Figure 4-3 (a) with Figure 4-3 (b), since the latter uses a 30% heavier vehicle, its curve is less affected by those influencing factors. The window length in these two cases is randomly selected with 54 sampling

intervals for a comparison and illustration. Therefore, following this idea, if a smaller window can be used, more components caused by the moving load can be extracted. However, due to the limitation of PCA algorithm, the window's length cannot be less than the number of input signal's channels. Additionally, a small window length may lose the important information caused by the moving loads. Thus, the Gaussian window is proposed.

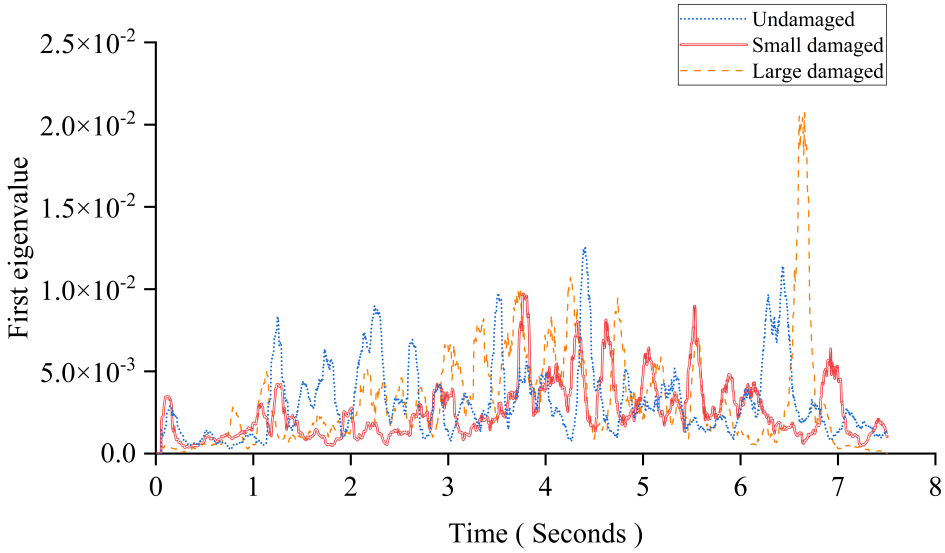

(a) The moving load is 10.6 kN

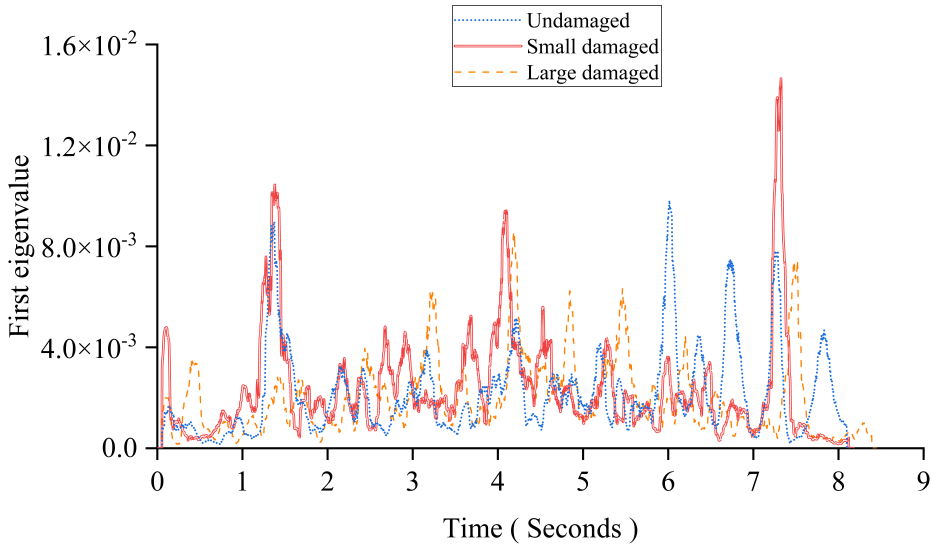

(b) The moving load is 15kN

Figure 4-3. The first eigenvalue curve in experimental study

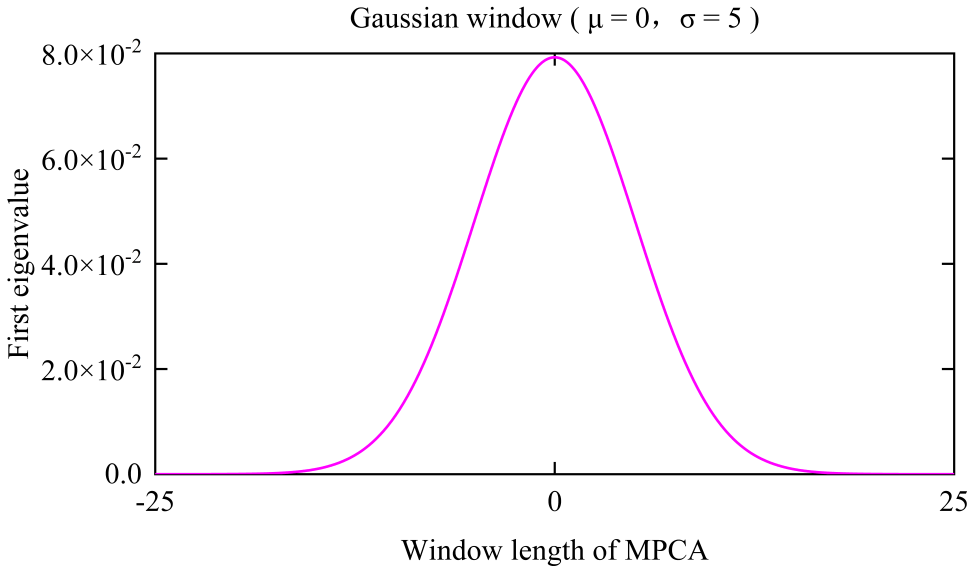

Figure 4-4. The Gaussian window

The Gaussian window draws on the idea of regularization. Figure 4-4 shows a Gaussian window (σ (0,5)) when the normal window's length is 50 sampling intervals. It is equivalent to add a penalty term: the farther the time is from the current moment, the smaller the impact on the current moment. The greater the weight in the middle, the deeper the consideration of instantaneous effects. The influencing factors' impact on the time axis is diffuse, so their effects can be significantly reduced by the Gaussian window and the proportion of the vehicle excitation in this window is magnified at the same time. In other words, PCA is a multi-channel data processing method and the additional normal moving window expands the eigenvalue along the time axis. Through the expansion of eigenvalues, not only the same overall movement trend of each measuring point on the bridge is displayed along the time axis, but also each interference factor is expanded on the time axis. Therefore, the Gaussian window realigns this expansion on the time axis again. This minimizes the effect of interference factors on the detection results.

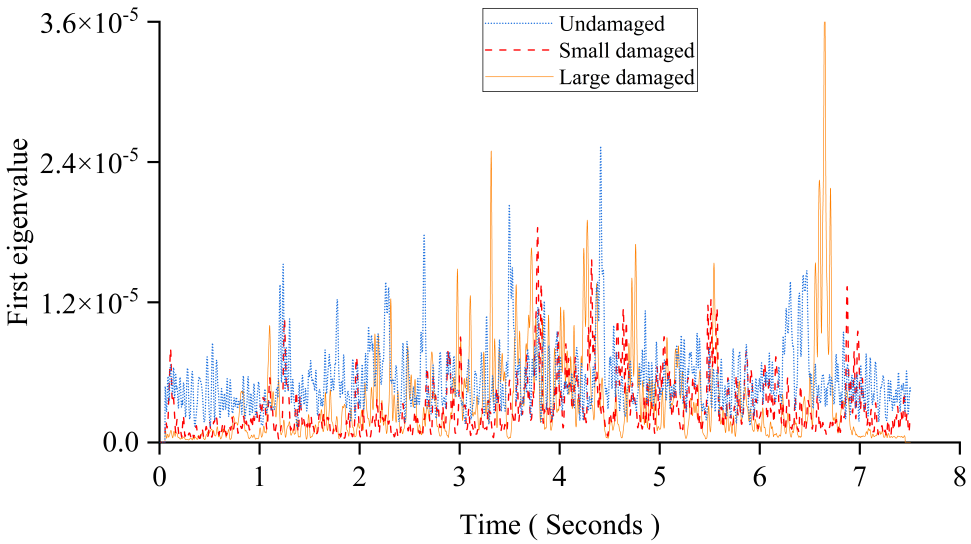

(a) The moving load is 10.6 Kn

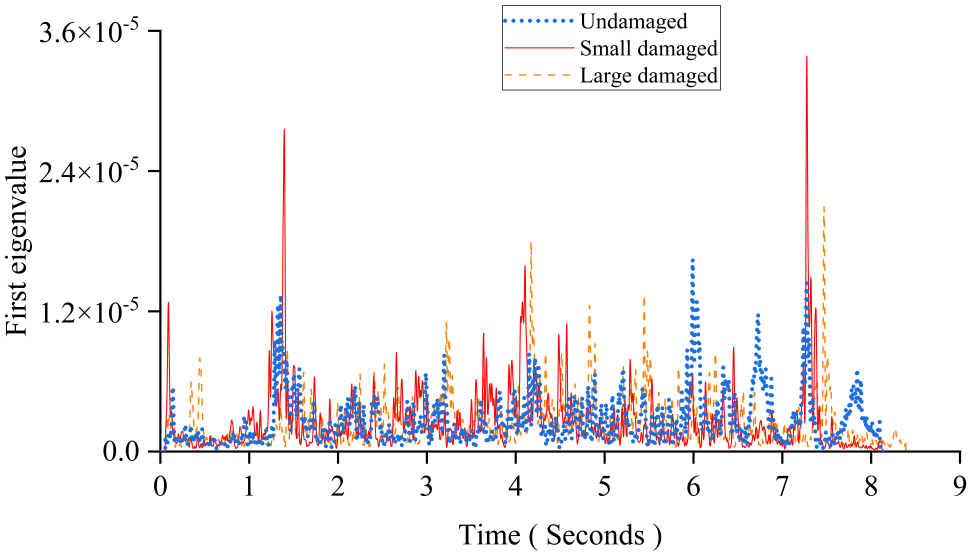

(b) The moving load is 15kN

Figure 4-5. The first eigenvalue curve with the Gaussian window in experimental study

In Figure 4-3, the first eigenvalue curve has many distortions or buckling caused by the noise, the vehicle bridge interaction or other factors like human interference or operational error. Figure 4-5 shows the first eigenvalue curves smoothed by the Gaussian window. The Gaussian window can reduce the effect from those factors and pay more attention on the data which are closer to the current time by giving more coefficient weight.

4.2.2 Parametric study

4.2.2.1 The effect of the window length

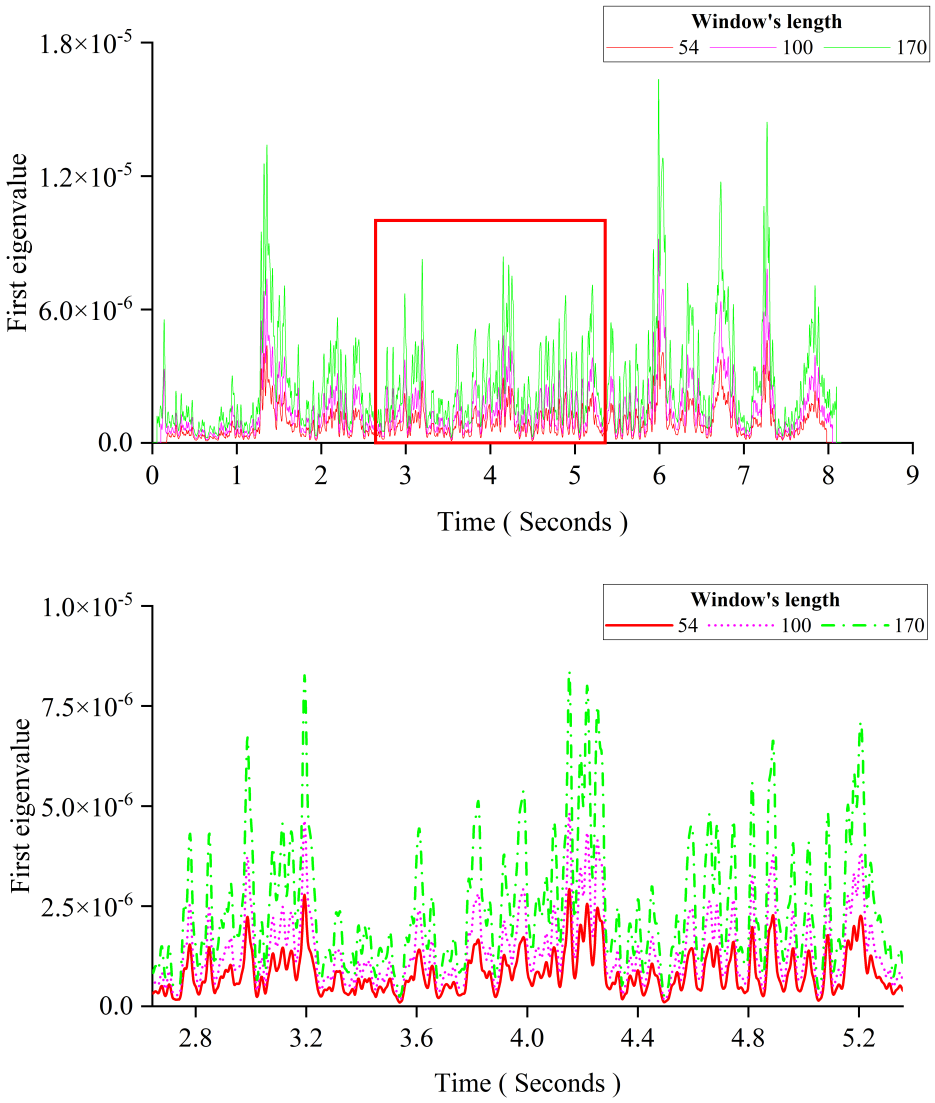

Figure 4-6. The effect of the Gaussian window's length

This section will discuss the selection of the window's parameters. The first is to investigate the influence of the window length on the first eigenvalue curve. In this section, the responses of the undamaged experimental beam under the 10.6 kN moving load are used. Figure 4-6 shows the first eigenvalue curves obtained under three commonly used lengths of the window. The image below is an enlarged view of the area in the red box of the image above. It is not recommended to use a length more than 200 times the sampling interval since a large window will greatly increase the MPCA's computational cost. From the first eigenvalue curves under different window lengths, we can see they have the same shape. Their only difference is the magnitude. The window length will not influence the damage detection since the damage influences the distance between each pair of adjacent peaks instead of the magnitude. Therefore, the second contribution of the Gaussian window is that it simplifies the problem of the window length's selection. The Gaussian window transforms the selection of the window length into the hyperparameter σ's selection of itself and allows the use of a small window to reduce the amount of calculation.

4.2.2.2 Hyperparameter of the Gaussian window

The choice of the hyperparameter σ will affect the Gaussian window's attention degree to the current moment and the tolerance of the influencing factors. If the value is too small, the anticipated effect cannot be achieved. If the value is too large, all the information carried in the data will be destroyed (only taking the value at the current time t into account). The numerical model is used to find the optimal value. The parameters of the simulated beam are same as Case 1 in Section 3.3.2 and the length for both normal and Gaussian windows is 50 sampling intervals.

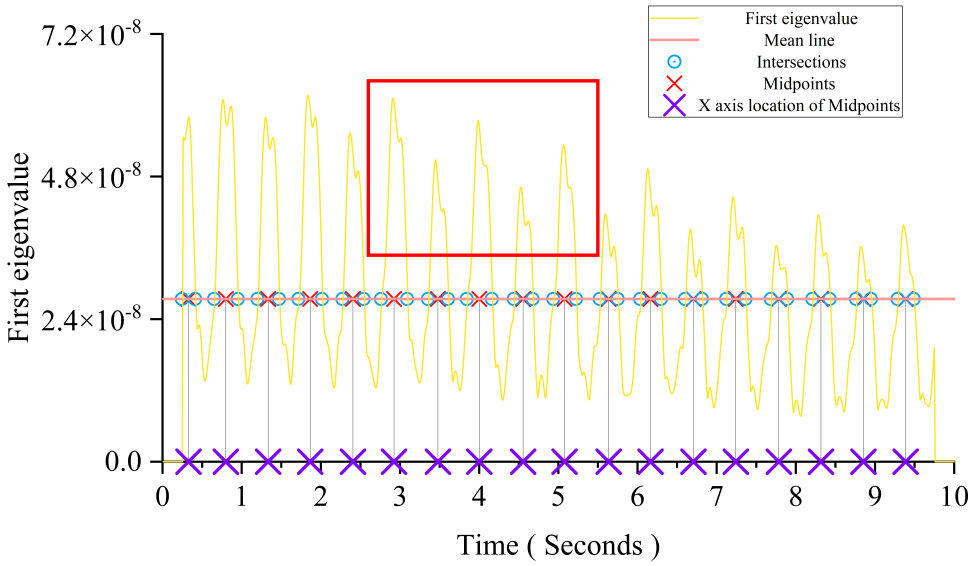

(a) Overall

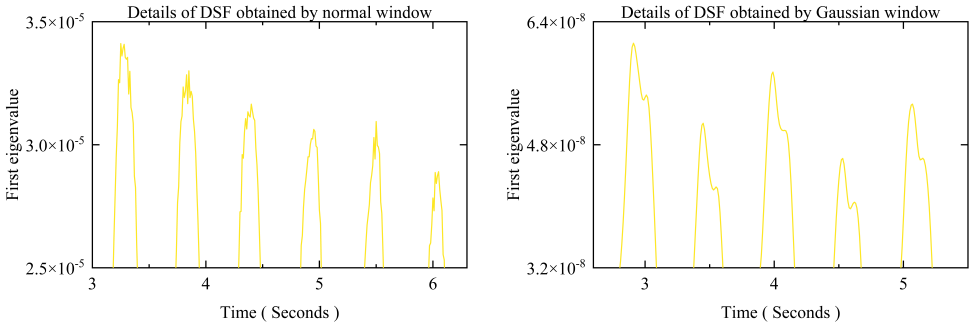

(b) Comparison of two windows' detail

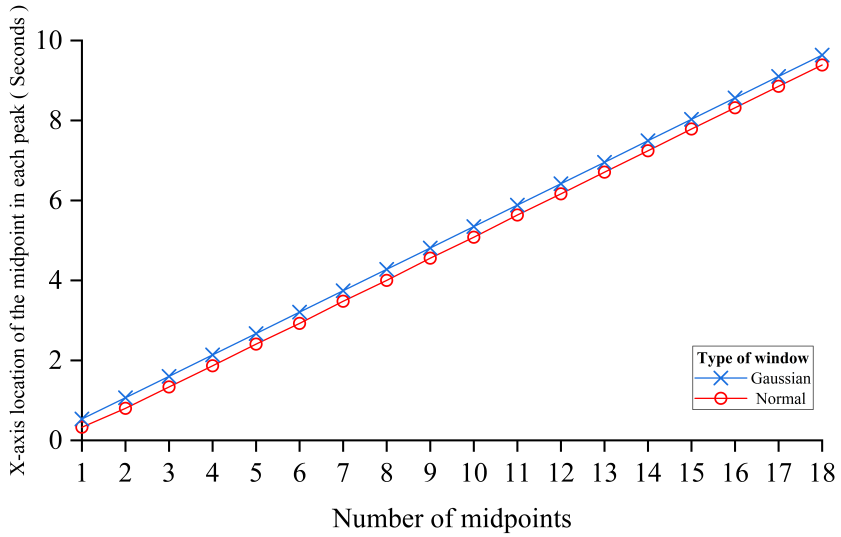

(c) Comparison of DSFs obtained by two windows

Figure 4-7. The result of numerical study proceeded by two types of window

Figure 4-7 (a) shows the first eigenvalue curve processed by the Gaussian window (σ (0,5)). Comparing with the curves in Figure 3-12, the curve obtained by the Gaussian window is much smooth. The Figure 4-7 (b) is the enlarged view of the area in the red box of Figure 3-12 and Figure 4-7 (a) correspondingly. Figure 4-7 (b) reveals that the Gaussian window can erase the distortions near the peak and trough areas of the first eigenvalue curve. Except for the window's type, the damage conditions and other parameters for obtaining the DSFs in Figure 3-12 and Figure 4-7 (a) are the same. Figure 4-7 (c) shows that the DSFs obtained by the normal window and the Gaussian window are almost the same. They both have the same gradient which could be an indicator of the beam's damage extent. Thus, the σ (0,5) can be used as the optimal hyperparameter of this study. The Gaussian window (σ (0,5)) can smooth the first eigenvalue curve without affecting the accuracy of the DSF for eliminating the influence of interference factors.

4.3 Experimental results and discussions

Figure 4-8 shows that the proposed DSF can distinguish the beam's damage extent well on the experimental dataset. Since the heavier vehicle can better excite the response due to the crack, the result in Figure 4-8 (b) is better than Figure 4-8 (a) in distinguishing the damage extent. Due to the existence of the elastic spring, the wheel can better maintain the contact with the concrete surface. The result in Figure 4-8 (b) is smoother and more continuous than that in Figure 4-8 (a). The size of the gradient reflects the "rhythm" of the beam. The cracks weaken the effective cross-sectional area of the beam, thereby hindering the transmission of information in the beam. In this case, the speed at which the first eigenvalue reaches each local extreme value will slow down and the gradient will become larger. Due to the existence of the elastic spring, part of energy in the response is transferred in the beam using the vehicle as the

transmission path. This leads to an increase in the information transmission bandwidth of the beam. When a visible crack zone occurs in the beam, the load in this area will be more borne by the steel bars. Since the vehicle in Figure 4-8 (b) is 30% heavier than the one in Figure 4-8 (a), this phenomenon will become deeper as the load increases. Since the load carried by the steel bars increases as the cracks deepen, the overall "rhythm" of the beam becomes faster and the gradient becomes smaller. Thus, these two points will reverse the change pattern of the DSF when the cracks grow but require a further study.

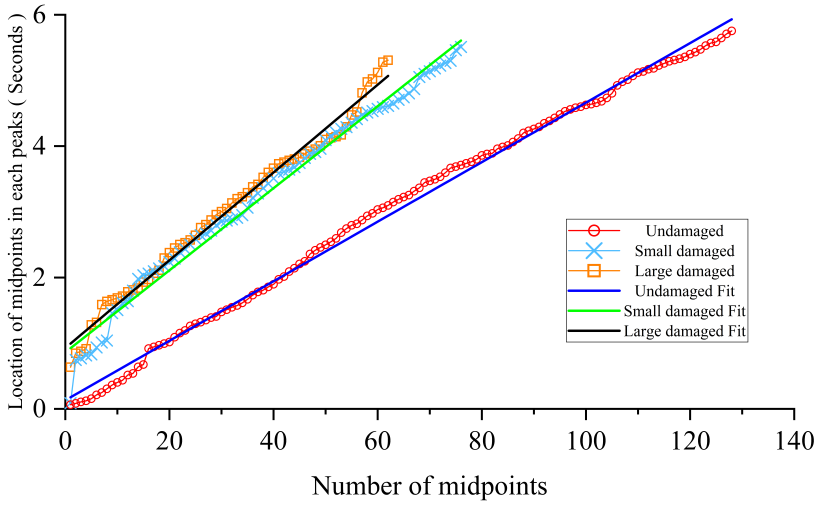

(a) The moving load is 10.6 kN

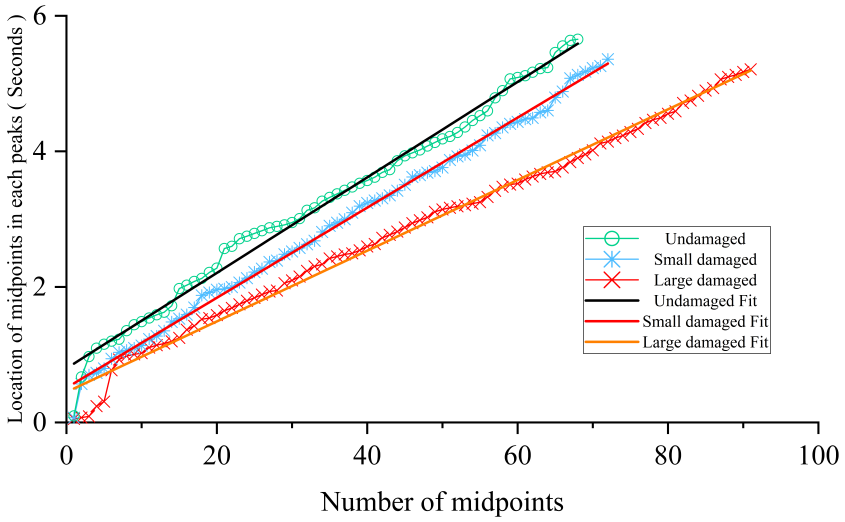

(b) The moving load is 15kN

Figure 4-8. The result of proposed DSF

4.4 Summary

- Experimental setup

This experimental study is a laboratory test. The whole experimental beam is composed of three T-section reinforcement concrete beams and the main beam which is the subject for the damage detection is 5.0 m long. The vehicle is at a speed of approximately 0.5 m/s. Three different damage cases (the undamaged, small and large damage) with two different vehicles' weight are used to verify the proposed damage sensitive feature. The elastic spring is deployed on the heavier vehicle to simulate the real vehicle axle load.

- Gaussian window

The existence of measurement noise and the vehicle-bridge interaction (VBI) will severely affect the result of the proposed damage sensitive feature. Therefore, a new type of the window called the Gaussian window is proposed for MPCA. This window gives more weight to the data near the current moment t on the time axis to pay more attention on the same movement trend caused by the vehicle movement. The addition of a Gaussian distribution to the window realigns the components expanded by the normal window on the time axis. By the parametric study on the numerical model and experimental data, this window can achieve the following without affecting the detection accuracy:

1. Reduce the influence of these factors (e.g., noise or VBI) that are more diffused on the time axis.

2. Simplify the problem of the window length's selection to the selection of the Gaussian window's hyperparameter.

3. Reduce the computing cost.

- The selection of the hyperparameter of the Gaussian window

The choice of the hyperparameter σ represents the attention of the Gaussian window to the current moment and the tolerance of the influencing factors. The selection of this hyperparameter is related to many factors: the length of bridge, distribution of measuring points, accuracy of sensors, interference degree of environmental factors, vehicle weights, traffic flow and so on.

The responses of the undamaged experimental beam under the 10.6 kN moving load in Section 4.2.2.1 are used as an example. Referring to Section 3.4.1, there are two major criteria for the selection of the hyperparameter σ:

1. Cleanly strip as many of the accompanying peaks as possible from the main peaks. This is to clearly expose each peak's two limbs that are the critical principal components of the first eigenvalue curve.
2. The mean line of the first eigenvalue curve should intersect the peaks obtained in the previous step as many as possible.

Figure 4-9 shows the first eigenvalues curve processed by the Gaussian window under different hyperparameters σ to illustrate the two criteria mentioned above. The image above in each subpicture of Figure 4-9 is the entire eigenvalue curve. The image below in each subpicture is an enlarged view of the area in the red box of the image above in each subpicture of Figure 4-9, correspondingly.

In the case of $\sigma=1$ in Figure 4-9 (a), the value of σ is too small. In the enlarged view, there are still many accompanying peaks at the two limbs of each main peak. This causes many jagged distortions in the desired two limbs and seriously affects the extraction of the midpoints. Additionally, the accompanying peak and the main peak are entangled without a clear separation. In this way, the effect of increasing the attention degree to the same instantaneous movement trend of the beam cannot be achieved. In other words, some disturbing factors still occupy a certain proportion in the first eigenvalue curve.

In the case of σ=5 in Figure 4-9 (b), the Gaussian window successfully smooths the desired two limbs. The accompanying peaks are stripped clean to the greatest extent, and the mean line can smoothly intersect each main peak without the interference. Therefore, σ=5 is the most ideal hyperparameter value for this study and is adopted accordingly.

Admittedly, in the case of σ=9 in Figure 4-9 (c), the Gaussian window can also distinguish the damage extent of the beam. But this does not mean that the larger the value of the hyperparameter, the better the effect. Firstly, overly large hyperparameters will further reduce the position of the mean line. This makes the mean line miss the chance to intersect some of the peaks and lose the information about those peaks. Secondly, in the enlarged view, some not negligible main peaks are also stripped away. The excessively large hyperparameter overemphasizes the Gaussian window's attention degree to the current moment, so that the causal continuity of the entire vibration process in the time dimension is ignored. In this way, key information may be lost in some cases, thereby affecting the accuracy of the results.

In short, when the two criteria are satisfied, the hyperparameter value can be flexibly selected according to the actual situation of the bridge without affecting the DSF's results.

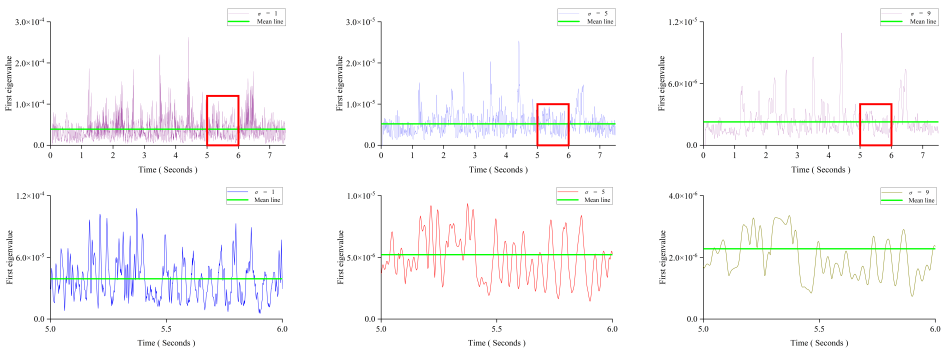

(a) $\sigma = 1$ (b) $\sigma = 5$ (c) $\sigma = 9$

Figure 4-9. The first eigenvalue curves under different hyperparameters

- Results and discussion

The result shows that the proposed damage sensitive feature can distinguish the damaged extent of the beam under the different vehicle weights. In the discussion part of the experimental results, several vehicle conditions that affect the change pattern of the damage sensitive feature are discussed. These conditions can be used as the entry point for a more in-depth study of the proposed damage sensitive feature.

Chapter 5 Field study

To further verify the proposed method in Chapter 3, the field bridge monitoring data are used. In this chapter, the bridge monitoring system and collected data for analysis are introduced. The detection results are introduced according to different environmental conditions separately. The discussion summaries these results from the different environments for comparison.

5.1 Introduction

(a) Field bridge model

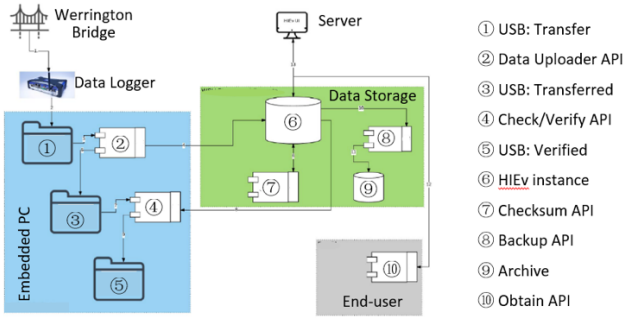

(b) Data acquisition and stroage

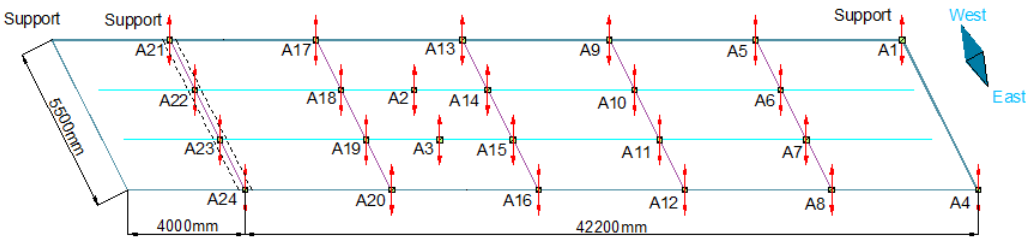

(c) Sensor locations

Figure 5-1. The monitoring system of a cable-stayed bridge

Figure 5-1 (a) shows the cable-stayed bridge located in Werrington, New South Wales, Australia. The bridge is over the Great Western Highway with a span 46 m. It is a single lane highway bridge with a 5 meters width. The bridge has been fully instrumented with a wired monitoring system in 2016 through the collaboration project with DATA61. There are totally 64 channels in the monitoring system including 31 channels for accelerations, 31 channels for strain, one for temperature and one for optical sensors to detect the presence of vehicles. There are 24 accelerometers on the bridge deck and Figure 5-1 (c) shows the sensor locations. The data acquisition system continuously records the data in the local computer from sensors with a 600 Hz sampling rate. The recorded data can be uploaded to the central storage through the fibre optic cable. Details of the data acquisition and storage system are shown in Figure 5-1 (b). With support from DATA61, the data collected from this bridge system since 2016 is available for verifying the methods developed.

5.2 Data pre-analysis

The single A-shaped steel tower is connected to the bridge deck by 16 stay cables with a semi fan arrangement. The bridge has a composite steel-concrete deck with four I-shape beam steel girders. A group of evenly separated cross girders are used to attach these girders internally. As a connection between two campuses of Western Sydney University, numerous different vehicles pass this bridge at various speeds from two directions. In this study, two acceleration signals of the bridge at different times on February 11, 2017, are used for analysis. A series of information such as the vehicle weight, vehicle speed, driving direction or passing time are unknown. This is closer to the actual bridge health monitoring scene and can better reflect the value for the practical use of this method.

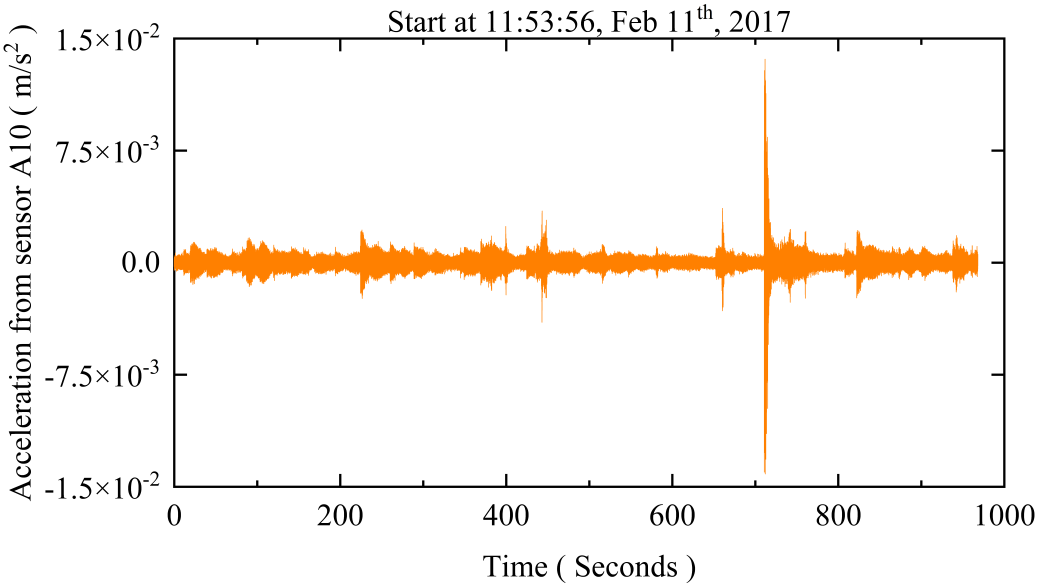

(a) Sample 1

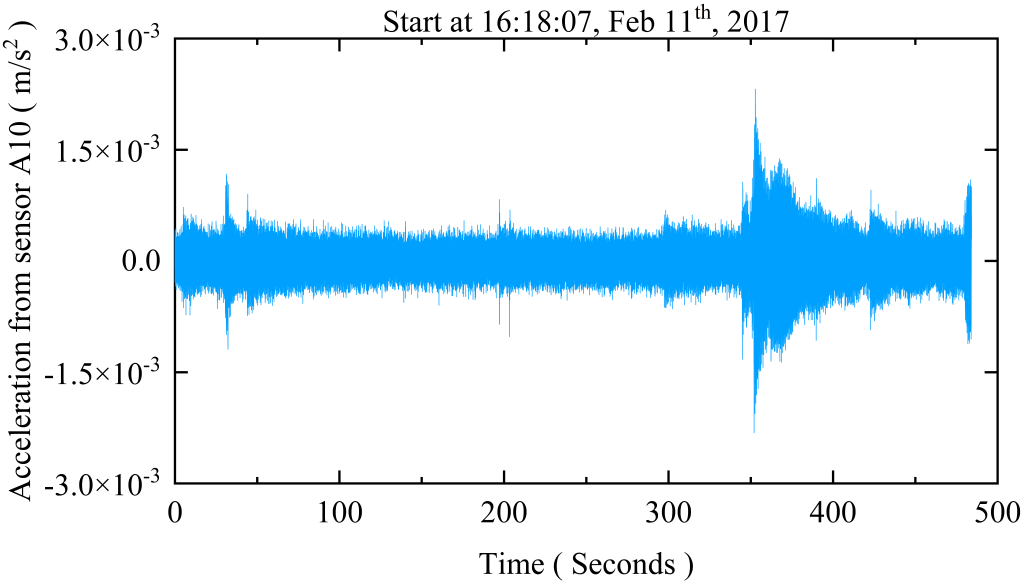

(b) Sample 2

Figure 5-2. Monitored data for analysis

Figure 5-2 shows the two segments of the acceleration signal monitored by Sensor A10. In Figure 5-2 (a), the signal starts at 11:53:56 and lasts 968 seconds. In Figure 5-2 (b), the signal starts at 16:18:07 and lasts 484 seconds. On February 11, 2017, the average temperature in Sydney was 31 degrees at 12 noon and 38 degrees at 4 p.m. The responses fall into three categories in terms of the magnitude: a) 10 to the negative 4th power corresponds to the response when no vehicle is on the bridge. b) 10 to the negative 3rd power corresponds to the response of small vehicles passing the bridge. c) 10 to the negative 2nd power corresponds to the response of the large vehicle passing the bridge. In Figure 5-2 (a), a large vehicle entered the bridge at 710 seconds. The following discussion of the data is based on this classification. In this field study, the window of MPCA is the proposed Gaussian window with 54 sampling intervals' length and the hyperparameter σ (0,5).

5.3 Results

5.3.1 No vehicle on the bridge

Two 10-second-long acceleration signals are intercepted from the monitored data for studying the pattern of the first eigenvalue curve when there is no vehicle on the bridge. Figure 5-3 (a) shows the first segment of the signal intercepted from the signal showed in Figure 5-2 (a). The start time of this first segment is located 640 seconds after the start time of the signal in Figure 5-2 (a). Figure 5-3 (b) shows the second segment of the signal intercepted from the signal showed in Figure 5-2 (b). The start time of this second segment is located 280 seconds after the start time of the signal in Figure 5-2 (b). The data of sensors A6, A10, A14 and A18 are used as the input data of MPCA.

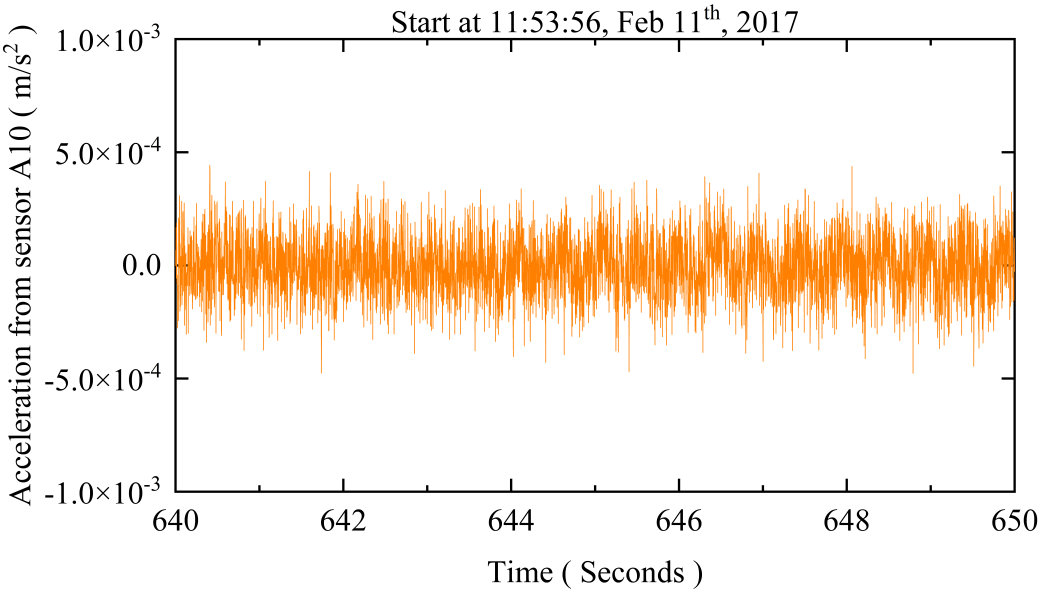

(a) Sample 1

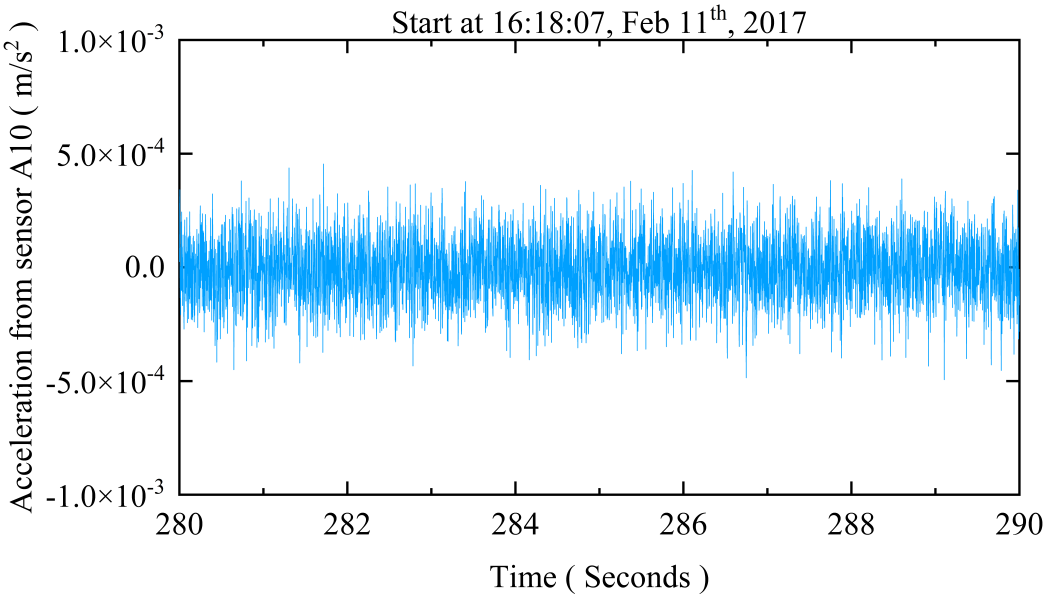

(b) Sample 2

Figure 5-3. Accelerations when no vehicle on bridge

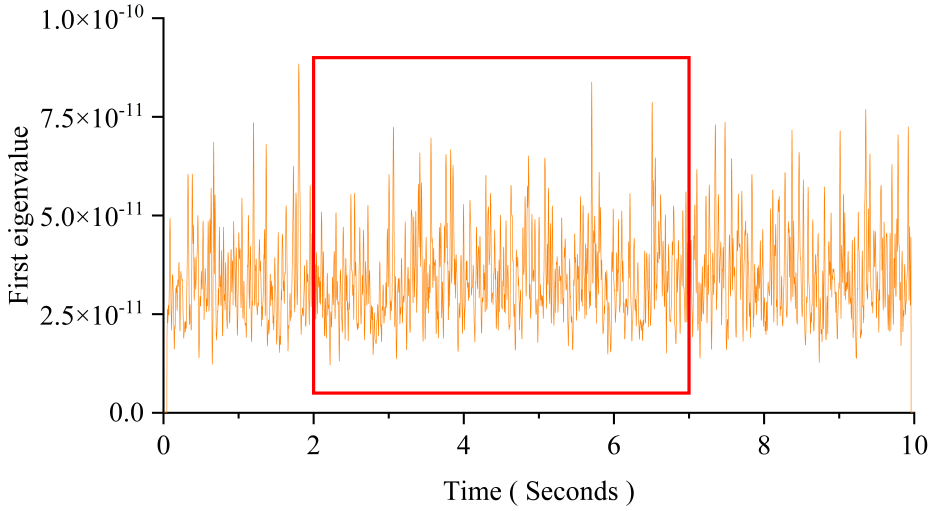

(a) MPCA for Figure 5-3 (a)

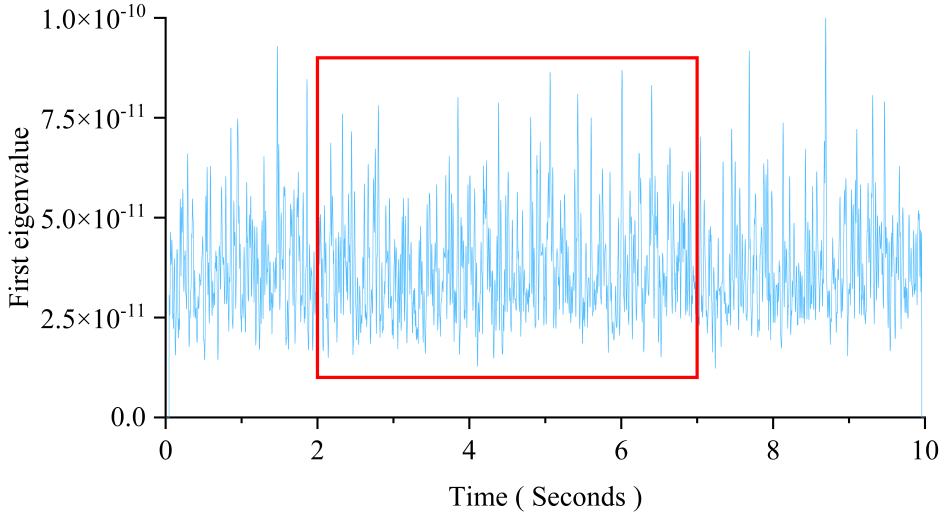

(b) MPCA for Figure 5-3 (b)

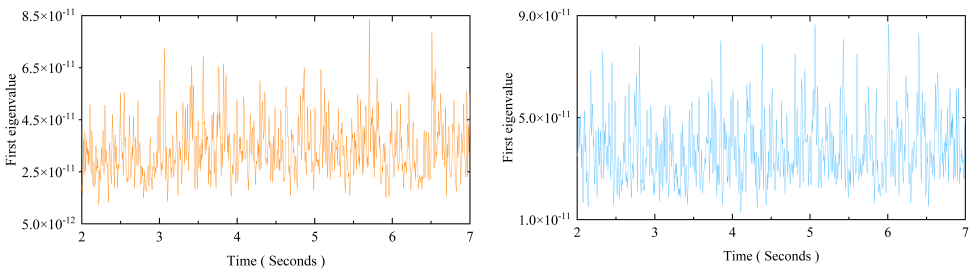

(c) Eigenvalue curves

Figure 5-4. The first eigenvalue curve when no vehicle on bridge

Figure 5-4 shows the obtained results by MPCA from the signals in Figure 5-3. The input data of Figures 5-4 (a) and (b) correspond to Figures 5-3 (a) and (b), respectively. The Figures on the left- and right-hand side in Figure 5-4 (c) are enlargements of the eigenvalue curves from the second to seventh seconds in the red box of Figures 5-4 (a) and (b), respectively. When no vehicle is on the bridge, the first eigenvalue curve fluctuates randomly within a single order of the magnitude. Without an obvious external excitation, the first eigenvalue curve has no obvious change pattern.

5.3.2 A single small vehicle passing the bridge

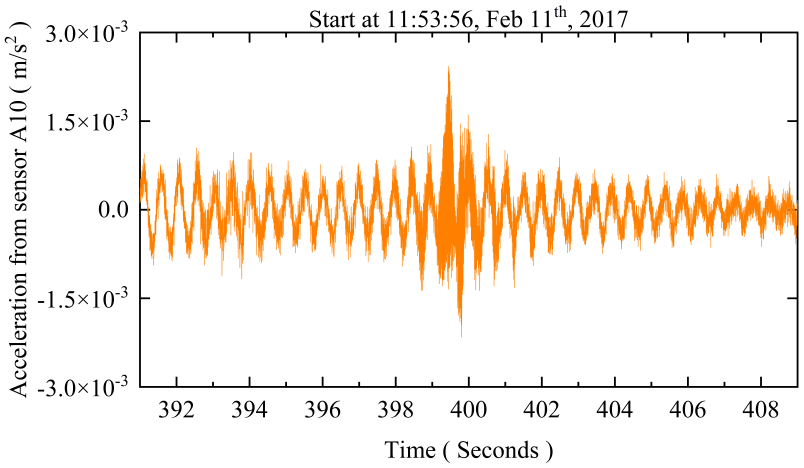

(a) The first segment of the signal in Figure 5-2 (a)

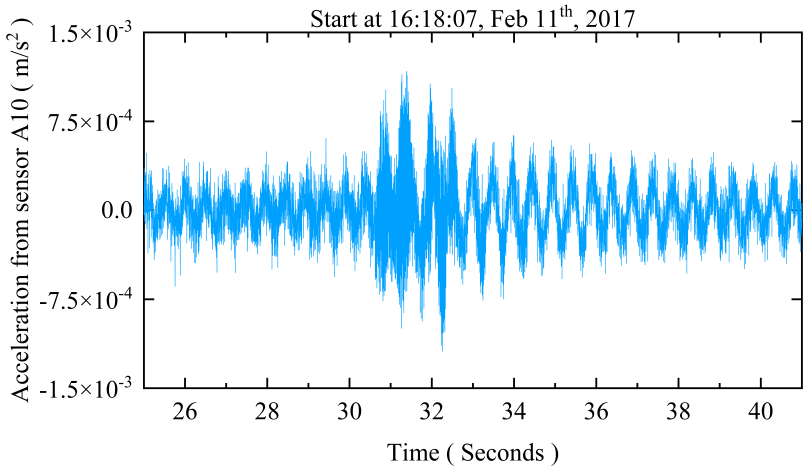

(b) The second segment of the signal in Figure 5-2 (b)

Figure 5-5. Accelerations when a single small vehicle passing bridge

Two 5-second-long acceleration signals are intercepted from the monitored data for studying the pattern of the first eigenvalue curve when there is a small vehicle passing the bridge. Figure 5-5 (a) shows the first segment of the signal intercepted from the signal showed in Figure 5-2 (a). The start time of this first segment is located 397 seconds after the start time of the signal in Figure 5-2 (a). Figure 5-5 (b) shows the second segment of the signal intercepted from the signal showed in Figure 5-2 (b). The start time of this second segment is located 30 seconds after the start time of the signal in Figure 5-2 (b). The data of sensors A6, A10, A14 and A18 are used as the input data of MPCA.

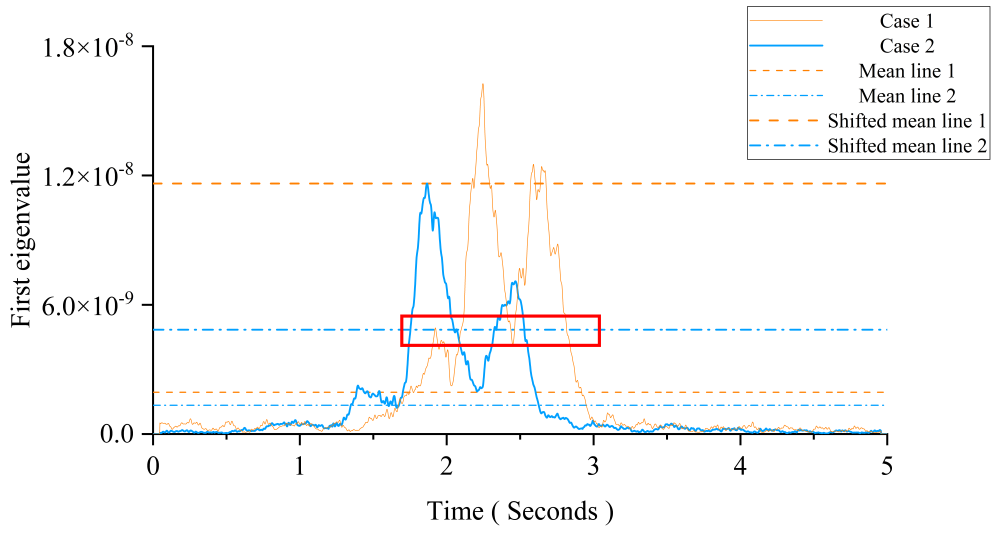

Figure 5-6. The first eigenvalue curve when a single small vehicle passing bridge

As mentioned earlier (Section 3.4.3), for simply supported beams, the uniaxial moving load is sufficient for MPCA to capture a continuous peak fluctuation of the same magnitude in the first eigenvalue curve. In this field study, a single vehicle is not sufficient to excite continuous peak fluctuations in the first eigenvalue curve. Due to the existence of the stay cables, only the continuous

passing of vehicles can ensure that the overall acceleration trend of the bridge is consistent. This phenomenon can be observed in the next section. But the transient effects caused by the entry of a single vehicle are enough for MPCA to extract the valuable information from them.

Figure 5-6 are the obtained results by MPCA from Figure 5-5. The input data of Cases 1 and 2 in Figure 5-6 correspond to Figures 5-5 (a) and (b), respectively. It can be seen from the peak height that the vehicle weight of Case 1 is larger than that of Case 2. From the peak distance and vehicle type (the distance between the front and rear axles of a small vehicle is 3 meters), it can be estimated that the speed of two vehicles when they are entering the bridge is 27 km/h and 18 km/h respectively. In order to make the mean line cut to the only two peaks, the original mean lines of Cases 1 and 2 (dashed line) are shifted to the appropriate positions (bold line). The intercepted results will be discussed together in Section 5.3.5.

5.3.3 Small vehicles passing the bridge continuously

Two 10-second-long acceleration signals are also intercepted from the monitored data for studying the pattern of the first eigenvalue curve when small vehicles enter the bridge continuously. Figure 5-7 (a) shows the first segment of the signal intercepted from the signal showed in Figure 5-2 (a). The start time of this first segment is located 224 seconds after the start time of the signal in Figure 5-2 (a). Figure 5-7 (b) shows the second segment of the signal intercepted from the signal showed in Figure 5-2 (b). The start time of this second segment is located 352 seconds after the start time of the signal in Figure 5-2 (b). The data of sensors A6, A10, A14 and A18 are used as the input data of MPCA.

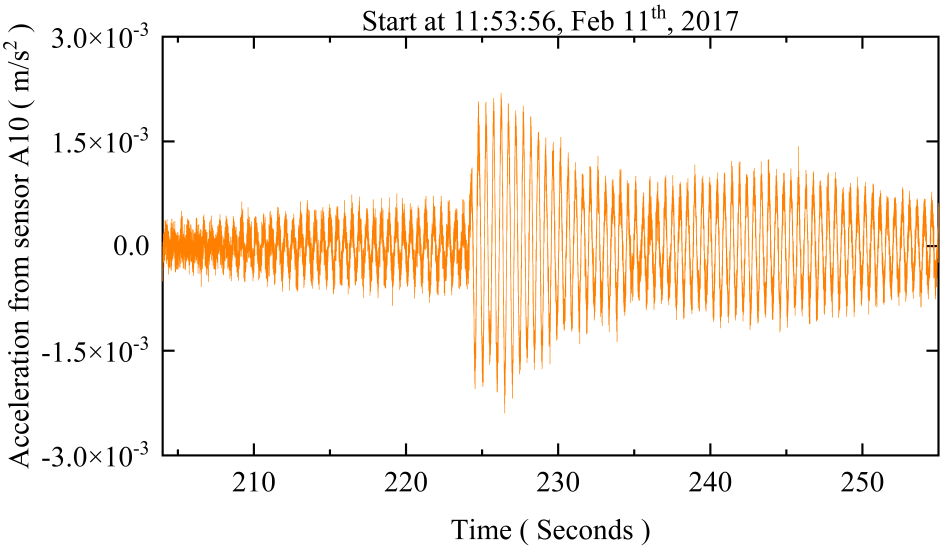

(a) The first segment of the signal in Figure 5-2 (a)

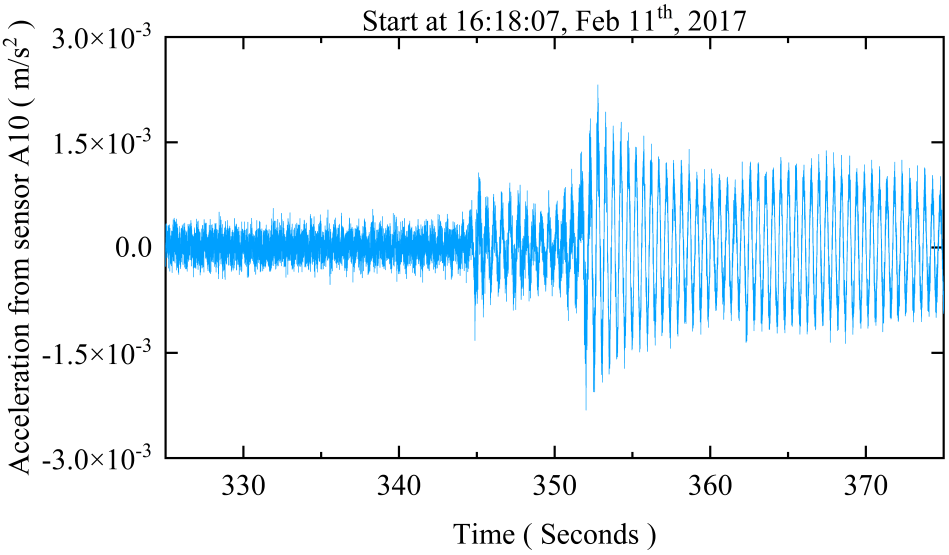

(b) The second segment of the signal in Figure 5-2 (b)

Figure 5-7. Accelerations when small vehicles passing bridge continuously

Figure 5-8 are the obtained results by MPCA from Figure 5-7. The input data of Cases 1 and 2 in Figure 5-8 correspond to Figures 5-7 (a) and (b), respectively. The change pattern of the first eigenvalue curve in Figure 5-8 is in accordance with the result in the numerical study. In Case 2, the eigenvalue curve shows a

slow downward trend, which reflects that the vehicles are crossing the bridge one after another. The small fluctuations in the downtrend are due to the fact that the load of a small vehicle is two-axle. In the numerical simulation, a single moving force is considered as the excitation of the bridge. The entry of the second axle will generate a slight recovery in the downtrend. Within the first five seconds of Case 1, the total mass of vehicles passing on the bridge is greater than Case 2. The peak value of the eigenvalue curve drops rapidly in the first second of Case 1. This shows that the vehicle entering in this second is faster. About the 2 s of Case 1, the peak value of the eigenvalue curve shows an upward trend. This means that the rear axle of the vehicle entering in this second weighs more than the front axle. In the third second of Case 1, another car got on the bridge. The weight of this car is relatively close to the one entered the bridge in the first second. These discussions illustrate that this method also has the potential for moving load identification but requires a further study.

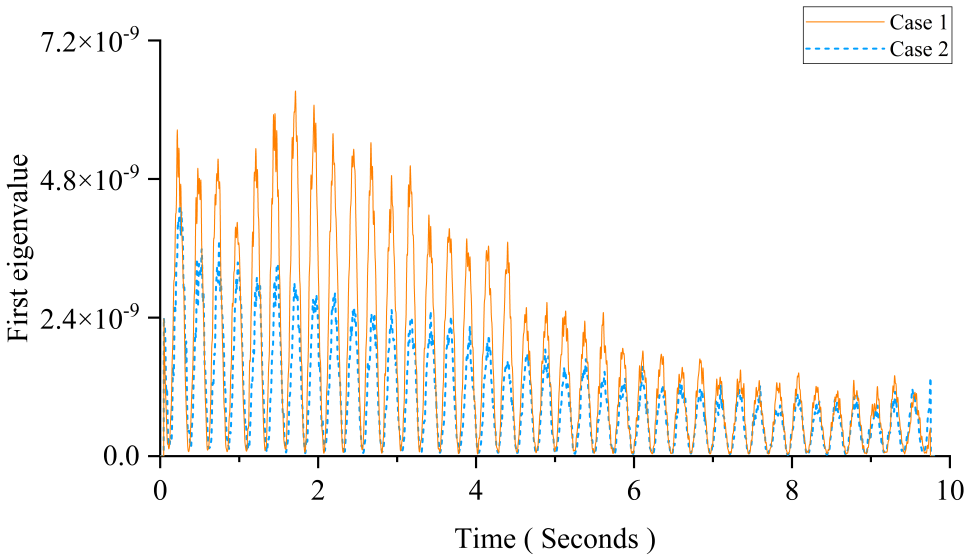

Figure 5-8. The first eigenvalue curve when small vehicles passing bridge continuously

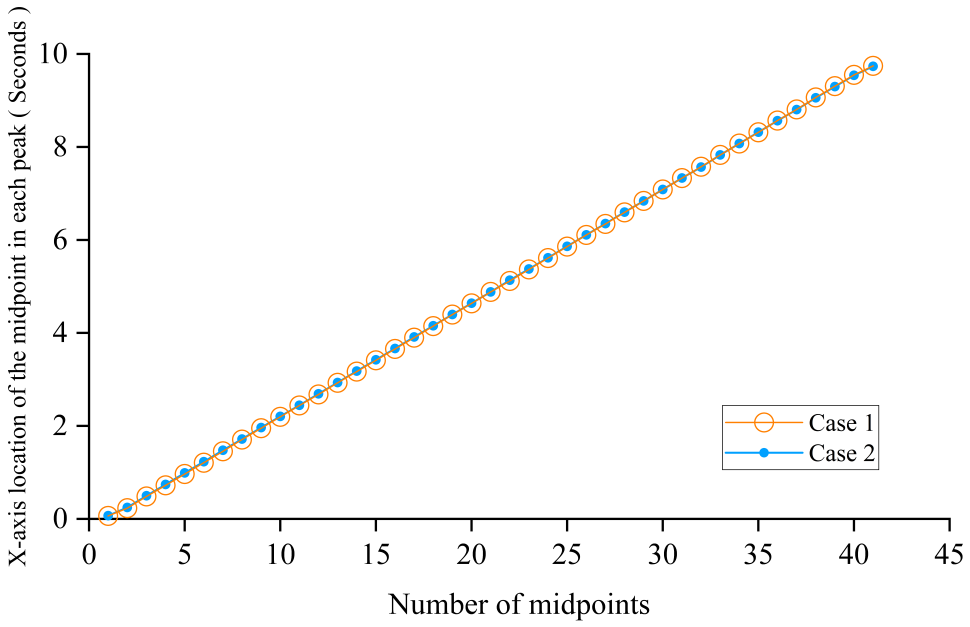

Figure 5-9. The DSF when small vehicles enter bridge

Figure 5-9 is the obtained DSFs from Figure 5-8. In the case of the different temperature, vehicle speed and vehicle weight, the results obtained from two cases are consistent. The average temperature of Sydney in Case 2 (4 p.m.) is 7 degrees Celsius higher than in Case 1 (12 noon). During these four hours, the increase in the average temperature is mainly caused by the intense sun exposure in midsummer. The larger vertical temperature difference caused by the strong sunlight increases the bending stiffness of the bridge. Therefore, the effects of the average temperature increase and vertical temperature difference offset each other on the DSF. The midpoints in both cases form a straight line since the steel I-beams are closer to the continuum assumption than reinforced concrete. This agrees with the results in the numerical study. This also shows that the integrity of the bridge movement is good and the bridge is in a healthy condition. Within a certain range, the variation of the vehicle weight will not affect the DSFs.

5.3.4 A single large vehicle passing the bridge

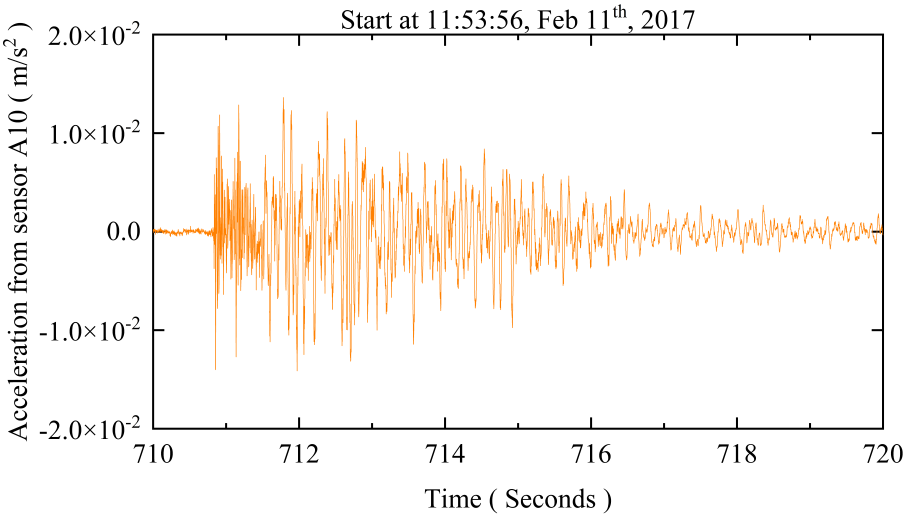

Figure 5-10. Acceleration when a single large vehicle passing bridge

A 5.7-second-long acceleration signal is intercepted from the monitored data for studying the pattern of the first eigenvalue curve when a large vehicle enters the bridge. Figure 5-10 shows the segment of the signal intercepted from the signal showed in Figure 5-2 (a). The start time of this segment is located 710 seconds after the start time of the signal in Figure 5-2 (a). The selection of sensors is divided into two groups. The first sensor group is A6, A10, A14 and A18 and the second is A7, A11, A15 and A19. The data of two sensor groups are respectively used as the input data of MPCA.

Figure 5-11 are the obtained results by MPCA from Figure 5-10. The first eigenvalue curve shows that it is a large two-axle vehicle. Similar to the results in Section 5.3.2, a single large vehicle is not enough to excite the motion of the bridge as a whole. The pattern of the eigenvalue curve in Figure 5-11 is different from the one in Figure 5-8. This difference reveals that the passage of a large vehicle on the bridge brings more local excitation effects. This phenomenon will be detailed discussed in the next section. The peak caused by the rear axle is higher than the front axle, indicating that the rear axle is heavier than the front axle of this car. The peak induced by the rear axle in the second group is greater

than the one at the same time in the first group, which indicates that the centroid of the vehicle is closer to the side of the second group sensors while passing the bridge. From the distance between two peaks on the time axis, it can be estimated that the vehicle's speed is at least 40 km/h. Also, to make the mean lines cut to the only two peaks, the original mean lines of Groups 1 and 2 (dashed line) are shifted to the appropriate positions (bold line). The intercepted results will be discussed together in the next section.

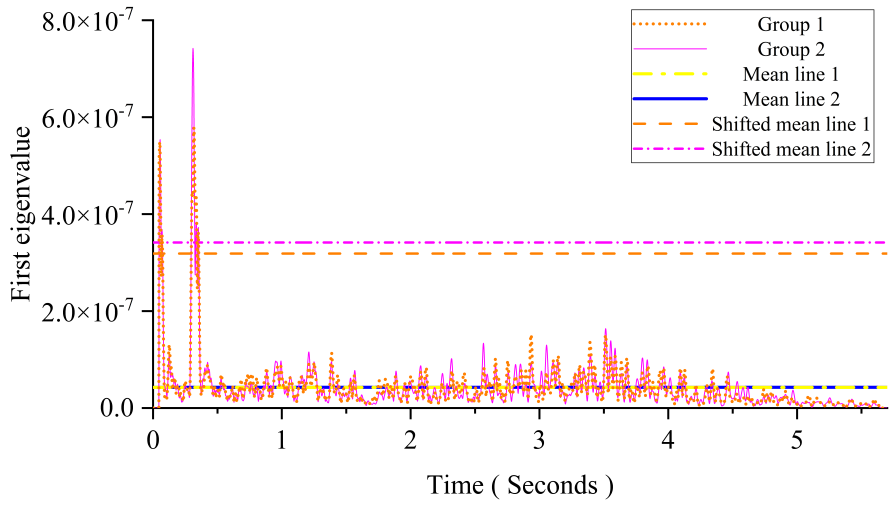

Figure 5-11. The first eigenvalue curve when a single large vehicle passing bridge

5.3.5 Discussion

Table 5-1 summarizes the value of the features from Sections 5.3.1 to 5.3.4 for comparison. The classification of vehicles and time is consistent with Section 5.2. The classification of sensors' group is consistent with Section 5.3.4. The DSF's value in Table 5-1 is calculated from the gradient of the DSF line by the arc tangent function.

Table 5-1. Comparison of DSF's value

Vehicle	Quantity	Time	Sensor group	Origin mean line	Shifted mean line
No		12 noon	1	1.5269225	
			2	1.5289591	
		4 p.m.	1	1.5319806	
			2	1.5268278	
Small	Single	12 noon	1		1.5614776
			2		1.5625422
		4 p.m.	1		1.5618204
			2		1.5625856
Large		12 noon	1		1.5561754
			2		1.5514023
Small	Continuously	12 noon	1	1.5639835	
			2	1.5639855	
		4 p.m.	1	1.5639658	
			2	1.5640453	

- When no vehicle on the bridge

The bridge is in a state of random vibration when there is no vehicle on the bridge. In this state, the vibration of each measuring point on the bridge has no obvious trend, so the eigenvalue curve fluctuates frequently and the value of the proposed DSF with the magnitude of the first eigenvalue curve is at a local minimum. The value under this state can be regarded as the ground state value of the bridge vibration.

- When a single small vehicle on the bridge

In this study, since it is difficult for a single vehicle to excite the bridge as a whole, the obtained value of the DSF depends on many factors. This allows us to extract the useful information from the peaks corresponding to the transient effects.

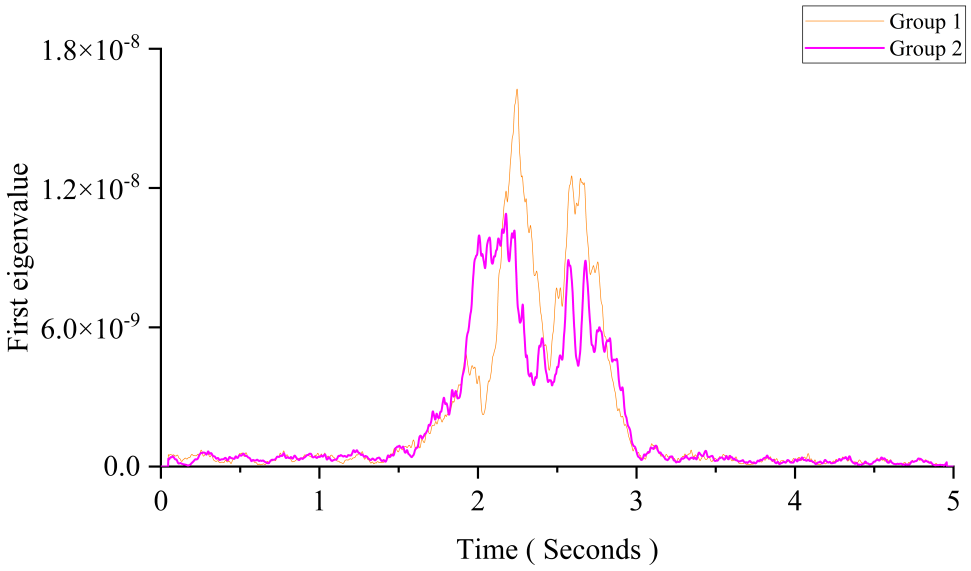

(a) 12 noon

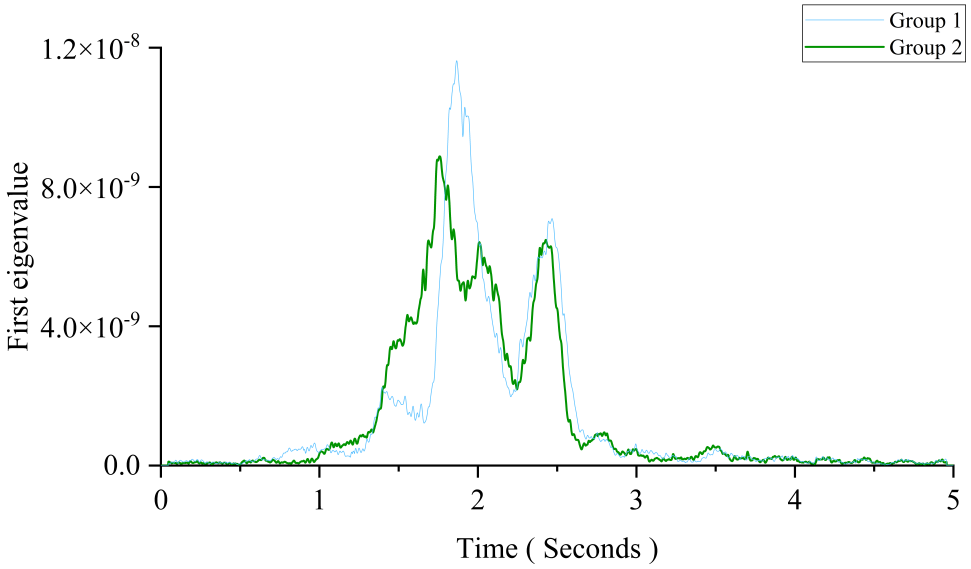

(b) 4 p.m.

Figure 5-12. Comparison of peak's height when the single small vehicle passing bridge

From the height of peaks, it can be judged which group of sensors is closer to the vehicle that is entering the bridge. Figure 5-12 compares the peaks corresponding to different sensor groups when the same vehicle enters the bridge. Figures 5-12 (a) and (b) correspond to the different vehicles enter the bridge at 12 noon and 4 p.m., respectively. In both cases, the peak's height of the first sensor group is higher than that of the second sensor group. This reflects that the centroids of both vehicles are closer to the first group of sensors when entering. Figure 5-12 also reveals that the peak excited by the same vehicle shares a similar change pattern.

Only two main peaks can be detected in the first eigenvalue curve when a single small vehicle is passing the bridge. Sometimes the mean line cannot ideally reach the two limbs of each peak. So it is necessary to shift the mean line to an appropriate position. Generally, four intersected midpoints are enough to accurately reflect the information of the vehicle and the bridge. These midpoints contain the intersections of the main peaks and several accompanying peaks attached on the main peaks. Peaks of different scales are induced by different influencing factors. The DSF obtained from these midpoints can reflect the overall condition of the bridge and the information of the vehicle.

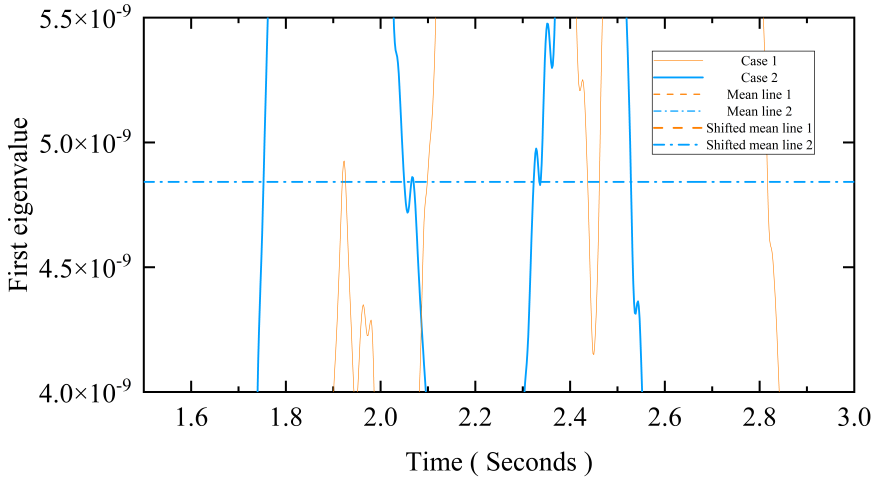

Figure 5-13. Local detail of Figure 5-6

Figure 5-13 is the enlarged view of the area in the red box of Figure 5-6. It shows two intercepted peaks that are not easily visible in Case 2 of Figure 5-6. The number of intersected midpoints for all single vehicle cases in this study is 4. In Table 5-1, the first sensor group's DSF value in both cases is lower than that of the second sensor group. The group of sensors with a lower DSF value represents that the centroid is closer to them when the vehicle passes by since a closer distance brings more intense vibrations.

- When a single large vehicle on the bridge

In this case, both the velocity and weight of the vehicle are much greater than the case of a single small vehicle. This leads to the impact of different sensor groups on the feature value will become more obvious. Additionally, this stronger vibration shock leads to a lower feature value (on the second decimal place). When a large vehicle passes through, the stay cables are stressed heavier. The stay cables fully participate in the bridge movement, and the overall 'rhythm' of the bridge is accelerated (the rate of exchange between kinetic and potential energy is accelerated). This phenomenon is similar to that in Section 4.3. In the laboratory study, the concrete cracked but the rebar does not yield. The heavier vehicle weight and cracks increase the participation degree of the rebar in the vibration, while the elastic spring improves the overall consistency of the vehicle-bridge’s motion. So the overall 'rhythm' of the experimental beam becomes faster, which causes the DSF value to decrease in Figure 4-8 (b). The single large vehicle is still not enough to fully excite the whole bridge. There are only two main peaks in Figure 5-11.

- When small vehicles passing the bridge continuously

Figure 5-7 shows the acceleration pattern of small vehicles passing through continuously is similar to that of a one-dimensional simply supported beam

subjected to a moving load in the numerical study. The continuous vehicle entry provides enough energy to bring the bridge into a stable vibration state. The main vibration direction of the stay cables and bridge deck is the direction of gravity. The bridge vibration under this state has an overall trend, which is similar to the vibration pattern of the simply supported beams subjected to a moving load. So the results obtained from the bridge under this state share the same form with the one in the numerical study. The fluctuation of the eigenvalue curve represents the energy exchange of the vehicle-bridge system and the feature value reflects the bridge's vibration 'rhythm'.

5.4 Summary

In this chapter, the field bridge monitoring data collected from a cable-stayed bridge are used to verify the proposed method. The bridge has a composite steel-concrete deck with four I-shape beam steel girders. A group of evenly separated cross girders are used to attach these girders internally. The single A-shaped steel tower is connected to the bridge deck by 16 stay cables with a semi fan arrangement. The detection results are introduced according to the different environmental conditions separately. When the bridge is fully excited, the pattern of the proposed feature is consistent with the results in the numerical study. This illustrates the accuracy of the numerical model and the reliability of the proposed feature. This feature can accurately and timely reflect the health condition of the bridges without being affected by the variation of the vehicle weight and temperature. Besides, this feature can also reveal the interesting information in the transient effects induced by the single vehicle entry such as the entering vehicle's axle-load, the velocity and wheel path. This shows the variations of this feature have their own physical meaning and can easily correspond to the actual situations on the bridge. The value of this feature can accurately reflect the bridge's overall vibration 'rhythm' which is reliable to

reveal the bridge's instantaneous vibration state. The discussion summaries these results from the different environments for comparison. In this field study, the proposed feature shows a promising future for addressing the research gaps mentioned in Section 2.7. The proposed feature can achieve the *real-time* since the bridge vibration state can be instantaneously obtained from the vehicle excitation response without the requirement of the prerequisite information and the preparation work such as the detailed information of the vehicle or the model calibration. The proposed feature also can achieve the *monitoring* since it can provide the more relevant information about the bridge from the obtained responses, such as the entering vehicle's axle-load, the velocity and wheel path. This means the information from the results of the proposed feature is more reliable since we can read the actual condition on the bridge from the changes in the feature. These two points reveal the strong practicability of the proposed feature with significant application potential.

Chapter 6 Conclusions and recommendations

6.1 Conclusions

With the development and expansion of human habitations, the scale and level of highway networks are also increasing. As a critical component in highway networks, highway bridges are the linkage for crossing obstacles. Within cities, they are often built above the existing road network to alleviate traffic pressure. Such bridges within cities generally have smaller spans, similar bridge types and larger traffic flow. The closure of them will affect the smoothness of urban traffic. Thus, for the aging bridges, an easy-transplantable SHM system that can conveniently track their status in the real time is urgently needed.

Since the vehicle loads are the most frequent live loads in bridges with obvious response patterns, they provide another orientation to achieve the real-time detection. The pattern of moving vehicle excited responses can be extracted into the feature space by MPCA from time domain responses and the variations on these extracted patterns induced by damage can be intuitively observed. This opens up the possibility of deploying a narrower window for MPCA. The vehicle-bridge interaction induced bridge responses will take the dominant place comparing to other environmental load induced responses under normal conditions. The inherent feature of bridge health conditions can be accurately extracted since the other environmental load's effect will be decreased when vehicles are passing on the bridge. The computational cost of this idea is low since the vehicle will pass the bridge in a short period. The bridge acceleration data are the better choice as the input data since they are more sensitive to the load variation comparing with the strain and deflection. It can provide the enough information within a time window in seconds. Moreover, the results obtained by MPCA from the vehicle induced responses are better interpretable.

The form of the damage and excitation in different studies are inconsistent. This will lead to the results obtained by MPCA are not interpretable and impede the comparison between different studies. The result obtained by PCA from the data in a specific pattern is interpretable. If the vehicle loads are taken as the main environmental factor, the results obtained by MPCA are easier to match the variations between the changes of external factors and results.

This project develops a bridge real-time monitoring method considering temperature and traffic effects using the moving principal component analysis (MPCA). In this study, the real-time monitoring is defined as: no bridge closure, no requirement of finite element model, no need of the training data that cover various bridge states, no need of accurate vehicle information; only several acceleration response segments of vehicles passing the bridge at different time with corresponding temperature conditions are required for evaluating the health of the bridge in real-time.

Through the numerical study, the inherent feature which reflects the existence of the breathing crack on the bridge is excavated by using MPCA. The robustness of this feature is verified. The changes on this feature induced by a moving vehicle are orthogonal with the changes induced by the breathing crack. The changes caused by the temperature difference are an order of the magnitude different from the changes caused by the breathing crack. The influence of the crack depth and location on the proposed feature is discussed in detail. From the perspective of mechanics and MPCA, the mechanism and meaning behind the feature changes are analysed. This feature provides the bridge information from a dynamic perspective and is strongly interpretable.

In the first experimental study, a Gaussian window is proposed to improve the performance of MPCA on actual datasets. This window can filter out the impact of interference factors like measurement noise and the vehicle-bridge interaction.

It also simplifies the selection of the MPCA window's length to the selection of the Gaussian window's hyperparameter σ. It can reduce the computational cost of MPCA without affecting the accuracy of the damage detection. The result shows that this feature can detect and distinguish the crack damage of different extents under the different vehicle's weight.

In the second experimental study, the pattern of the proposed feature is consistent with the results in the numerical study. This illustrates the accuracy of the numerical model and the reliability of the proposed feature. When the bridge is fully excited, the results show that this feature can accurately and timely reflect the health condition of the bridge without being affected by the variation of the vehicle weight and temperature. In the cases of a single vehicle passing the bridge, the mechanism of the feature change is discussed. The transient effects induced by the single vehicle entry are extracted by MPCA to provide the valuable information such as the entering vehicle's axle-load, the velocity and wheel path. This illustrates the variations of the feature have their own physical meaning and are easy to interpreter. The value of the feature can accurately reflect the bridge's overall vibration 'rhythm' which is reliable to reveal the bridge's instantaneous vibration state.

There is a special case in both laboratory and field studies. The variation of the proposed feature in these two special cases is consistent with the analysis based on the actual situation. This illustrates that this feature is not limited to several few pre-considered parameters but reflects the beam's damage extent from a dynamic perspective. Additionally, both numerical and experimental study illustrate that this feature also has the potential for moving load identification but requires further study.

6.2 Recommendations

- Real-time monitoring

For the proposed method, only several acceleration response segments of vehicles passing the bridge at different time with corresponding temperature conditions are required for evaluating the health of the bridge.

- Accuracy and Robustness

The proposed method can detect and distinguish the crack damage of different extents under the different vehicle's weight and temperature conditions in both the numerical study and laboratory test. In the numerical study, the changes on the feature induced by a moving vehicle are orthogonal with the changes induced by the breathing crack. The changes caused by the temperature difference are an order of the magnitude different from the changes caused by the breathing crack. In the field study, the intense sun exposure in midsummer induced average temperature increase and vertical temperature difference does not influence the detection result of the proposed method. When the bridge is fully excited, the pattern of the proposed feature is consistent with the results in the numerical study since the steel I-beams are closer to the continuum assumption than the reinforced concrete.

- Interpretability

The variation of the damage sensitive feature in the proposed method has its own physical meaning and is easy to interpreter. Not only the bridge damage condition, but the other interesting information also can be derived from the feature variations such as the entering vehicle's axle-load, the velocity and wheel path. This allows us to read the actual situation on bridge in real time from the changes in the proposed feature.

In bridge, the cracks are actually formed by the accumulation of small cracks distributed in different positions. The equivalent crack depth reflected by the proposed feature can more accurately measure the damage extent caused by these distributed cracks on the bridge. This feature provides the bridge information from a dynamic perspective and is strongly interpretable. Since MPCA is a muti-channel data processing method, it is easy for the proposed method to capture the overall movement trend in the bridge vibration signals.

There is a special case in both experiments. The variation of the proposed feature in these two special cases is consistent with the analysis based on the actual situation. This illustrates that this feature is not limited to several few pre-considered parameters and the value of this feature can accurately reflect the bridge's overall vibration 'rhythm' which is reliable to reveal the bridge's instantaneous vibration state.

- Gaussian window

In MPCA, the problem of the window length’s selection is always a big issue and will directly relate to the performance of MPCA. Existence of the measurement noise and vehicle-bridge interaction (VBI) will severely affect the result of traditional MPCA. Therefore, a new type of window called Gaussian window is proposed for MPCA. This window gives more weight to the data near the current moment t on the time axis to pay more attention on the measuring points’ same movement trend caused by the vehicle movement. The normal window expands the eigenvalue along the time axis, and the additional Gaussian distribution of the window realigns the components expanded by the normal window on the time axis.

This window can achieve the following without affecting the detection accuracy:

1. Reduce the influence of these factors (e.g., noise or VBI) that are more diffused on the time axis.

2. Simplify the problem of the window length's selection to the selection of the Gaussian window's hyperparameter.

3. Reduce the computing cost.

The choice of the hyperparameter σ represents the attention of the Gaussian window to the current moment and the tolerance of the influencing factors. The selection of this hyperparameter is related to many factors: the length of bridge, distribution of measuring points, accuracy of sensors, interference degree of environmental factors, vehicle weights, traffic flow and so on.

- Real-world deployment

For a better application of the proposed method in real-world practical use, some noteworthy recommendations are as follows:

1. According to the actual situation of the bridge, it is better to choose the signal excited by the same kind of the load with obvious characteristics as the input. For example, in windy areas, the signals caused by wind loads can be selected as the input.
2. It is better to arrange the sensors evenly along the whole bridge to reflect the overall state information of the bridge more accurately.
3. For the case where the vehicle excitation is used as the input, some standard vehicles (vehicles with the same weight and speed when passing) can be set up as a calibration method for the regular test of the system. In this way, abnormalities in daily results, such as sensor failures, can be found more easily by comparison.

References

An, Y., Chatzi, E., Sim, S. H., Laflamme, S., Blachowski, B., and Ou, J. (2019). Recent progress and future trends on damage identification methods for bridge structures. *Structural Control and Health Monitoring, 26*(10), e2416. https://doi.org/10.1002/stc.2416

Austroads. (2012). Investigating the Development of a Bridge Assessment Tool for Determining Access for High Productivity Freight Vehicles, Sydney, A4, pp 114, AP-R398-12.

Avci, O., Abdeljaber, O., Kiranyaz, S., Hussein, M., Gabbouj, M., and Inman, D. J. (2021). A review of vibration-based damage detection in civil structures: From traditional methods to Machine Learning and Deep Learning applications. *Mechanical Systems and Signal Processing, 147*, 107077. https://doi.org/10.1016/j.ymssp.2020.107077

Bao, Y., Chen, Z., Wei, S., Xu, Y., Tang, Z., and Li, H. (2019). The state of the art of data science and engineering in structural health monitoring. *Engineering, 5*(2), 234-242. https://doi.org/10.1016/j.eng.2018.11.027

Cao, L., He, W.-Y., and Ren, W.-X. (2021). Damage localization and quantification for beam bridges based on frequency variation of parked vehicle-bridge systems. *Structures, 31*, 357-368. https://doi.org/10.1016/j.istruc.2021.01.098

Carden, E. P., and Brownjohn, J. M. (2008). ARMA modelled time-series classification for structural health monitoring of civil infrastructure. *Mechanical Systems and Signal Processing, 22*(2), 295-314. https://doi.org/10.1016/j.ymssp.2007.07.003

Cavadas, F., Smith, I. F., and Figueiras, J. (2013). Damage detection using data-driven methods applied to moving-load responses. *Mechanical Systems and Signal Processing, 39*(1-2), 409-425. https://doi.org/10.1016/j.ymssp.2013.02.019

Cawley, P. (2018). Structural health monitoring: Closing the gap between research and industrial deployment. *Structural Health Monitoring, 17*(5), 1225-1244. https://doi.org/10.1177/1475921717750047

Cheema, P., Alamdari, M. M., Vio, G., Zhang, F., and Kim, C. (2021). Infinite mixture models for operational modal analysis: An automated and principled approach. *Journal of sound and vibration, 491*, 115757. https://doi.org/10.1016/j.jsv.2020.115757

Dackermann, U., Li, J., and Samali, B. (2010). Dynamic-based damage identification using neural network ensembles and damage index method.

Advances in Structural Engineering, 13(6), 1001-1016. https://doi.org/10.1260/1369-4332.13.6.1001

Das Khan, S., Topdar, P., and Datta, A. K. (2020). Applicability of Fuzzy-Based Visual Inspection Approach for Condition Assessment of Bridges in Developing Countries: A State-of-the-Art Review. *Journal of The Institution of Engineers (India): Series A, 101*(4), 835-846. https://doi.org/10.1007/s40030-020-00465-1

de Almeida Cardoso, R., Cury, A., and Barbosa, F. (2019). Automated real-time damage detection strategy using raw dynamic measurements. *Engineering Structures, 196*, 109364. https://doi.org/10.1016/j.engstruct.2019.109364

Deraemaeker, A., Reynders, E., De Roeck, G., and Kullaa, J. (2008). Vibration-based structural health monitoring using output-only measurements under changing environment. *Mechanical Systems and Signal Processing, 22*(1), 34-56. https://doi.org/10.1016/j.ymssp.2007.07.004

Deraemaeker, A., and Worden, K. (2018). A comparison of linear approaches to filter out environmental effects in structural health monitoring. *Mechanical Systems and Signal Processing, 105*, 1-15. https://doi.org/10.1016/j.ymssp.2017.11.045

Entezami, A., Sarmadi, H., Behkamal, B., and Mariani, S. (2020). Big data analytics and structural health monitoring: a statistical pattern recognition-based approach. *Sensors, 20*(8), 2328. https://doi.org/10.3390/s20082328

Entezami, A., Shariatmadar, H., and Karamodin, A. (2019). Data-driven damage diagnosis under environmental and operational variability by novel statistical pattern recognition methods. *Structural Health Monitoring, 18*(5-6), 1416-1443. https://doi.org/10.1177/1475921718800306

Erazo, K., Sen, D., Nagarajaiah, S., and Sun, L. (2019). Vibration-based structural health monitoring under changing environmental conditions using Kalman filtering. *Mechanical Systems and Signal Processing, 117*, 1-15. https://doi.org/10.1016/j.ymssp.2018.07.041

Favarelli, E., and Giorgetti, A. (2021). Machine Learning for Automatic Processing of Modal Analysis in Damage Detection of Bridges. *IEEE Transactions on Instrumentation and Measurement, 70*, 1-13. https://doi.org/10.1109/TIM.2020.3038288

Fuh-Gwo, Y., Sakib Ashraf, Z., Qiuyi, C., and Shaohan, W. (2020). *Machine learning for structural health monitoring: challenges and opportunities.* Paper presented at the Sensors and Smart Structures Technologies for Civil, Mechanical, and Aerospace Systems 2020. https://doi.org/10.1117/12.2561610

Gu, J., Gul, M., and Wu, X. (2017). Damage detection under varying

temperature using artificial neural networks. *Structural Control and Health Monitoring, 24*(11), e1998. https://doi.org/10.1002/stc.1998

Guidio, B., and Jeong, C. (2021). On the feasibility of simultaneous identification of a material property of a Timoshenko beam and a moving vibration source. *Engineering Structures, 227*, 111346. https://doi.org/10.1016/j.engstruct.2020.111346

Gul, M., and Catbas, F. N. (2008). Ambient vibration data analysis for structural identification and global condition assessment. *Journal of Engineering Mechanics, 134*(8), 650-662. https://doi.org/10.1061/(ASCE)0733-9399(2008)134:8(650)

Guo, W., Zhao, H., Gao, X., Kong, L., and Li, Y. (2018). An efficient representative for object recognition in structural health monitoring. *The International Journal of Advanced Manufacturing Technology, 94*(9), 3239-3250. https://doi.org/10.1007/s00170-016-9309-6

Han, Q., Ma, Q., Xu, J., and Liu, M. (2021). Structural health monitoring research under varying temperature condition: a review. *Journal of Civil Structural Health Monitoring, 11*(1), 149-173. https://doi.org/10.1007/s13349-020-00444-x

Hester, D., and González, A. (2015). A bridge-monitoring tool based on bridge and vehicle accelerations. *Structure and Infrastructure Engineering, 11*(5), 619-637. https://doi.org/10.1080/15732479.2014.890631

Hotelling, H. (1933). Analysis of a complex of statistical variables into principal components. *Journal of educational psychology, 24*(6), 417-441. https://doi.org/10.1037/h0071325

Huang, M.-S., Gül, M., and Zhu, H.-P. (2018). Vibration-based structural damage identification under varying temperature effects. *Journal of Aerospace Engineering, 31*(3), 04018014. https://doi.org/10.1061/(ASCE)AS.1943-5525.0000829

Jayasundara, N., Thambiratnam, D., Chan, T. T., and Nguyen, A. (2020). Locating and quantifying damage in deck type arch bridges using frequency response functions and artificial neural networks. *International Journal of Structural Stability and Dynamics, 20*(10), 2042010. https://doi.org/10.1142/S0219455420420109

Jesus, A., Brommer, P., Westgate, R., Koo, K., Brownjohn, J., and Laory, I. (2019). Bayesian structural identification of a long suspension bridge considering temperature and traffic load effects. *Structural Health Monitoring, 18*(4), 1310-1323. https://doi.org/10.1177/1475921718794299

Jin, S.-S., Cho, S., and Jung, H.-J. (2015). Adaptive reference updating for vibration-based structural health monitoring under varying environmental

conditions. *Computers & Structures, 158*, 211-224. https://doi.org/10.1016/j.compstruc.2015.06.001

Jin, S.-S., and Jung, H.-J. (2018). Vibration-based damage detection using online learning algorithm for output-only structural health monitoring. *Structural Health Monitoring, 17*(4), 727-746. https://doi.org/10.1177/1475921717717310

Kim, J.-T., Park, J.-H., and Lee, B.-J. (2007). Vibration-based damage monitoring in model plate-girder bridges under uncertain temperature conditions. *Engineering Structures, 29*(7), 1354-1365. https://doi.org/10.1016/j.engstruct.2006.07.024

Kostić, B., and Gül, M. (2017). Vibration-based damage detection of bridges under varying temperature effects using time-series analysis and artificial neural networks. *Journal of Bridge Engineering, 22*(10), 04017065. https://doi.org/10.1061/(ASCE)BE.1943-5592.0001085

Kromanis, R., and Kripakaran, P. (2016). SHM of bridges: characterising thermal response and detecting anomaly events using a temperature-based measurement interpretation approach. *Journal of Civil Structural Health Monitoring, 6*(2), 237-254. https://doi.org/10.1007/s13349-016-0161-z

Kromanis, R., and Kripakaran, P. (2017). Data-driven approaches for measurement interpretation: analysing integrated thermal and vehicular response in bridge structural health monitoring. *Advanced Engineering Informatics, 34*, 46-59. https://doi.org/10.1016/j.aei.2017.09.002

Kulprapha, N., and Warnitchai, P. (2012). Structural health monitoring of continuous prestressed concrete bridges using ambient thermal responses. *Engineering Structures, 40*, 20-38. https://doi.org/10.1016/j.engstruct.2012.02.001

Kumar, K., Biswas, P. K., and Dhang, N. (2019). Damage diagnosis of steel truss bridges under varying environmental and loading conditions. *The International Journal of Acoustics and Vibration, 24*(1), 56-67. https://doi.org/10.20855/ijav.2019.24.11255

Lanata, F., Posenato, D., and Inaudi, D. (2007, November 13-16). *Data Anomaly Identification in Complex Structures Using Model Free Data Statistical Analysis.* Paper presented at the 3rd International Conference on Structural Health Monitoring of Intelligent Infrastructure (SHMII-3), Vancouver, British Columbia, Canada.

Law, S.-S., and Zhu, X.-Q. (2009). *Damage Models and Algorithms for Assessment of Structures under Operating Conditions: Structures and Infrastructures Book Series* (1st ed. Vol. 5). London: CRC Press. https://doi.org/10.1201/b10991

Law, S.-S., and Zhu, X.-Q. (2011). *Moving Loads-Dynamic Analysis and Identification Techniques: Structures and Infrastructures Book Series* (1st ed. Vol. 8). London: CRC Press. https://doi.org/10.1201/b10561

Law, S., and Zhu, X. (2006). Vibration of a beam with a breathing crack subject to moving mass. In G. R. Liu, V. B. C. Tan, & X. Han (Eds.), *Computational Methods* (pp. 1963-1968). Dordrecht: Springer Netherlands. https://doi.org/10.1007/978-1-4020-3953-9_141

Li, H. (2019). *Statistical Learning Method* (2nd ed.). Beijing: Tsinghua University Press.

Li, L., Liu, H., Zhou, H., and Zhang, C. (2020). Missing data estimation method for time series data in structure health monitoring systems by probability principal component analysis. *Advances in Engineering Software, 149*, 102901. https://doi.org/10.1016/j.advengsoft.2020.102901

Ma, X., Lin, Y., Nie, Z., and Ma, H. (2020). Structural damage identification based on unsupervised feature-extraction via Variational Auto-encoder. *Measurement, 160*, 107811. https://doi.org/10.1016/j.measurement.2020.107811

Mao, L., Weng, S., Li, S.-J., Zhu, H.-P., and Sun, Y.-H. (2020). Statistical damage identification method based on dynamic response sensitivity. *Journal of Low Frequency Noise, Vibration and Active Control, 39*(3), 560-571. https://doi.org/10.1177/1461348418784828

Martinez, D., Malekjafarian, A., and OBrien, E. (2020a). Bridge flexural rigidity calculation using measured drive-by deflections. *Journal of Civil Structural Health Monitoring, 10*(5), 833-844. https://doi.org/10.1007/s13349-020-00419-y

Martinez, D., Malekjafarian, A., and OBrien, E. (2020b). Bridge health monitoring using deflection measurements under random traffic. *Structural Control and Health Monitoring, 27*(9), e2593. https://doi.org/10.1002/stc.2593

Mei, Q., Gül, M., and Boay, M. (2019). Indirect health monitoring of bridges using Mel-frequency cepstral coefficients and principal component analysis. *Mechanical Systems and Signal Processing, 119*, 523-546. https://doi.org/10.1016/j.ymssp.2018.10.006

Meixedo, A., Ribeiro, D., Santos, J., Calçada, R., and Todd, M. (2021). Progressive numerical model validation of a bowstring-arch railway bridge based on a structural health monitoring system. *Journal of Civil Structural Health Monitoring, 11*(2), 421-449. https://doi.org/10.1007/s13349-020-00461-w

Meruane, V., and Heylen, W. (2012). Structural damage assessment under

varying temperature conditions. *Structural Health Monitoring, 11*(3), 345-357. https://doi.org/10.1177/1475921711419995

Miguel, L. F. F., Miguel, L. F. F., Kaminski Jr, J., and Riera, J. D. (2012). Damage detection under ambient vibration by harmony search algorithm. *Expert Systems with Applications, 39*(10), 9704-9714. https://doi.org/10.1016/j.eswa.2012.02.147

Moughty, J. J., and Casas, J. R. (2016). *Vibration based damage detection techniques for small to medium span bridges: A review and case study*. Paper presented at the 8th European Workshop on Structural Health Monitoring (EWSHM 2016), Bilbao, Spain.

Murphy, B., and Yarnold, M. (2018). Temperature-driven structural identification of a steel girder bridge with an integral abutment. *Engineering Structures, 155*, 209-221. https://doi.org/10.1016/j.engstruct.2017.10.074

Nguyen, K. V. (2013). Comparison studies of open and breathing crack detections of a beam-like bridge subjected to a moving vehicle. *Engineering Structures, 51*, 306-314. https://doi.org/10.1016/j.engstruct.2013.01.018

Nguyen, V., Dackermann, U., Li, J., Alamdari, M. M., Mustapha, S., Runcie, P., and Ye, L. (2015). Damage identification of a concrete arch beam based on frequency response functions and artificial neural networks. *Electronic Journal of Structural Engineering, 14*(1), 75-84. https://doi.org/10.56748/ejse.141921

Nie, Z., Guo, E., Li, J., Hao, H., Ma, H., and Jiang, H. (2020). Bridge condition monitoring using fixed moving principal component analysis. *Structural Control and Health Monitoring, 27*(6), e2535. https://doi.org/10.1002/stc.2535

Niu, Y., Ye, Y., Zhao, W., and Shu, J. (2021). Dynamic monitoring and data analysis of a long-span arch bridge based on high-rate GNSS-RTK measurement combining CF-CEEMD method. *Journal of Civil Structural Health Monitoring, 11*(1), 35-48. https://doi.org/10.1007/s13349-020-00436-x

Pai, S. G., Reuland, Y., and Smith, I. F. (2019). Data-Interpretation Methodologies for Practical Asset-Management. *Journal of Sensor and Actuator Networks, 8*(2), 36. https://doi.org/10.3390/jsan8020036

Pan, H., Azimi, M., Yan, F., and Lin, Z. (2018). Time-frequency-based data-driven structural diagnosis and damage detection for cable-stayed bridges. *Journal of Bridge Engineering, 23*(6), 04018033. https://doi.org/10.1061/(ASCE)BE.1943-5592.0001199

Posenato, D., Lanata, F., Inaudi, D., and Smith, I. F. (2008). Model-free data interpretation for continuous monitoring of complex structures. *Advanced*

Engineering Informatics, 22(1), 135-144. https://doi.org/10.1016/j.aei.2007.02.002

Rogers, T., Worden, K., Fuentes, R., Dervilis, N., Tygesen, U., and Cross, E. (2019). A Bayesian non-parametric clustering approach for semi-supervised Structural Health Monitoring. *Mechanical Systems and Signal Processing, 119*, 100-119. https://doi.org/10.1016/j.ymssp.2018.09.013

Roveri, N., Milana, S., Culla, A., and Carcaterra, A. (2019, June 16-19). *Damage Diagnostic Technique Combining Machine Learning Approach With a Sensors Swarm.* Paper presented at the INTER-NOISE and NOISE-CON Congress and Conference Proceedings, Madrid, Spain.

Sadeghi Eshkevari, S., Pakzad, S. N., Takáč, M., and Matarazzo, T. J. (2020). Modal identification of bridges using mobile sensors with sparse vibration data. *Journal of Engineering Mechanics, 146*(4), 04020011. https://doi.org/10.1061/(ASCE)EM.1943-7889.0001733

Sakiyama, F. I. H., Lehmann, F., and Garrecht, H. (2021). A Novel Runtime Algorithm for the Real-Time Analysis and Detection of Unexpected Changes in a Real-Size SHM Network with Quasi-Distributed FBG Sensors. *Sensors, 21*(8), 2871. https://doi.org/10.3390/s21082871

Santos, J., Crémona, C., and Silveira, P. (2020). Automatic Operational Modal Analysis of Complex Civil Infrastructures. *Structural Engineering International, 30*(3), 365-380. https://doi.org/10.1080/10168664.2020.1749012

Santos, J. P., Crémona, C., Calado, L., Silveira, P., and Orcesi, A. D. (2016). On‐line unsupervised detection of early damage. *Structural Control and Health Monitoring, 23*(7), 1047-1069. https://doi.org/10.1002/stc.1825

Sarmadi, H., and Karamodin, A. (2020). A novel anomaly detection method based on adaptive Mahalanobis-squared distance and one-class kNN rule for structural health monitoring under environmental effects. *Mechanical Systems and Signal Processing, 140*, 106495. https://doi.org/10.1016/j.ymssp.2019.106495

Sen, D., Erazo, K., Zhang, W., Nagarajaiah, S., and Sun, L. (2019). On the effectiveness of principal component analysis for decoupling structural damage and environmental effects in bridge structures. *Journal of sound and vibration, 457*, 280-298. https://doi.org/10.1016/j.jsv.2019.06.003

Shahbaznia, M., Dehkordi, M. R., and Mirzaee, A. (2020). An Improved Time-Domain Damage Detection Method for Railway Bridges Subjected to Unknown Moving Loads. *Periodica Polytechnica Civil Engineering, 64*(3), 928-938. https://doi.org/10.3311/PPci.15813

Shokrani, Y., Dertimanis, V. K., Chatzi, E. N., and N. Savoia, M. (2018). On the

use of mode shape curvatures for damage localization under varying environmental conditions. *Structural Control and Health Monitoring, 25*(4), e2132. https://doi.org/10.1002/stc.2132

Silva, M., Santos, A., Santos, R., Figueiredo, E., Sales, C., and Costa, J. C. (2017). Agglomerative concentric hypersphere clustering applied to structural damage detection. *Mechanical Systems and Signal Processing, 92*, 196-212. https://doi.org/10.1016/j.ymssp.2017.01.024

Tada, H., Paris, P. C., and Irwin, G. R. (2000). *The analysis of cracks handbook* (3rd ed.). New York: ASME Press. https://doi.org/10.1115/1.801535

Voggu, S., and Sasmal, S. (2021). Dynamic nonlinearities for identification of the breathing crack type damage in reinforced concrete bridges. *Structural Health Monitoring, 20*(1), 339-359. https://doi.org/10.1177/1475921720930990

Wang, Y., and Ni, Y. (2020). Bayesian dynamic forecasting of structural strain response using structural health monitoring data. *Structural Control and Health Monitoring, 27*(8), e2575. https://doi.org/10.1002/stc.2575

Wang, Z., Huang, M., and Gu, J. (2020). Temperature effects on vibration-based damage detection of a reinforced concrete slab. *Applied Sciences, 10*(8), 2869. https://doi.org/10.3390/app10082869

Yeung, W., and Smith, J. (2005). Damage detection in bridges using neural networks for pattern recognition of vibration signatures. *Engineering Structures, 27*(5), 685-698. https://doi.org/10.1016/j.engstruct.2004.12.006

Yu, L., and Zhu, J. H. (2011). Effect of Computational Patterns of PCA on Moving Force Identification. *Advanced Materials Research, 163-167*, 2678-2682. https://doi.org/10.4028/www.scientific.net/AMR.163-167.2678

Yuen, K.-V. (2010). *Bayesian methods for structural dynamics and civil engineering*. Singapore: John Wiley & Sons (Asia) Pte Ltd. https://doi.org/10.1002/9780470824566

Zhang, G., Tang, L., Zhou, L., Liu, Z., Liu, Y., and Jiang, Z. (2019). Principal component analysis method with space and time windows for damage detection. *Sensors, 19*(11), 2521. https://doi.org/10.3390/s19112521

Zhang, H., Gül, M., and Kostić, B. (2019). Eliminating temperature effects in damage detection for civil infrastructure using time series analysis and autoassociative neural networks. *Journal of Aerospace Engineering, 32*(2), 04019001. https://doi.org/10.1061/(ASCE)AS.1943-5525.0000987

Zhang, W., Li, Y. X., and Sun, L. M. (2021). SHM-Oriented Hybrid Modeling for Stress Analysis of Steel Girder Bridge. *Journal of Bridge Engineering, 26*(6), 05021002. https://doi.org/10.1061/(ASCE)BE.1943-5592.0001710

Zhou, X., Cao, L., Khan, I., and Li, Q. (2018). Data inspecting and denoising method for data-driven stochastic subspace identification. *Shock and vibration, 2018*, 3926817. https://doi.org/10.1155/2018/3926817

Zhou, X. T., Ni, Y. Q., and Zhang, F. L. (2014). Damage localization of cable-supported bridges using modal frequency data and probabilistic neural network. *Mathematical Problems in Engineering, 2014*, 837963. https://doi.org/10.1155/2014/837963

Zhou, Y., Xia, Y., and Fujino, Y. (2021). Analytical formulas of beam deflection due to vertical temperature difference. *Engineering Structures, 240*, 112366. https://doi.org/10.1016/j.engstruct.2021.112366

Zhu, X., and Hao, H. (2007). Structural damage detection using wavelet support vector machine. In A. L. Wicks (Ed.), *Proceedings of the IMAC XXV: A Conference & Exposition on Structural Dynamics* (Orlando, Florida, USA ed., Vol. 1, pp. 9). Florida, USA: Society for Experimental Mechanics, Inc.

Zhu, X. Q., and Law, S. S. (2006). Wavelet-based crack identification of bridge beam from operational deflection time history. *International Journal of Solids and Structures, 43*(7-8), 2299-2317. https://doi.org/10.1016/j.ijsolstr.2005.07.024.

Zhu, Y., Ni, Y.-Q., Jesus, A., Liu, J., and Laory, I. (2018). Thermal strain extraction methodologies for bridge structural condition assessment. *Smart Materials and Structures, 27*(10), 105051. https://doi.org/10.1088/1361-665X/aad5fb

Zhu, Y., Ni, Y.-Q., Jin, H., Inaudi, D., and Laory, I. (2019). A temperature-driven MPCA method for structural anomaly detection. *Engineering Structures, 190*, 447-458. https://doi.org/10.1016/j.engstruct.2019.04.004.